การพัฒนาแบบจำลองค่าการนำความร้อนของวัสดุพอลิเมอร์คอมโพสิตที่รวมผลของความต้านทานทางความร้อนที่ส่วนต่อประสานระหว่างเฟส

นายณัฐกานต์ ขัตตเนตร์

วิทยานิพนธ์นี้เป็นส่วนหนึ่งของการศึกษาตามหลักสูตรปริญญาวิศวกรรมศาสตรมหาบัณฑิต
สาขาวิชาวิศวกรรมเคมี ภาควิชาวิศวกรรมเคมี
คณะวิศวกรรมศาสตร์ จุฬาลงกรณ์มหาวิทยาลัย
ปีการศึกษา 2557

DEVELOPMENT OF THERMAL CONDUCTIVITY MODEL OF POLYMER COMPOSITES WITH INTERFACIAL THERMAL RESISTANCE EFFECT

Mr. Nuttakan Kuttanate

A Thesis Submitted in Partial Fulfillment of the Requirements
for the Degree of Master of Engineering Program in Chemical Engineering
Department of Chemical Engineering
Faculty of Engineering
Chulalongkorn University
Academic Year 2014

Thesis Title	DEVELOPMENT OF THERMAL CONDUCTIVITY MODEL OF POLYMER COMPOSITES WITH INTERFACIAL THERMAL RESISTANCE EFFECT
By	Mr. Nuttakan Kuttanate
Field of Study	Chemical Engineering
Thesis Advisor	Varun Taepaisitphongse, Ph.D.

Accepted by the Faculty of Engineering, Chulalongkorn University in Partial Fulfillment of the Requirements for the Master's Degree

.....Dean of the Faculty of Engineering

(Professor Bundhit Eua-arporn, Ph.D.)

THESIS COMMITTEE

.....Chairman

(Associate Professor Sarawut Rimdusit, Ph.D.)

.....Thesis Advisor

(Varun Taepaisitphongse, Ph.D.)

.....Examiner

(Assistant Professor Amornchai Arpornwichanop, D.Eng.)

.....External Examiner

(Sunan Tiptipakorn, D.Eng.)

ณัฐกานต์ ขัตตเนตร์ : การพัฒนาแบบจำลองค่าการนำความร้อนของวัสดุพอลิเมอร์คอมโพสิตที่รวมผลของความต้านทานทางความร้อนที่ส่วนต่อประสานระหว่างเฟส (DEVELOPMENT OF THERMAL CONDUCTIVITY MODEL OF POLYMER COMPOSITES WITH INTERFACIAL THERMAL RESISTANCE EFFECT) อ.ที่ปรึกษาวิทยานิพนธ์หลัก: อ. ดร.วรัญ แต้ไพสิฐพงษ์, 156 หน้า.

ค่าการนำความร้อนของวัสดุพอลิเมอร์สามารถถูกปรับปรุงได้โดยการผสมสารเติมแต่งนำความร้อนลงในพอลิเมอร์ ค่าการนำความร้อนของวัสดุพอลิเมอร์คอมโพสิตขึ้นอยู่กับหลายปัจจัย งานวิจัยนี้มุ่งศึกษาเฉพาะผลของความต้านทานทางความร้อนที่ส่วนต่อประสานระหว่างเฟส (interfacial thermal resistance) อัตราส่วนระหว่างค่าการนำความร้อนของสารเติมแต่งและพอลิเมอร์ ปริมาณและขนาดของอนุภาคสารเติมแต่ง ที่มีต่อค่าการนำความร้อนยังผล (effective thermal conductivity) ของวัสดุพอลิเมอร์คอมโพสิต

แบบจำลองเชิงทฤษฎีสำหรับทำนายค่าการนำความร้อนของคอมโพสิตได้รับการพัฒนาขึ้นบนพื้นฐานของวิธีผลเฉลยอย่างง่าย โดยพิจารณาค่าความต้านทางความร้อนเป็นแบบเรียงต่อกันเชิงอนุกรมตามทิศทางการถ่ายเทความร้อนของหน่วยปริมาตรตัวแทนที่มีการจัดเรียงอนุภาคสารเติมแต่งที่แตกต่างกันสามรูปแบบ ได้แก่ ลูกบาศก์อย่างง่าย (simple cubic) ลูกบาศก์กลางตัว (body-centered cubic) และลูกบาศก์กลางหน้า (face-centered cubic) แบบจำลองทั้งสามที่ได้ถูกพัฒนาขึ้นโดยไม่รวมผลของความต้านทานทางความร้อนที่ส่วนต่อประสานระหว่างเฟสทำนายว่า ค่าการนำความร้อนยังผลเพิ่มขึ้นตามการเพิ่มขึ้นของปริมาณสารเติมแต่งและอัตราส่วนระหว่างค่าการนำความร้อนของสารเติมแต่งและพอลิเมอร์ อย่างไรก็ตามแบบจำลองทั้งสามประเมินค่าการนำความร้อนยังผลได้มากกว่าค่าที่วัดได้จากการทดลอง แบบจำลองแบบลูกบาศก์อย่างง่ายให้ค่าการทำนายที่เหมาะสมมากกว่าแบบจำลองแบบอื่น ดังนั้นแบบจำลองลูกบาศก์อย่างง่ายจึงได้รับการปรับปรุงโดยการเพิ่มผลกระทบของความต้านทานทางความร้อนที่ส่วนต่อประสานระหว่างเฟสโดยใช้หลักการของรัศมีคาปิตซา (Kapitza radius) และวิธีนี้ทำให้ผลกระทบของขนาดอนุภาคสารเติมแต่งได้ถูกรวมเข้าไปในการพัฒนาแบบจำลองด้วย แบบจำลองลูกบาศก์อย่างง่ายที่ได้รับการปรับปรุงทำนายว่า ค่าการนำความร้อนยังผลลดลงตามการเพิ่มขึ้นของค่าความต้านทานทางความร้อนที่ส่วนต่อประสานระหว่างเฟส และเมื่อสารเติมแต่งมีอนุภาคขนาดเล็กลงทำให้ความต้านทานทางความร้อนที่ส่วนต่อประสานระหว่างเฟสมีค่าเพิ่มขึ้น นอกจากนั้นแล้วแบบจำลองทำนายว่า ความต้านทานที่ส่วนต่อประสานระหว่างเฟสมีค่าลดลงเมื่อปริมาณของสารเติมแต่งเพิ่มขึ้น

ภาควิชา วิศวกรรมเคมี ลายมือชื่อนิสิต .....

สาขาวิชา วิศวกรรมเคมี ลายมือชื่อ อ.ที่ปรึกษาหลัก .....

ปีการศึกษา 2557

5570185821 : MAJOR CHEMICAL ENGINEERING
KEYWORDS: THERMAL CONDUCTIVITY / INTERFACIAL THERMAL RESISTANCE / POLYMER COMPOSITES / MATHEMATHICAL MODEL

NUTTAKAN KUTTANATE: DEVELOPMENT OF THERMAL CONDUCTIVITY MODEL OF POLYMER COMPOSITES WITH INTERFACIAL THERMAL RESISTANCE EFFECT. ADVISOR: VARUN TAEPAISITPHONGSE, Ph.D., 156 pp.

Thermal conductivity of polymers can be enhanced by incorporating the thermally conductive fillers into the polymer matrix. Various factors affect the thermal conductivity of polymer composites. The effects of interfacial thermal resistance, ratio between thermal conductivity of filler and polymer matrix, content and size of filler particles on the effective thermal conductivity of polymer composites were investigated in this work.

The theoretical models for predicting the thermal conductivity of composite were derived based on the simplified solution by considering a series of thermal resistance along the heat flow direction of the representative volume element with three different arrangements of filler particles, i.e. simple cubic , body-centered cubic, and face-centered cubic. The three models derived without the interfacial thermal resistance effect predicted that the effective thermal conductivity increased with increasing filler content and the ratio between thermal conductivity of filler and polymer matrix. However, these three models overestimated the effective thermal conductivity compared with the experimental data. Among these models, simple cubic model gave a more appropriate and reasonable prediction than the others and thus it was further developed by including the effect of the interfacial thermal resistance using the Kapitza radius concept. By this way, the effect of particle size was also incorporated into the model. The modified simple cubic model indicated that the effective thermal conductivity decreased with increasing interfacial thermal resistance. The smaller filler particle size resulted in the higher interfacial thermal resistance. In addition, the model predicted that the interfacial thermal resistance decreased with increasing filler content.

Department: Chemical Engineering Student's Signature .....
Field of Study: Chemical Engineering Advisor's Signature .....
Academic Year: 2014

ACKNOWLEDGEMENTS

I am profoundly indebted to my advisor, Dr. Varun Taepaisitphongse, for his inspiring and invaluable guidance and support throughout the course of this thesis. In addition, I gratefully thank members of my thesis committee for their substantial advice and helpful comments for completing my thesis.

Furthermore, I would like to thank the Department of Chemical Engineering, Faculty of Engineering, Chulalongkorn University for the opportunity to study and develop my skills and knowledge which has been a big part in my successful completion of this thesis.

Thanks to all my friends and colleagues in the Polymer Engineering Laboratory, Chulalongkorn University for their friendly encouragement.

Finally, I would like to thank my family for their blessings, constant encouragement, and full support throughout my entire study.

CONTENTS

Page

Page

Page

Page

LIST OF TABLES

LIST OF FIGURES

LIST OF NOMENCLATURE

Symbol	Definition	SI Units
A	Area	m^2
Ag	Silver	
Al	Aluminum	
AlN	Aluminum nitride	
a	Length of RVE	m
a_K	Kapitza Radius	m
a_r	Aspect Ratio	
a_s	Speed of Sound in Solid State	m/s
a_1, a_2	Integration Constants in Eq. (2.12)	
a_1, a_2, a_3	Semiaxes of Ellipsoid	
B	Parameter in Eq. (2.42)	
$BaTiO_3$	Barium Titanate	
BCC	Body-centered Cubic	
BN	Boron nitride	
b	Radius of Circle in Each Layer of RVE (Smaller)	m
C'	Parameter in Eq. (2.42)	
$\hat{C}_p$	Specific Heat Capacity at Constant Pressure	J/K-kg
$\hat{C}_{v,e}$	Specific Heat Capacity of Each Electron	J/electron-K
$\hat{C}_{v,l}$	Lattice Specific Heat Capacity	J/K-kg
Cu	Copper	
D	Diameter	m
d	Radius of Circle in Each Layer of RVE (Larger)	m
EVA	Ethylene Vinyl Acetate	
e_c	Electron Charge	C
FCC	Face-centered Cubic	
Ge	Germanium	
HDPE	High Density Polyethylene	

h	Thermal Conductance	W/°C
h_B	Skin Constant	W/m^{2}K
h_{int}	Thermal Interfacial Conductance	W/m^{2}K
h_{21}	Contact Conductance at the Interface between the Spherical Particle and Continuous Medium	W/m^{2}K
J_e	Electric Current	A
k	Thermal Conductivity of Solid	W/m-K
k_b	Boltzman Constant	J/K
k_E	Generalized Einstein Coefficient	
k_e	Free Electron Thermal Conductivity	W/m-K
k_{eff}	Effective Thermal Conductivity	W/m-K
k_f	Thermal Conductivity of Filler Particle	W/m-K
k_{int}	Interfacial Thermal Conductivity	W/m-K
k_m	Thermal Conductivity of Matrix	W/m-K
k_{mn}	Thermal Conductivity Ratio	
L	Geometrical Factor	
l	Distance between Centers of Adjacent Spheres	m
Δl	Thickness of Ideal Matrix Material	m
m_e	Electron mass	kg
n	Shape Factor	
n_e	Number of Free Electrons per Unit Volume	electrons/m^3
n_f	Number of Spherical Particles in RVE	
P_1	One-dimensional Porosity (Line Fraction)	
PP	Polypropylene	
PS	Polystyrene	
Q	Heat Flow	W
q	Heat Flux	W/m^2
$\boldsymbol{q}$	Heat Flux Vector	W/m^2
R	Parameter in Eq. (2.54)	
R	Thermal Resistance	K/W
R_Σ	Total Thermal Resistance	K/W

R_f	Filler Thermal Resistance	K/W
R_{int}	Interfacial Thermal Resistance	m^2K/W
R_m	Polymer Matrix Thermal Resistance	K/W
RVE	Representative Volume Element	
r	Radius	m
r'	Effective Radius of Filler	m
S	Shape Parameter	
SC	Simple Cubic	
Si	Silicon	
$\boldsymbol{s}$	Unit Vector	m
T	Temperature	°C or K
ΔT	Temperature Difference	°C or K
$\boldsymbol{\nabla} T$	Temperature Gradient	°C/m or K/m
T_{max}	Maximum Temperature	°C or K
t	Time	s
Δt	Period of Time	s
$t_{1/2}$	Half Time	s
u_e	Mean Electron Speed	m/s
u_p	Mean Phonon Velocity	m/s
V	Total Volume or Volume of RVE	m^3
V'	Volume of RVE with Interfacial Layer	m^3
V_f	Volume of Filler	m^3
V_f'	Effective Volume of Filler	m^3
V_K	Volume of Interfacial Layer	m^3
V_m	Volume of Matrix Material	m^3
v_f	Volume Fraction of Filler Particles	
v_f'	Effective Volume Fraction of Filler Particles	
v_{f3}	Volume Ratio between Spherical Particle and Continuous Medium	
$v_{f,max}$	Maximum Packing Volume Fraction	

v_K	Volume Fraction of Interfacial Layer	
v_{3f}	Volume Ratio between Continuous Medium and Spherical Particle	
X	Materials Axis	
X'	Local Particle Axis	
Δx	Thickness	m

Greek Symbols

α	Thermal Diffusivity	m^2/s
α_K	Interfacial Thermal Resistance Factor	
β	Parameter in Eq. (3.10)	
β_{BCC1}	Parameter in Body-centered Cubic Model Defined in Eq. (4.76)	
β_{FCC1}	Parameter in Face-centered Cubic Model Defined in Eq. (4.136)	
β_2	Parameter in Eq. (3.20)	
γ_{BCC1}	Parameter in Body-centered Cubic Model Defined in Eq. (4.45)	
γ_{FCC1}	Parameter in Face-centered Cubic Model Defined in Eq. (4.105)	
γ_{SC1}	Parameter in Simple Cubic Model Defined in Eq. (4.17)	
δ	Thickness of Interface Layer	m
δ_{BCC1}	Parameter in Body-centered Cubic Model Defined in Eq. (4.85)	
δ_{FCC1}	Parameter in Face-centered Cubic Model Defined in Eq. (4.144)	
ε_K	Interfacial Volume Factor	
Θ_D	Parameter in Eq. (3.20)	
Θ_N	Parameter in Eq. (3.20)	

θ	Angle between Material Axis and Local Particle Axis	rad
λ_e	Electron Mean Free Path	m
λ_p	Phonon Mean Free Path	m
μ	Mean	
ρ	Density	kg/m^3
σ	Standard Deviation	
σ_e	Electrical Conductivity	1/ohm-m
τ_e	Electron Residence Time	s
φ	Electrical Potential	Volt
Ψ	Sphericity	
Ψ_2	Parameter in Eq. (3.20)	

Subscripts

1	Side 1, Node 1
$1'$	Internode 1
2	Side 2, Node 2
$2'$	Internode 2
$\mathrm{BCC1-1}$	Body-centered Cubic Model with v_f < 0.131
$\mathrm{BCC1-2}$	Body-centered Cubic Model with v_f = 0.131
$\mathrm{BCC1-3}$	Body-centered Cubic Model with v_f > 0.131
$\mathrm{FCC1-1}$	Face-centered Cubic Model with v_f < 0.262
$\mathrm{FCC1-2}$	Face-centered Cubic Model with v_f = 0.262
$\mathrm{FCC1-3}$	Face-centered Cubic Model with v_f > 0.262
i	Section Number of Element
j	Layer Number
l	Longitudinal Wave
$\mathrm{SC1-1}$	SC1 Model with v_f < 0.524
$\mathrm{SC1-2}$	SC1 Model with v_f = 0.524
$\mathrm{SC2}$	Modified Simple Cubic Model

t	Transverse Wave
x	x Direction

CHAPTER 1
INTRODUCTION

1.1 Introduction

Polymer materials are presently used instead of the metal parts in the electronic devices because of their advantages such as lightweight, high corrosive resistance, and easy processing [1]. However, the thermal conductivity of neat polymer is usually lower than that of the ceramics and metal as shown in Table 1.1.

Table 1.1 Thermal conductivity of materials

Material	Thermal conductivity (W/m-K)	Ref.
Copper (Cu)	400	[2]
Boron nitride (BN)	275	[2]
Aluminum (Al)	230	[3]
Aluminum nitride (AlN)	200	[2]
Polybenzoxazine/78.5% BN (225 μm)	32.5	[4]
Polypropylene/60% Al (125 μm)	4.12	[5]
Polypropylene/40% Cu (40 μm)	2.14	[5]
HDPE/26% Al oxide	1.65	[6]
HDPE/24% Cu	1.07	[6]
High density polyethylene (HDPE)	0.44	[7]
PS/10% AlN (<10 μm)	0.33	[8]
Polypropylene (PP)	0.24	[5]
Polystyrene (PS)	0.14	[7]

Note: Concentration of filler is in percent by volume.

The materials used in the electronic devices should possess the high thermal conductivity to protect the damage of the devices from the heat generated inside the

devices themselves [3, 9]. Thus the thermal conductivity of the polymer materials have to be enhanced. This is a technological progress in the field of the thermal management for the electrical and electronic devices [10]. A simple method for improving the thermal conductivity of the polymer materials is to prepare them as the composite by adding the thermally conductive filler, such as graphite, carbon black, carbon fiber, ceramic particles, and metal particles, into the polymers [11]. By this method, the polymer composite that conducts the heat well and is an electrical insulator can be prepared. However, the thermal conductivity of the composite depends on many factors such as shape, size, and content of filler particles as shown by the experimental data depicted in Figure 1.1. Thus, it is essential to understand the effect of those factors to successfully design the highly thermal conductive materials.

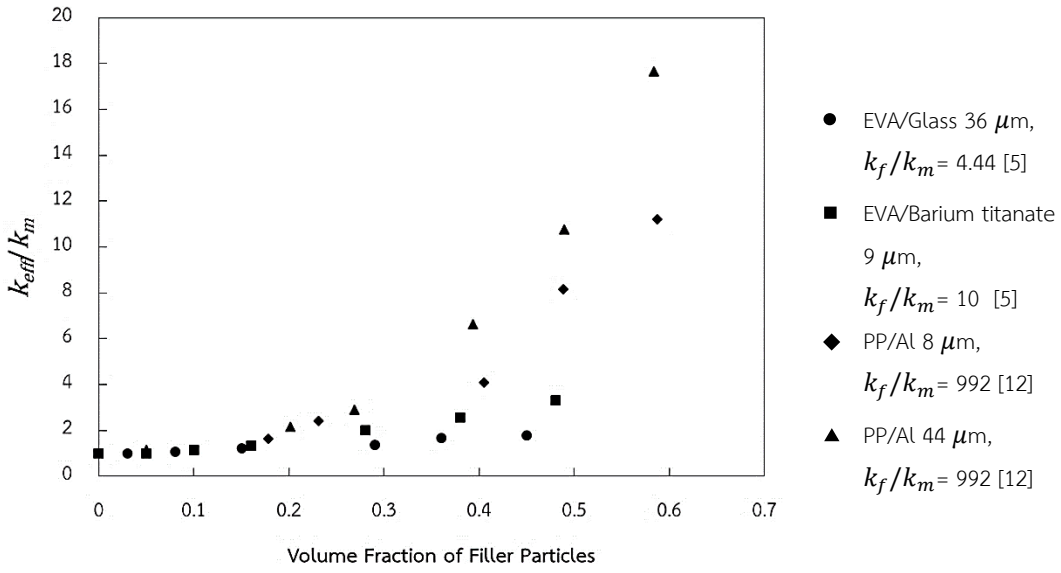

Figure 1.1 Relationship between the effective thermal conductivity and the volume fraction of filler particles where k_f is thermal conductivity of filler, k_m is thermal conductivity of polymer matrix, and k_{eff} is effective thermal conductivity

The modelling of the thermal conductivity of the composite is a way to understand the effect of such factors on the thermal transport in the composite. Many researches paid the attention to develop the analytical models that were classified into theoretical model [13-18], empirical model [13], and semi-empirical model [19].

Furthermore, the theoretical model can be classified into two classes depending on their solution method, i.e., exact and simplified solutions [20]. For example, Maxwell model [13] and Bruggeman model [13] are classified as the exact solution, while Cheng and Vachon model [14] and Liang and Liu model [15] are classified as the simplified solution. As frequently found, those models gave the prediction in good agreement with the experimental data only at some range of filler content, especially at low filler loading [21]. In addition, the numerical models were presented by applying the numerical methods [22, 23]. However, the analytical models are preferred more because they possess more physical meaning, simpler calculation, and lower cost in calculation than the numerical models [24, 25].

The comparison between the experimental data and the theoretical models as shown in Figure 1.2. indicated that the basic theoretical models, namely series and parallel models, cannot give the appropriate prediction due to the complicated structure of the composites [26]. Other more complicated theoretical models showed more possibility to fit the experimental data but there is no single model that can precisely fit the curve. In addition, these models cannot describe the effect of the particle size on the thermal conductivity of the composites. This led to the effort to modify the analytical models in many researches [27-31].

A cause of the deviation of the classical model comes from the fact that these models were focused on the idealized case of perfect interface contact between the matrix and the filler particles. However, even though the interface contact is perfect, a temperature drop usually occurs at the interface. This phenomena was first discovered by Kapitza at a boundary between liquid helium and metals [32]. This disturbance of the heat flow can be explained by means of the interfacial thermal resistance. This thermal resistance is due to the scattering of heat carriers (phonon or electron) at the interface of both materials which have the differences in vibrational and electronic properties [33]. Many experiments revealed that the interfacial thermal resistance had a dramatical effect on the effective thermal conductivity of the composites [31]. The theoretical models which included the effect of the interfacial thermal were presented by using the Kapitza radius concept [27, 31, 34]. By this way, the effect of the particle size was automatically incorporated into the models. These

modified models showed the potential for describing the effect of the interfacial thermal resistance and particle size on the effective thermal conductivity [27, 31]. However, only the theoretical models based on the exact solution were modified.

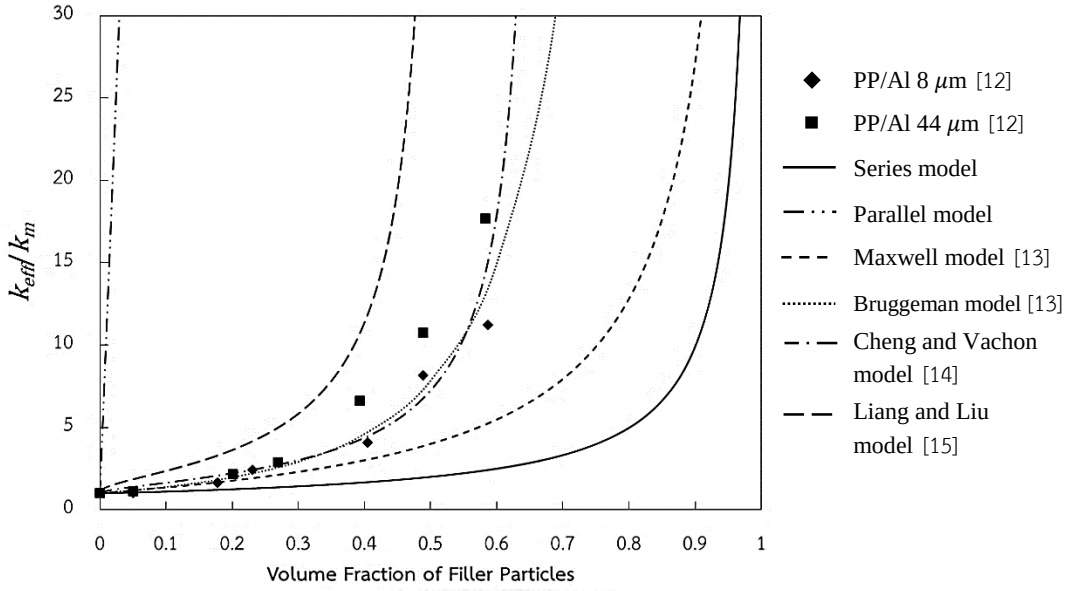

Figure 1.2 Comparison between the experimental data and the prediction by the analytical models of composite thermal conductivity where k_m is thermal conductivity of polymer matrix, and k_{eff} is effective thermal conductivity

It was therefore interesting to modify the theoretical model based on the simplified solution to include the effect of the interfacial thermal resistance and the particle size. Due to the simplicity of the simplified solution, it was further expected that the effect of the interfacial thermal resistance and the particle size may be easier to be included and understood. This work was organized as follows. First, the effective thermal conductivity models were derived based on the simplified solution and then their performance were investigated. Second, the suitable model were modified by applying the Kapitza radius concept and the effect of the interfacial thermal resistance and particle size on the effective thermal conductivity were discussed.

1.2 Objectives

This work aimed to develop the thermal conductivity model based on the simplified solution and to include the effect of the interfacial thermal resistance between the matrix and filler particles and to examine the possibility to use this modified model to predict the thermal conductivity of the polymer composite.

CHAPTER 2
THEORY

2.1 Thermal Property of Solid Material

Thermal property is the response of the material to heat. While solid material absorbs energy in the form of heat, its temperature and volume will increase. The difference of temperature between any positions in the bulk of material causes the heat transport phenomena. Energy is always transferred from high- to low-temperature regions of material. There are three mechanisms of heat transport, i.e. conduction, convection, and radiation. In case of heat transport in solid, only heat conduction will be considered.

2.1.1 Heat Conduction

Heat conduction or thermal conduction is the phenomenon in which heat is transferred from a hot section to a cool section of material by molecular mechanism. The simple relationship between the rate of heat transfer and temperature gradient for steady state heat conduction through a solid in one-dimension (*x*-dimension) is

$$q_x = -k\frac{dT}{dx} \tag{2.1}$$

where q_x is the local rate of heat flow per unit area (heat flux) in the positive x direction. The minus sign in the expression (2.1) indicates that the direction of heat flow is from hot region to cold region or down the temperature gradient [35]. This Eq. (2.1) is called Fourier's law of heat conduction.

The three-dimensional form of Fourier's law is expressed as

$$\boldsymbol{q} = -k\boldsymbol{\nabla}T \tag{2.2}$$

where $\boldsymbol{q}$ is the heat flux vector and $\boldsymbol{\nabla}T$ is the gradient of temperature. For the Cartesian coordinate system $\boldsymbol{\nabla}T$ is given by

$$\boldsymbol{\nabla} T = \frac{\partial T}{\partial x}\boldsymbol{s}_x + \frac{\partial T}{\partial y}\boldsymbol{s}_y + \frac{\partial T}{\partial z}\boldsymbol{s}_z \tag{2.3}$$

where $\boldsymbol{s}_x$, $\boldsymbol{s}_y$, and $\boldsymbol{s}_z$ are the unit vectors.

This Eq. (2.2) describes the molecular transport of heat in isotropic media. The word "isotropic" means that the properties of material is uniform in all directions; therefore, heat is conducted with the same thermal conductivity in all directions [36].

Considering a stationary volume element of solid as a system, heat may enter and leave the system by heat conduction and internal energy of system may be changed. Because of a stationary solid, rate of kinetic and internal energy addition by convective transport and rate of work done on system by molecular mechanisms and external forces can be omitted. Thus, the equation of change for temperature for a stationary solid can be expressed as follows:

$$\rho \hat{C}_p \frac{\partial T}{\partial t} = k\boldsymbol{\nabla}^2 T \tag{2.4}$$

Eq. (2.4) is the heat balance equation for solid [36].

2.1.2 Heat Conduction Mechanism and Thermal Conductivity

The conduction heat transfer is the carrying of heat by molecular contact among molecules in thermal nonequilibrium. For solids, conduction occurs between adjacent molecules by propagation of the quantized lattice-vibrational waves which is called phonon heat carriers, or by the drift and collision of free electrons which is called electron heat carriers. These are described by phonon and electron mean-free paths (λ_p and λ_e). The mean-free path is the average distance traveled between these collisions. In conduction, the ability of the heat carriers to move in the medium, before a significant loss of their heat content, makes them effective heat carriers. Since the heat losses occur during collisions, the longer the length between collisions, the longer the mean-free path and the higher the heat transfer rate [37].

Thermal conductivity is a transport or nonequilibrium property of a material that characterizes the ability of a material to transfer heat per unit of time and per unit of area and in the presence of a unit temperature difference (ΔT) over a unit length (Δx) within the medium. Thermal conductivity has a unit of J-m/s-m^2-K or W/m-K. The thermal conductivity depends on the ability of micro heat carriers, i.e. phonon and electron, of heat to travel to exchange this heat [37]. This travel is in the form of fluctuations or random-motion displacement about an equilibrium location. The ability to transfer heat by conduction is related to the ability of electrons and holes for metallic and semimetallic solids, and phonons for solids (dominant in nonmetals) to store and release thermal energy, and the ability of the electrons and phonons to travel before losing their energy.

For heat conduction in solid, electrons and phonons are the micro heat carriers. To point out the roles of the conduction electrons and the phonons, an electrical classification of solids (metals, nonmetals, and semiconductors) is used. The conduction electrons play a significant role in conducting heat for the solid metals due to their large number of conduction electrons. The thermal lattice vibration or phonons are the main heat conduction carrier for nonmetals (electrical insulators). The semiconductors have an intermediate electrical behavior between metals and nonmetals, however, their thermal conduction is similar to nonmetals [37].

I) Metals

Metals have a large number of conduction or free electrons (larger than 10^{22} conduction electrons/cm^3) because the atomic binding in crystalline metals reduces the energy of the valence electrons as compared to electrons in free atoms and makes a large number of valence electrons free to move [37]. The high thermal conductivity of metals is due to the acceleration of the conduction electrons in the presence of a temperature gradient and it is closely related to their high electrical conductivity σ_e (1/ohm-m). The accelerated conduction electrons are stopped when the electrons collide with atoms in the crystal, with other electrons, or with other heat carriers. The average distance traveled between collisions is the mean-free path of the electron λ_e. The approximate electrical conductivity due to free electrons is given by

$$\sigma_e = \frac{n_e e_c^2 \lambda_e}{m_e u_e} \tag{2.5}$$

where n_e is the number of free electrons per unit volume (number of electrons/m^3), e_c is the electron charge (Coulomb), m_e is the electron mass (kg), and u_e is the mean electron speed (the carrier group velocity) (m/s) [37]. The ratio between λ_e and u_e is called the electron residence time τ_e (or electron relaxation time, s).

By assuming the temperature-gradient accelerated electrons travel the same average distance, i.e. mean-free path, before transferring their excess thermal energy to the atoms, the free electron thermal conductivity k_e is expressed as

$$\begin{aligned} k_e &= \frac{1}{3} n_e \hat{C}_{v,e} u_e \lambda_e \\ &= \frac{1}{3} n_e \hat{C}_{v,e} u_e^2 \tau_e \end{aligned} \tag{2.6}$$

where $\hat{C}_{v,e}$ is the specific heat capacity of each electron (J/electron-K) [37]. The value of $\hat{C}_{v,e}$ and λ_e depend on the temperature and λ_e may be much larger than the intermolecular spacing. In addition, the electron mean-free path (or relaxation time) is influenced by the electron-electron, electron-phonon, and electron-lattice defect scattering mechanisms [37]. From the quantum-statistical mechanics, the relation between electrical and thermal conductivity for free electrons is given in the form of Wiedemann-Franz law as

$$\frac{k_e}{\sigma_e T} = \frac{\pi^2}{3}\left(\frac{k_b}{e_c}\right)^2 = 2.442 \times 10^{-8} \text{ W-ohm/K}^2 \tag{2.7}$$

where T is the absolute temperature and k_b is the Boltzmann constant. Eq. (2.7) shows that the ratio of k_e and $\sigma_e T$ is a constant. This equation holds well for the pure metals.

II) Nonmetals

Due to the absence of conduction electrons in solid nonmetals because the electron conduction-gap energy is large, the heat conduction is dominated by nonelectronic heat carriers. The presence of temperature gradient in the solid causes a nonuniform elastic thermal lattice vibration that transfers heat in form of vibrational energy along the solid. This heat carrier is phonon. In analogy with photons of electromagnetic waves, phonons are the quanta of energy in each mode of vibration traveling in the solid phase. The solid lattice is characterized as crystalline with periodic structure or amorphous with nonperiodic structure. The phonon internal energy is the sum of energy in all possible vibrational states and all polarizations. The vibration frequencies, which are associated with the concerted harmonic motion of all atoms and are called the normal modes, are orders of terahertz (10^{12} Hz) [37]. The lattice or phonon thermal conductivity can be expressed as

$$k_p = \frac{1}{3}\rho \hat{C}_{v,l} u_p \lambda_p \tag{2.8}$$

where ρ is the density of solid material, $\hat{C}_{v,l}$ is the lattice specific heat capacity, u_p is mean phonon velocity (also called lattice heat-carrier group velocity), and λ_p is the phonon mean-free path (also called heat-carrier mean-free path) [37]. The mean phonon velocity u_p can be determined as the speed of sound in the solid state (a_s), thus it is called “acoustic phonons”. The plane longitudinal wave speed is generally used, however, the average phonon speed is also used and is defined as

$$3u_p^{-3} = 2u_{p,t}^{-3} + u_{p,l}^{-3} \tag{2.9}$$

where subscript t denotes the two transverse and l denotes the single longitudinal wave speeds [37]. The mean-free path of the phonons is temperature and defect dependent. Around the room temperature, the interphonon collisions are significant. At low temperatures, the interphonon interactions become less significant and the electron-lattice-defect and boundary scattering (elastic and inelastic) become

important [37]. The mean free path is the most important parameter related to the thermal conductivity. If the size of the system is greater than the mean free path, scattering events will happen. But if the mean free path is greater than the system size, no scattering event can occur prior to reaching the ends of the system [35].

Polymer is classified as a nonmetal. The thermal conductivities for most polymers are on the order of 0.3 W/m-K [35]. These materials possess the lowest thermal conductivities compared with metals and nonmetals. Heat transport in polymers is accomplished by the vibration and rotation of the chain molecules. The main thermal energy carriers are the phonons [38]. In contrast to ceramics or nonmetals, the conduction is carried out with extremely small phonons mean free path, i.e. a few angstroms, owing to their scattering from many defects, leading to a very low thermal conductivity [38]. The magnitude of the thermal conductivity depends on the degree of crystallinity. A polymer with a highly crystalline and ordered structure will have a better conductivity than the equivalent amorphous materials because of the better effective coordinated vibration of the molecular chains for the crystalline state [35]. In addition, the thermal conductivity of polymer depends on many factors such as chemical composition, strength of chemical bond, type of structure, side group, molecular weight, molecular weight distribution, defects in structure, processing condition, and temperature [7]. The thermal conductivity of polymeric materials can be improved by adding high thermally conductive materials such as Cu, Al, and Si [12, 39].

III) Semiconductors

Semiconductors (e.g., Ge, Si) have conduction electron less than 10^{17} conduction electron/cm^3. Their thermal conductivity is involved with the electrons k_e and the lattice vibration k_p, and the total conductivity is the sum of the two contributions as expressed by

$$k = k_e + k_p \tag{2.10}$$

A semiconductor is intrinsic when it has no imperfections and its electronic properties are dominated by electrons thermally excited from valence to conduction band. Semiconductors (e.g., Si) are made impure by adding other elements such as P, As, and Sb; this is called doping and the resulting materials are called an extrinsic materials. If impurities can provide free electrons, they are called donor elements and the resulting material is called the *n*-type because the electrical conduction is by electrons. In contrast, if these impurities are deficient in electrons, they are called acceptor elements and the resulting material is called the *p*-type because the electrical conduction is by hole. Electrons and holes are the electronic contributions in semiconductors. However, the thermal conductivity of semiconductors is generally dominated by phonon. The presence of impurities (dopants) can increase or decrease the thermal conductivity depending on the extent of the extra scattering caused by the impurities [37].

2.1.3 Thermal Resistance and Electrical Circuit Analogy

The analogy between electrical and heat conduction is based on the fundamental similarity between voltage and temperature, current conduction and heat conduction. Electrical conduction occurs in response to a voltage difference while heat conduction occurs in response to a temperature difference. Starting with heat conduction in only one direction (e.g., x direction) through a thin slab with a uniform conduction cross-sectional area A, the heat flux q_x is constant along x axis for the case of no energy conversion. This is shown in Figure 2.1(a). Assuming that heat conduction is steady-state and thermal conductivity k does not vary with x, Eq. (2.4) can be written as

$$k\frac{d^2T}{dx^2} = 0 \tag{2.11}$$

Eq. (2.11) is integrated to give

$$T(x) = a_1 x + a_2 \tag{2.12}$$

where a_1 and a_2 are the integration constants. The boundary conditions are determined by the prescribed temperature on the bounding surface as

$$T(x = 0) = T_1, T(x = \Delta x) = T_2 \tag{2.13}$$

Using the boundary conditions in Eq. (2.12), both integration constants are solved, and the results are

$$a_1 = \frac{T_2 - T_1}{\Delta x} \tag{2.14}$$

and

$$a_2 = T_1 \tag{2.15}$$

Substituting for a_1 and a_2 in Eq. (2.12), the temperature distribution is given as

$$T(x) = T_1 + \frac{T_2 - T_1}{\Delta x} x \tag{2.16}$$

Eq. (2.16) describes a linear distribution of temperature along the x axis. The heat flux at any location x is determined by

$$q_x = -k \frac{dT}{dx} = -k \frac{T_2 - T_1}{\Delta x} \tag{2.17}$$

Eq. (2.17) indicates that q_x is uniform throughout the planar layer which perpendicular to x axis. For any locations x and $x + \Delta x$, the heat flux can be written as

$$q_x = -k\frac{dT}{dx} = -k\frac{T(x+\Delta x) - T(x)}{\Delta x} \tag{2.18}$$

The heat flow rate Q_x is the product of the heat flux q_x and the cross-sectional area A through which heat is transferred as

$$Q_{x,1-2} = Aq_x = -Ak\frac{T_2 - T_1}{\Delta x} = \frac{T_1 - T_2}{\frac{\Delta x}{Ak}} = \frac{\Delta T}{\frac{\Delta x}{Ak}} \tag{2.19}$$

where the subscript $1-2$ means the heat transfers from the wall on side 1 to the wall on side 2 as shown in Figure 2.1. Since it is a one-dimensional heat flow, the subscript x can be neglected.

Eq. (2.19) is the Fourier law in terms of a linear, one-dimensional temperature distribution that can be compared to the Ohm law. By considering an electric current flow J_e when an electrical potential $\Delta\varphi$ or $\varphi_1 - \varphi_2$ is applied across a conductor of thickness Δx with an electrical conductivity σ_e, and a cross-section area A, the relationship of these parameters can be written as

$$J_{e,1-2} = \frac{\Delta\varphi}{R_{e,1-2}} = -\frac{\varphi_2 - \varphi_1}{\frac{\Delta x}{\sigma_e A}} \tag{2.20}$$

where $R_{e,1-2}$ is the electrical resistance. It is worth to notice that Eq. (2.19) is similar to Eq. (2.20). Based on this analogy, the thermal resistance R_{1-2} (°C/W or K/W) can be defined as

$$R_{1-2} \equiv \frac{T_1 - T_2}{Q_{1-2}} = \frac{\Delta x}{Ak} \tag{2.21}$$

Eq. (2.21) is the heat conduction resistance for a slab. The thermal resistance is the measure of the temperature difference needed for the flow of one Watt of thermal energy through a layer of thermal conductivity k, thichness Δx, and area A. The magnitude of thermal resistance is between zero (ideal conductor) and infinity (ideal insulator) and it is always positive, i.e., $0 \leq R \leq \infty$. The thermal circuit model is also shown in Figure 2.1(b). The inverse of the thermal resistance is the thermal conductance h (W/°C) as expressed as

$$h = \frac{Ak}{\Delta x} \tag{2.22}$$

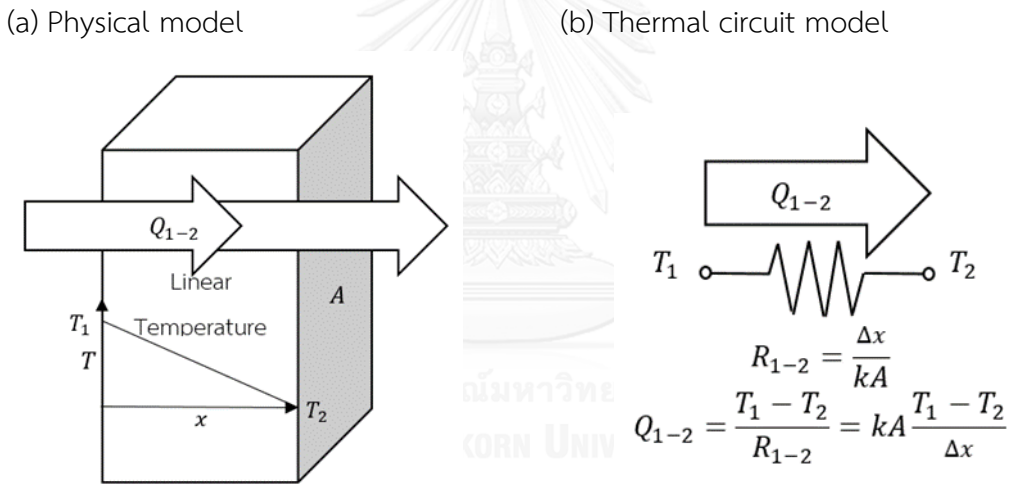

Figure 2.1 (a) A physical model of one-dimensional steady-state conduction through a slab and (b) Thermal circuit model for this conduction heat transfer (adapted from [37])

Composite is made of two or more distinct materials. Its thermal conductivity and thermal resistance can be determined by the inclusion of the resistance for each element of the composite. Composite can be divided into layered and nonlayered structures. The layers can be perpendicular to the heat flow direction, resulting in the series arrangement of the resistances. In contrast, the layers can be parallel to the

heat flow direction and this is called parallel arrangement of resistances. The rendering of these arrangements are shown in Figure 2.2(a). For nonlayered composite, one of materials is continuous and the others can be continuous or discontinuous in one or more directions. Figure 2.2(b) shows some examples of nonlayered composites.

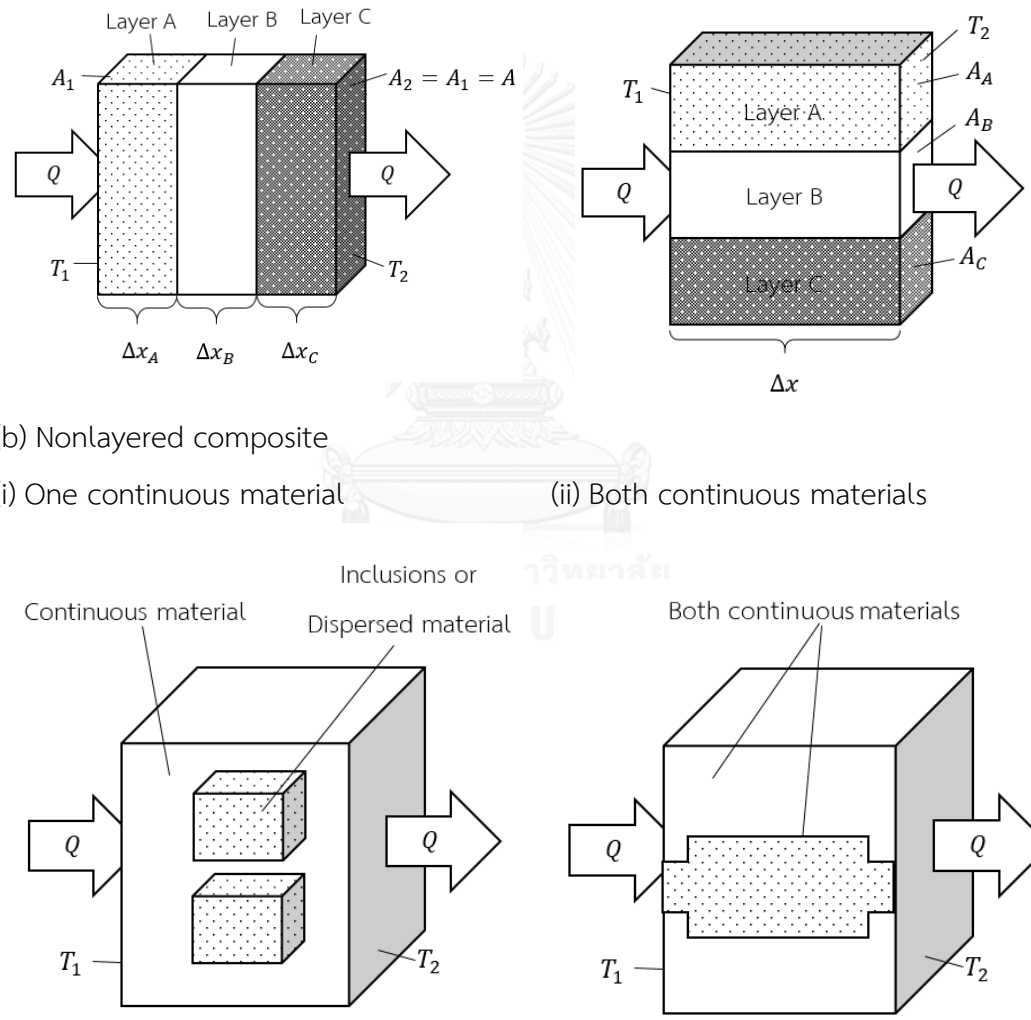

Figure 2.2 Schematic of (a) layered composite and (b) nonlayered composite (adapted from [37])

Considering a composite composed of three materials arranged in series as shown in Figure 2.3, the heat flows perpendicular to the interfaces. The heat flows out of the surface to the left as designated by $-Q_1$ and to the right as designated by $Q_{1-1'}$. The energy equation for surface node T_1 at steady state is written as

$$-Q_1 + Q_{1-1'} = 0 \text{ or } Q_1 = Q_{1-1'} \tag{2.22}$$

Likewise, this can be done for all surface nodes. Then the energy equations for each of the surface shown in Figure 2.3 are listed below.

$$-Q_1 + Q_{1-1'} = 0 \quad \text{for surface node } T_1 \tag{2.23a}$$
$$-Q_{1-1'} + Q_{1'-2'} = 0 \quad \text{for surface node } T_{1'} \tag{2.23b}$$
$$-Q_{1'-2'} + Q_{2'-2} = 0 \quad \text{for surface node } T_{2'} \tag{2.23c}$$
$$-Q_{2'-2} + Q_2 = 0 \quad \text{for surface node } T_2 \tag{2.23d}$$

From Eq. (2.23a) to (2.23d), it is found that

$$Q_1 = Q_{1-1'} = Q_{1'-2'} = Q_{2'-2} = Q_2 = Q_{1-2} \tag{2.24}$$

It should be noted that same heat flow rate Q_{1-2} flows through each resistance.

For each resistance, the heat flow can be expressed as

$$Q_{1-1'} = Q_{1-2} = -\frac{Ak_A}{\Delta x_A}(T_{1'} - T_1) = \frac{T_1 - T_{1'}}{\frac{\Delta x_A}{Ak_A}} = \frac{T_1 - T_{1'}}{R_{1-1'}} \tag{2.25}$$

$$Q_{1'-2'} = Q_{1-2} = -\frac{Ak_B}{\Delta x_B}(T_{2'} - T_{1'}) = \frac{T_{1'} - T_{2'}}{\frac{\Delta x_B}{Ak_B}} = \frac{T_{1'} - T_{2'}}{R_{1'-2'}} \tag{2.26}$$

$$Q_{2'-2} = Q_{1-2} = -\frac{Ak_C}{\Delta x_C}(T_2 - T_{2'}) = \frac{T_{2'} - T_2}{\frac{\Delta x_C}{Ak_C}} = \frac{T_{2'} - T_2}{R_{2'-2}} \tag{2.27}$$

$T_{1'}$ is solved by rearranging Eq. (2.25), and the result is

$$T_{1'} = T_1 - \frac{Q_{1-2}\Delta x_A}{Ak_A} \tag{2.28}$$

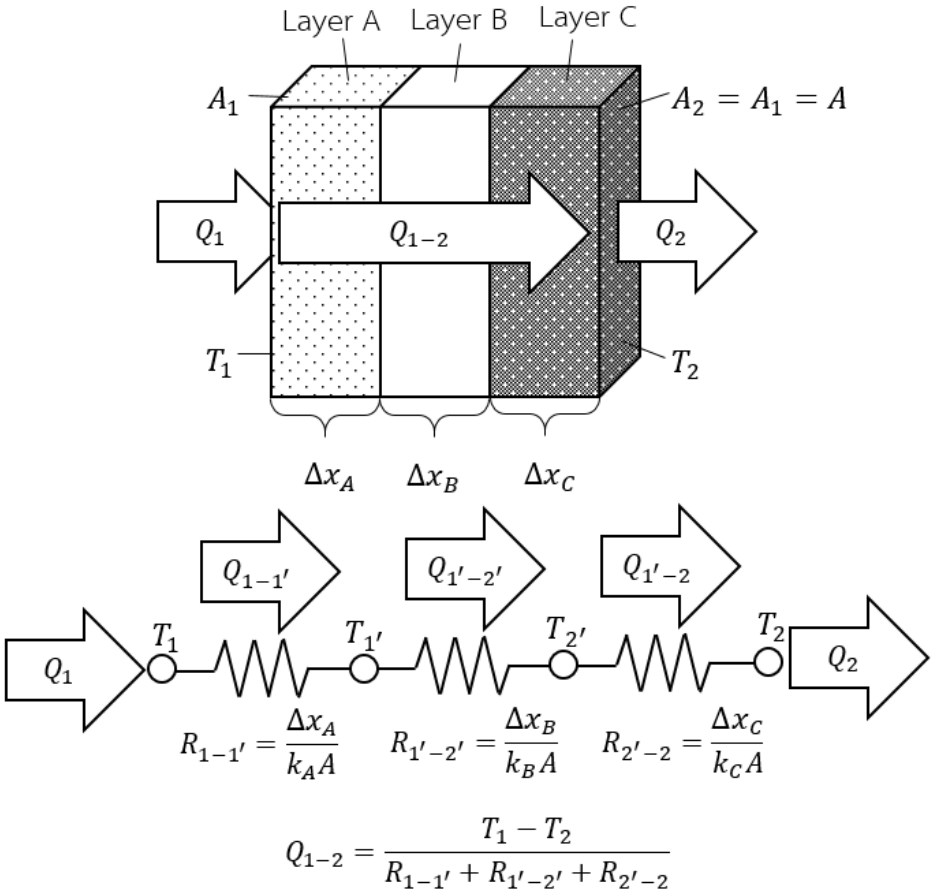

Figure 2.3 Illustration of physical model and thermal circuit model for series layered-composite (adapted from [37])

In the same manner, the result for $T_{2'}$ from Eq. (2.26) and when using Eq. (2.28) is

$$T_{2'} = T_{1'} - \frac{Q_{1-2}\Delta x_B}{Ak_B} = T_1 - \frac{Q_{1-2}\Delta x_A}{Ak_A} - \frac{Q_{1-2}\Delta x_B}{Ak_B} = T_1 - Q_{1-2}\left(\frac{\Delta x_A}{Ak_A} + \frac{\Delta x_B}{Ak_B}\right) \quad (2.29)$$

The result for T_2 from Eq. (2.27) and when using Eq. (2.29) is

$$T_2 = T_{2'} - \frac{Q_{1-2}\Delta x_C}{Ak_C} = T_1 - Q_{1-2}\left(\frac{\Delta x_A}{Ak_A} + \frac{\Delta x_B}{Ak_B} + \frac{\Delta x_C}{Ak_C}\right) \quad (2.30)$$

Eq. (2.30) is rearranged into the form of the temperature difference across the three layers as $T_1 - T_2$ and then using the definition of thermal resistance given by Eq. (2.21), the heat flow through the composite can be expressed as

$$Q_{1-2} = \frac{T_1 - T_2}{\frac{\Delta x_A}{k_A A} + \frac{\Delta x_B}{k_B A} + \frac{\Delta x_C}{k_C A}} = \frac{T_1 - T_2}{R_{1-1'} + R_{1'-2'} + R_{2'-2}} \quad (2.31)$$

Eq. (2.31) indicates that for this layered arrangement of layers perpendicular to the heat flow, the thermal resistances are added as series resistances with the temperature difference across the composite as the potential. This series arrangement of resistances is shown in Figure 2.3.

For n layers placed perpendicular (series arrangement) to the heat flow between surface 1 and 2, it can be generalized as

$$Q_{1-2} = \frac{T_1 - T_2}{\sum_{i=1}^{n} R_i} \equiv \frac{T_1 - T_2}{R_\Sigma}, \; R_\Sigma \equiv \sum_{i=1}^{n} R_i \quad \text{series resistances} \quad (2.32)$$

where R_Σ is the overall conduction resistance for the composite.

In the other way, layers can be arranged in parallel to form layered composite as shown in Figure 2.4. In this case, there are three heat flow rates. For surface nodes 1 and 2, the energy equation can be written as

$$-Q_1 + Q_{1-2,A} + Q_{1-2,B} + Q_{1-2,C} = 0 \quad \text{for surface 1} \tag{2.33}$$

$$-Q_{1-2,A} - Q_{1-2,B} - Q_{1-2,C} + Q_2 = 0 \quad \text{for surface 2} \tag{2.34}$$

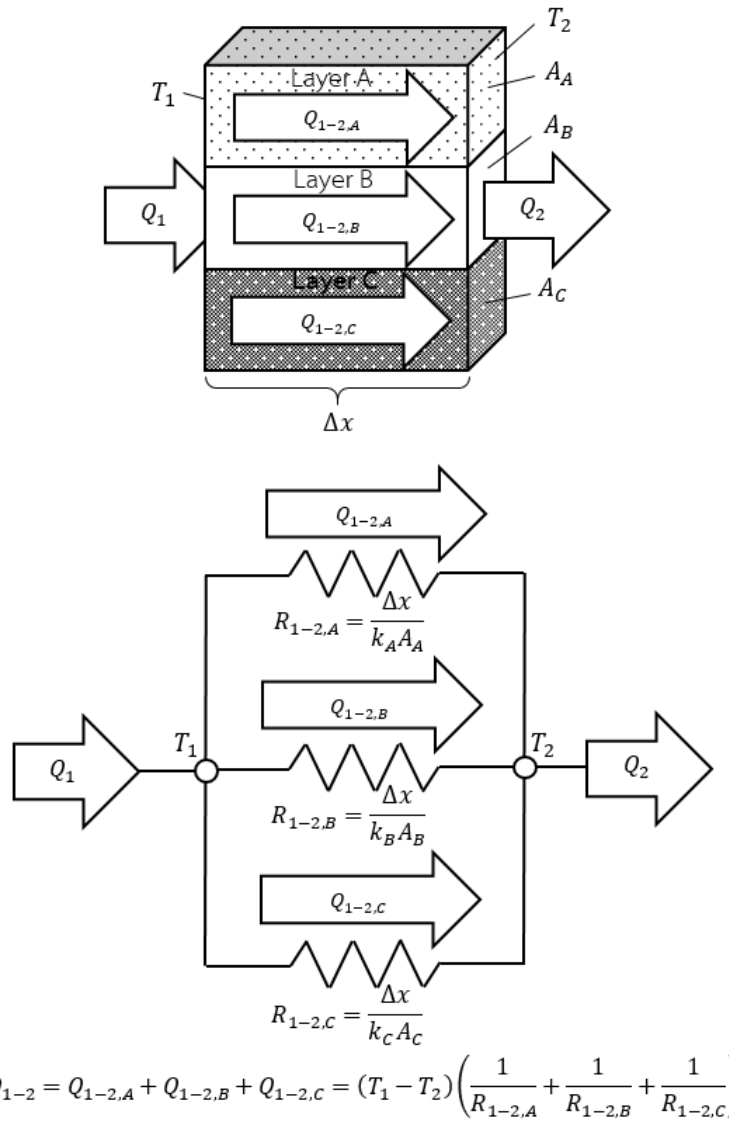

Figure 2.4 Illustration of physical model and thermal circuit model for parallel layered-composite (adapted from [37])

Then from Eq. (2.33) and (2.34), it can be shown that

$$Q_1 = Q_2 = Q_{1-2,A} + Q_{1-2,B} + Q_{1-2,C} \equiv Q_{1-2} \tag{2.35}$$

Using the definition of thermal resistance given by Eq. (2.21), the heat flow through the composite can be expressed as

$$\begin{aligned} Q_{1-2} &= Q_{1-2,A} + Q_{1-2,B} + Q_{1-2,C} \\ &= \frac{T_1 - T_2}{\frac{\Delta x}{A_A k_A}} + \frac{T_1 - T_2}{\frac{\Delta x}{A_B k_B}} + \frac{T_1 - T_2}{\frac{\Delta x}{A_C k_C}} \\ &= (T_1 - T_2)\left(\frac{1}{\frac{\Delta x}{A_A k_A}} + \frac{1}{\frac{\Delta x}{A_B k_B}} + \frac{1}{\frac{\Delta x}{A_C k_C}} \right) \end{aligned} \tag{2.36}$$

For *n* layers placed parallel to the heat flow, in parallel arrangement, the heat flow equation can be generalized as

$$Q_{1-2} = (T_1 - T_2) \sum_{i=1}^{n} \frac{1}{R_i} \equiv \frac{T_1 - T_2}{R_\Sigma}, \quad \frac{1}{R_\Sigma} = \sum_{i=1}^{n} \frac{1}{R_i} \quad \text{parallel resistances} \tag{2.37}$$

For nonlayered composite, there are many geometric variations where a material A is in a nonlayered arrangement with another material B. One material or more than one materials can be continuous, called continuous phase and co-continuous phase, respectively. While one of the materials can be dispersed or discontinuous in a continuous phase. In the case of composite composed of two materials, it can be thought that its structure is ordered periodic arrangement with one of the materials being discontinuous. This is also called ordered lattice. It is assumed that there are many of unit cells arranged in a periodic arrangement and local thermal equilibrium over a unit cell exists. An example is shown in Figure 2.5. The regular arrangement of dispersed spherical inclusions of diameter D in a square array

arrangement with the distance between centers of the adjacent spheres being l. Assuming a one-dimensional heat flow with parallel-series arrangement of the resistances in each unit cell, the thermal circuit model for each unit cell can be used for calculating the heat flow by the same method described above.

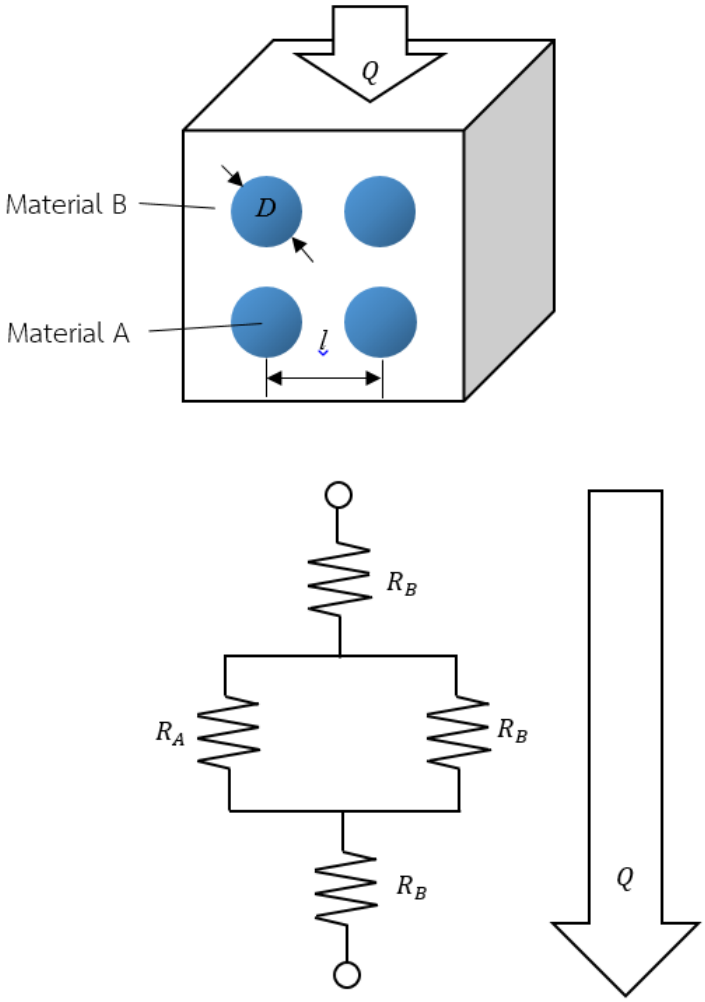

Figure 2.5 Physical model and thermal circuit model of square array of spherical inclusions (adapted from [37])

2.1.4 Interfacial Thermal Resistance

The idea of interfacial thermal resistance or thermal boundary resistance between two materials has been studied for a long period [32]. It is known as interfacial thermal resistance and refers to the combined effect of two thermal resistances, namely thermal contact resistance and thermal boundary resistance [33]. Thermal contact resistance is caused by poor mechanical and chemical bonding between constituent phases while thermal boundary resistance occurs due to differences in the physical properties of constituent materials [33]. This latter thermal resistance is also called Kapitza resistance in memory of P. Kapitza who was the first to discover a temperature drop at a boundary between liquid helium and metals in 1941 [32]. The interfacial thermal resistance (R_{int}) with a unit of m^2K/W can be defined as the ratio of the temperature difference at the interface ΔT to the heat flow rate Q per unit area A flowing across that interface [32, 33]:

$$R_{int} = \frac{\Delta T}{\frac{Q}{A}} = \frac{\Delta T}{q} \tag{2.38}$$

The difference in the physical properties of contacting materials causes the interfacial thermal resistance and leads to the temperature drop at the interface [40]. For example, a schematic of temperature profile for Si/Ge interface at a temperature of 500 K obtained from molecular dynamics simulations was shown in Figure 2.6. Heat is transferred in a solid by phonon transport or electronic transport as described previously. Because of different vibrational and electronic properties of each medium (material), a heat carrier in form of electron or phonon, arriving at the interface, reaches a physical end of the medium in which it originally propagates and must fulfill certain requirements to continue its propagation in the other medium, and there will be only some heat carriers that can pass the interface, although the mechanical contact between the two phases is perfect [40]. This makes the thermal boundary resistance different from the thermal contact resistance.

The interfacial thermal resistance may result from interdiffusion or corrosion of composite components, particle coating, particle electrochemical treatment, and moisture absorption. Poor adhesion causes imperfect mechanical contact and also increases the interfacial thermal resistance in term of thermal contact resistance. Furthermore, thermal expansion mismatch between constituents may lead to the formation of gas-filled gaps in the interfacial region; this gaps act as thermal resistance [33].

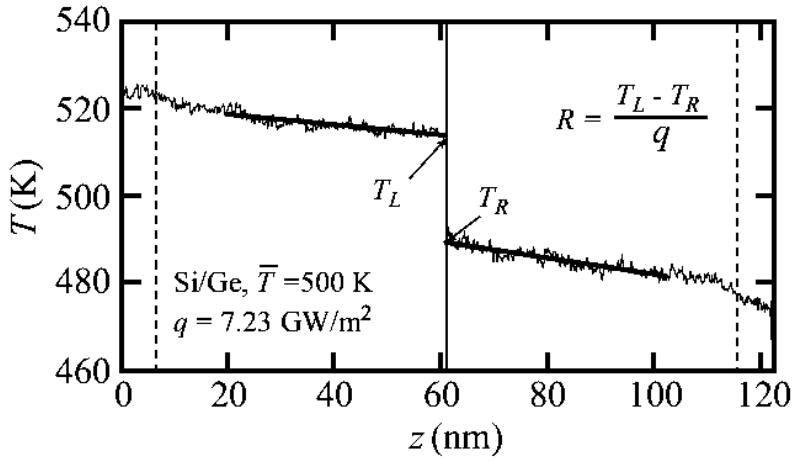

Figure 2.6 Temperature profile for the Si/Ge interface at an average temperature $\bar{T}$ of 500 K obtained from molecular dynamics simulation where T_L is temperature at interface of Si and T_R is temperature at interface of Ge [41]

The interfacial thermal resistance acts as a thermal barrier in composites. This negative effect increases when the filler particle size decreases, especially in high filler volume fraction as shown in Figure 2.7. This effect can be explained in terms of the interfacial thermal resistance which becomes increasingly dominant as the particles become smaller and have higher surface area to volume ratio [27]. The interfacial thermal resistance is an important parameter that affects the enhancement of the thermal conductivity of composites, especially in nanocomposites [13]. To determine the effective thermal conductivity of newly designed composites, it is essential to know the interfacial thermal resistance of those composites. The measurement of the interfacial thermal resistance can be separated into two types, i.e. direct method and

indirect method. However, there are many difficulties during interfacial thermal resistance measurement attempts due to the subtle nature of the phenomenon [40].

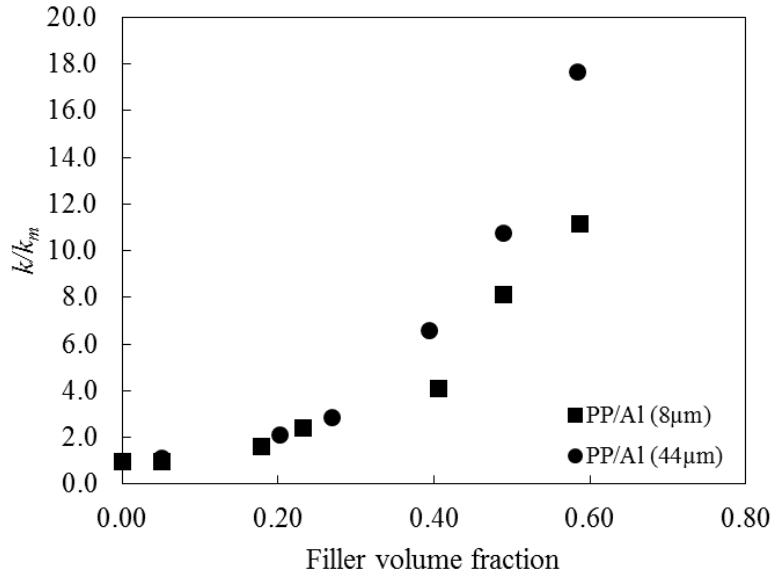

Figure 2.7 Relative thermal conductivity versus filler volume fraction of polypropylene filled with aluminum in form of spherical particles with average particle size of 8 μm and 44 μm (experimental data cited from [12])

2.2 Polymer Composites

Many modern technologies require materials with several special properties which may coexist in one. These are not found in typical materials. To response to the desirable requirement, composite materials are developed intensely. Composite is material with several phases, but at least 2 phases. The continuous phase is called “matrix”. The discontinuous phase surrounded by the matrix is called “dispersed phase” or “filler”. Each phase possesses innate property and different chemical structure which can be clearly separated. This makes the composite to have several properties depending on their composition. In addition, some properties of composites are better than the original materials. The whole properties of composites depend on type of original material, quantity and geometry of dispersed phase (shape and size), and distribution and orientation of dispersed phase [35].

2.2.1 Polymer Composite Preparation for Improving the Thermal Conductivity

There are several methods to prepare thermally conductive polymer composite. It depends on the type of matrix whether thermoplastic or thermoset. Furthermore, shapes of filler whether cylindrical, flake, or sphere usually also influence the processing method. However, all processing method has a similar purpose that is to gain the composite which has desirable property. The processing method should cause the uniform dispersion and distribution of filler without the fracture of filler. Especially in fiber filler, the fractured fiber has lower aspect ratio and incurs the decreasing in property. The satisfied processing method should make good interfacial between the matrix and filler. In addition, it should be able to control the orientation of filler particles and cause the anisotropic property as needed [2].

For thermoplastic, melt-mixing is very popular. The extruder and internal mixer are usually used in this method. Solvent casting is alternative method for filler coated with thermally sensitive chemical. After preparation, prepared composite is formed as specimen by compression or injection molding machine [2].

2.2.2 Thermally Conductive Fillers

The thermal conductivity of polymer can be improved by adding thermally conductive fillers such as graphite, carbon black, carbon fibers, ceramic particles and metal particles. The thermal conductivities of those materials depend on their purity, crystallinity, size of particle, or even the measurement technique. Especially in fiber or cylindrical filler, the axial thermal conductivity is normally higher than the transverse thermal conductivity [11]. The fillers used for improving the thermal conductivity of polymeric material are divided as three types, namely carbon-based fillers, metallic fillers, and ceramic fillers [11].

I) Carbon-based Fillers

Carbon-based filler is one of the appropriate fillers to improve the thermal conduction of polymeric materials due to their high thermal conductivity and low

weight. Typical carbon-based fillers are graphite, carbon fiber, and carbon black. Graphite is the best filler due to high thermal conductivity, affordability, and very good dispersion in polymer matrix. In one layer of graphite, graphene has the high thermal conductivity around 800 W/m-K or more than 5,300 W/m-K theoretically. However, graphite normally has the thermal conductivity of 100 to 400 W/m-K. The thermal conductivity of composite depends on the dispersion of graphite and its aspect ratio [11].

Carbon fiber is the hollow cylindrical filler. The axial thermal conductivity is different from the transverse thermal conductivity. The axial thermal conductivity is around 2000 W/m-K. The transverse thermal conductivity is around 10-110 W/m-K. Thus, the orientation of carbon fiber affects the thermal conduction of composite seriously [11].

II) Metallic Fillers

Metallic fillers may cause the increase in both of the thermal conductivity and electrical conductivity. Furthermore, the density of composite is increased. These are limitations for using this filler type. Metallic fillers for increasing the thermal conductivity are aluminum, silver, copper, nickel, etc. The efficiency of improving the thermal conductivity depends on the thermal conductivity of metallic particle, shape and size of particle, volume fraction, and orientation [11].

III) Ceramic Fillers

Ceramic fillers such as aluminum nitride, silicon carbide, beryllium oxide, etc., are widely used in electronics. They possess the interesting properties which are high thermal conductivity and electrical insulator. Their thermal conductivities depend on packing density, particle size, size distribution, and surface treatment [11].

2.3 Effective Thermal Conductivity Models

It is known that the thermal conductivity of polymer composite depends on several factors such as particle size and size distribution, volume fraction of filler, shape

of filler particle, dispersion state of fillers, interfacial thermal resistance , and so on [13, 42]. These factors make the thermal conductivity mechanism very complicated, especially for a highly filled system [42]. To interpret thermal measurement results and design materials for thermal applications, various theoretical, empirical, and semiempirical models have been developed with a variety of assumptions [13]. The result of modeling is a mathematical relationship involving at least the volume fraction and the properties of each component of composite [5]. Sundstrom and Lee [20] classified theoretical models into two classes depending on their solution method, i.e., exact or simplified solutions. In exact solution, the effective thermal conductivity is obtained by an analytical solution of the heat equation for a simple idealized geometry without any assumptions on heat flow or temperature patterns. The models are exact solutions such as Maxwell model [13] and Bruggeman model [43]. In contrast, simplified solutions generally assume that heat flow is unidirectional and isotherm planes are perpendicular to the heat flow. By this way, the problem is reduced to ordinary differential equation instead of a partial differential equation. Cheng and Vachon model [14] is a model derived from simplified solution. There is an alternative classification of thermal conductivity model that was proposed by Mottram [5, 26]. The models are divided into first, second, third and fourth order. First order models are the simplest model, i.e., series and parallel model. Most well-known models are organized in the second order group. The models that take into account the disturbance between the phases of the composites and the geometry of the inclusions are classified as the third and fourth order models. These models usually have a more complicated parameter, for example, the three-point parameter that take into account the statistical perturbation around each particle in Torquato model [44]. However, there are only a few models in the third and fourth order. In this section, some basic models of thermal conductivity based on exact and simplified solution were reviewed.

2.3.1 Model Based on Simplified Solution

2.3.1.1 Series Model

If two components arranged in series with respect to the heat flow direction, the effective thermal conductivity (k_{eff}) in this case can be written as

Series model: $$\frac{1}{k_{eff}} = \frac{v_m}{k_m} + \frac{v_f}{k_f} \quad (2.39)$$

where v_m is the matrix volume fraction, v_f is the filler volume fraction, k_m is the thermal conductivity of matrix, and k_f is the thermal conductivity of filler.

Series model typically gives an underestimation for a particulate composite due to the presumably complete localization of the contribution from the particles embedded in the matrix; in other words, neglecting the interaction among the fillers [13]. It can be imagined that the composite material responds as a homogeneous material in which each filler particle is an isolated entity [26]. Thus, the series model gives the lower bound for thermal conductivity of composites as shown in Figure 2.8.

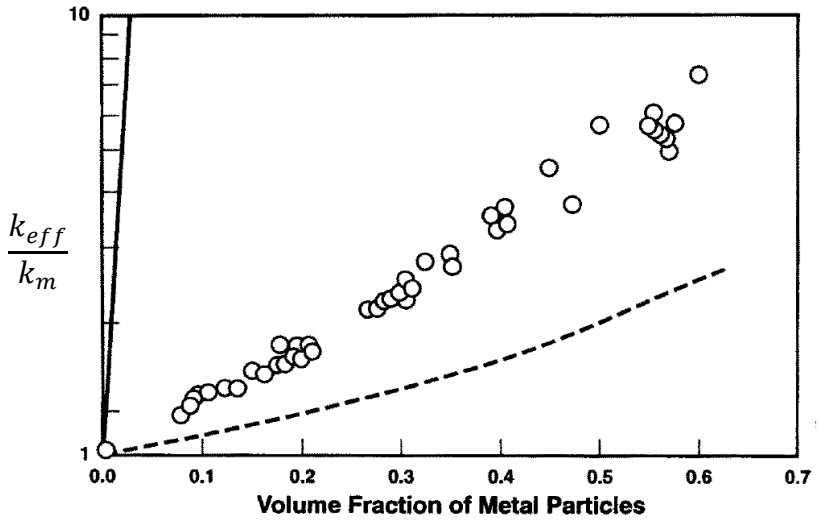

Figure 2.8 The predictions of the relative thermal conductivity of a two phase system as a function of volume fraction of the spherical metal particle where solid line is parallel model and dot line is series model [26]

2.3.1.2 Parallel Model

If two components arranged in parallel with respect to the heat flow, the effective thermal conductivity in this case can be written as

Parallel model: $$k_{eff} = v_m k_m + v_f k_f \tag{2.40}$$

which is also called the rule of mixture for thermal conductivity [13].

Parallel model accounts for the particle-particle interactions by assuming the perfect contact between particles in a fully percolating network [13, 26]. This model gives an overestimation of thermal conductivity for composites [13]. Therefore, it gives upper bound for thermal conductivity of composites as shown in Figure 2.8.

2.3.1.3 Cheng and Vachon Model

Based on the series and the parallel models, Tsao [45] developed a probabilistic model for the effective thermal conductivity of composites as follows:

$$\frac{1}{k_{eff}} = \int_0^1 \frac{dP_1}{k_m + (k_f - k_m)\int_{P_1}^1 \frac{1}{\sigma\sqrt{2\pi}} e^{-\frac{1}{2}\left(\frac{P_1 - \mu}{\sigma}\right)^2} dP_1} \tag{2.41}$$

where P_1 is the one-dimensional porosity (line fraction), μ is the mean of P_1, and σ is the standard deviation.

The values of μ and σ are derived from the experiment and it is specific for a composite. To solve this problem, Cheng and Vachon [14] postulated a parabolic distribution of the discontinuous phase in the matrix. The constants of the parabolic distribution are given as a function of the volume fraction of discontinuous phase. In case of composite filled with highly conductive filler ($k_f > k_m$), the formula is

$$\frac{1}{k_{eff}} = \frac{1}{\sqrt{C'(k_f - k_m)[k_m + B(k_f - k_m)]}} \ln \frac{\sqrt{k_m + B(k_f - k_m)} + \frac{B}{2}\sqrt{C'(k_f - k_m)}}{\sqrt{k_m + B(k_f - k_m)} - \frac{B}{2}\sqrt{C'(k_f - k_m)}} + \frac{1 - B}{k_m} \quad (2.42)$$

where $B = \left(\frac{3v_f}{2}\right)^{\frac{1}{2}}$ and $C' = \frac{4}{B}$.

The maximum volume fraction of filler in Cheng and Vachon model consequently was fixed to be 0.667 due to assuming the parabolic distribution curve. However, this value should depend on the dispersion state and the shape of the filler. Okamoto and Ishida [46] suggested that the maximum packing volume fraction ($v_{f,max}$) of the filler phase should be used as a new parameter applied to the Cheng and Vachon model. This new parameter reflects the dispersion state and the shape of the filler. They assumed that the dispersion state of the discontinuous phase does not change substantially throughout the volume fraction of the discontinuous phase under examination. The shape of the distribution curve at a certain volume fraction (v_f) is supposed to be geometrically similar to that at $v_{f,max}$, as shown in Figure 2.9. They defined the relationship between v_f and $v_{f,max}$ as follows:

$$v_f = B^2 v_{f,max} \quad (2.43)$$

Therefore, B and C can be rewritten as

$$B = \left(\frac{v_f}{v_{f,max}}\right)^{\frac{1}{2}} \quad (2.44)$$

and

$$C = -4\left(\frac{v_{f,max}}{v_f}\right)^{\frac{1}{2}} \quad (2.45)$$

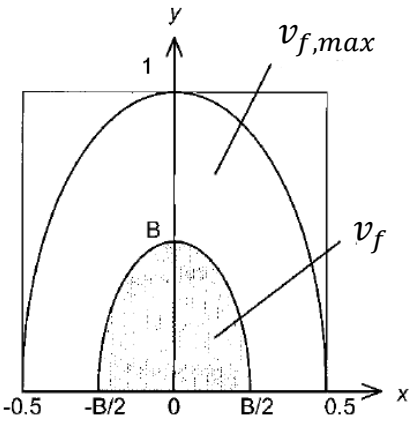

Figure 2.9 Schematic diagram of $v_{f,max}$ and v_f [46]

The value of $v_{f,max}$ of this model can be found by fitting the modified Cheng and Vachon model to the experimental data and it is very close to theoretical maximum volume fraction derived by calculation. By this way, the modified Cheng and Vachon model can account for the effects of the dispersion state and the shape of filler on the thermal conductivity of composite.

2.3.1.4 Liang and Liu Model

Liang and Liu [15] presented a heat transfer model of inorganic particulate-filled polymer composites based on the specific equivalent thermal resistance of the element of composites, when only heat conduction is considered. Thus, the calculation of the equivalent thermal conductivity for composites can be attributed to the determination of the equivalent thermal conductivity of the unit cell with the same specific equivalent thermal resistance. They supposed that an overall composite consists of a number of small squared elements, and each element only contains a spherical particle in the center. The element was divided into three parts. Part one and part three contain only neat polymer, while part two contains both spherical particle and polymer. The thermal conductivities of part one and part three are equal to thermal conductivity of neat polymer. For part two, the mean thermal conductivity is derived by considering the connection of polymer and particle in parallel. Then, the total thermal resistance was calculated by a series model of thermal resistance of

each part. From a definition of thermal resistance, the equation for effective thermal conductivity can be written as

$$k_{eff} = \frac{1}{\frac{1}{k_m} - \frac{1}{k_m}\left(\frac{6v_f}{\pi}\right)^{\frac{1}{3}} + \frac{2}{k_m\left(\frac{4\pi}{3v_f}\right)^{\frac{1}{3}} + \left(\frac{2v_f}{9\pi}\right)^{\frac{1}{3}}\pi\left(k_f - k_m\right)}} \tag{2.46}$$

Chauhan *et al.* [47] modified Liang and Liu model to consider the effect of geometry of filler particles on the effective thermal conductivity. Two different shapes, namely, elliptical and hexagonal, of filler particle were used in modeling.

For the elliptical shape of filler particle, the equation is

$$k_{eff} = \frac{1}{\frac{1}{k_m} - \frac{1}{k_m}\left(\frac{6v_f}{\pi}\right)^{\frac{1}{3}} + \frac{2}{\frac{k_m}{\sqrt{2}}\left(\frac{\pi}{6v_f}\right)^{\frac{1}{3}} + \left(\frac{2v_f}{9\pi}\right)^{\frac{1}{3}}\pi\left(k_f - k_m\right)}} \tag{2.47}$$

For the hexagonal shape of filler particle, the equation is

$$k_{eff} = \frac{1}{\frac{1}{k_m} - \frac{1.23}{k_m}\left(v_f\right)^{\frac{1}{3}} + \frac{2}{1.62\frac{k_m}{\left(v_f\right)^{\frac{1}{3}}} + 1.29\left(v_f\right)^{\frac{1}{3}}\left(k_f - k_m\right)}} \tag{2.48}$$

Although, the shapes of filler particle are different in Eq. (2.46), (2.47), and (2.48), the predictive values from these equations are quite similar [47].

2.3.2 Model Based on Exact Solution

2.3.2.1 Maxwell Model (Maxwell-Garnett Equation)

Maxwell solved the problem of determining the effective transport properties of multiphase materials [13]. He derived an exact solution for the effective specific resistance of a composite filled with spherical particles based on the continuity of potential and electric current at the interface, and on the assumption that the interactions among the spherical particles are neglected. This means the small spherical particles are located far enough from each other. When the solution was transformed to the thermal conductivity, the model can be written as

$$\frac{k_{eff}}{k_m} = 1 + 3v_f \frac{k_f - k_m}{2k_m + k_f - v_f(k_f - k_m)} \tag{2.49}$$

Eq. (2.49) is suitable for composites filled with spherical particles at very low content and good dispersion. The interfacial thermal resistance is not considered in this model. The effective thermal conductivity predicted by Maxwell model usually deviates from experimental thermal conductivity at a high volume fraction, because there is no consideration of mutual interaction of particles in this model [42]. Eq. (2.49) is also named Maxwell-Garnett (MG) equation in terms of electrical conductivity [13].

2.3.2.2 Hamilton and Crosser Model

Hamilton and Crosser defined volume-temperature gradient-averaged thermal conductivity of a composite as [13, 48]

$$k_{eff} = \frac{k_m v_m \left(\frac{dT}{dx}\right)_m + k_f v_f \left(\frac{dT}{dx}\right)_f}{v_m \left(\frac{dT}{dx}\right)_m + v_f \left(\frac{dT}{dx}\right)_f} \tag{2.50}$$

The ratio of the temperature gradient was determined from theoretical work of Maxwell under the assumption that interaction between particles is negligible, which relates to low filler concentration.

$$\frac{\left(\frac{dT}{dx}\right)_f}{\left(\frac{dy}{dx}\right)_m} = \frac{nk_m}{k_f + (n-1)k_m} \tag{2.51}$$

where n is shape factor depending on the shape of the dispersed particles and the ratio of the conductivity of the two phases, and should be determined experimentally for mixtures containing particles of arbitrary shapes. Substituting Eq. (2.51) into Eq. (2.50), the equation for effective thermal conductivity is given by

$$\frac{k_{eff}}{k_m} = \frac{1 + \frac{v_f(n-1)(k_f - k_m)}{k_f + (n-1)k_m}}{1 - \frac{v_f(k_f - k_m)}{k_f + (n-1)k_m}} \tag{2.52}$$

where $n = \frac{3}{\Psi}$, Ψ is sphericity being an empirical factor. The Ψ is defined as the ratio of the surface area of a sphere, with a volume equal to that of the particle, to the surface area of the particle.

2.3.2.3 Bruggeman Model

Bruggeman developed the differential effective medium (DEM) theory to estimate the effective properties of composites at high particle concentration. The principle of the DEM theory was briefly discussed in [49]. By considering the mutual interaction between the particles in the composite with high filler concentration, Bruggeman model was obtained by introducing the filler volume fraction under an integral transformation of Maxwell model as [42]

$$1 - v_f = \frac{k_f - k_{eff}}{k_f - k_m}\left(\frac{k_m}{k_{eff}}\right)^{\frac{1}{3}} \tag{2.53}$$

However, some research indicated that there are a smaller deviation between the experiment data and the predictive value of Bruggeman model [42].

2.3.2.4 Hatta and Taya Model

Equivalent inclusion method (EIM) was first introduced by Eshelby [50] for the determination of the elastic field of an ellipsoidal inclusion. By the principle of the analogy of heat conduction to elasticity, Hatta and Taya [17] applied EIM to the study of steady-state heat conduction in composite. In the EIM, an inhomogeneous region is converted to an equivalent inclusion filled by a uniformly distributed doublet such that the equivalent inclusion induces the same thermal intensity field as the particle. After the temperature fields in and around an inclusion are solved, the effective thermal conductivity of the composite can be computed. For a completely random distribution and intrinsically isotropic property of the fillers, the effective thermal conductivity is written as

$$\frac{k_{eff}}{k_m} = 1 + \frac{v_f(k_f - k_m)\left[(k_f - k_m)(2S_{33} + S_{11}) + 3k_m\right]}{3(k_f - k_m)^2(1 - v_f)S_{11}S_{33} + k_m(k_f - k_m)R + 3k_m^2} \tag{2.54}$$

where

$$R = 3(S_{11} + S_{33}) - v_f(2S_{11} + S_{33}) \tag{2.55}$$

and S depends on the shape of the filler particle as [17]:

(1) Sphere ($a_1 = a_2 = a_3$)

$$S_{11} = S_{22} = S_{33} = \frac{1}{3} \tag{2.56}$$

(2) Oblate spheroid ($a_1 = a_2 > a_3$)

$$S_{11} = S_{22} = \frac{a_1^2 a_3}{2(a_1^2 - a_3^2)^{\frac{3}{2}}} \left\{ \cos^{-1}\frac{a_3}{a_1} - \frac{a_3}{a_1}\left(1 - \frac{a_3^2}{a_1^2}\right)^{\frac{1}{2}} \right\} \tag{2.57}$$

$$S_{33} = 1 - 2S_{22} \tag{2.58}$$

(3) Prolate spheroid ($a_1 = a_2 < a_3$)

$$S_{11} = S_{22} = \frac{a_1^2 a_3}{2(a_3^2 - a_1^2)^{\frac{3}{2}}} \left\{ \frac{a_3}{a_1}\left(\frac{a_3^2}{a_1^2} - 1\right)^{\frac{1}{2}} - \cosh^{-1}\frac{a_3}{a_1} \right\} \tag{2.59}$$

$$S_{33} = 1 - 2S_{22} \tag{2.60}$$

where a_1, a_2, and a_3 are semiaxes of ellipsoid.

2.3.2.5 Hashin Model

A generalized self-consistent scheme method of approximation for effective properties was presented by Hashin [13]. The basic underlying assumption is that a typical basic element of a heterogeneous medium, such as a particle in a composite, can be regarded as being embedded in an equivalent homogeneous medium whose properties are the unknowns to be calculated. The idea of modeling is that a spherical particle of radius r_1, consisting of material of intrinsic conductivity k_f, is embedded in a concentric matrix shell of unspecified radius r_2, with the matrix conductivity being k_m. Therefore, the composite sphere obtained is embedded in an infinite body of

conductivity k_{eff}, which is the unknown to be found. By this way, Hashin derived a general quadratic equation as

$$2\left[2+a^*+\frac{k_f}{k_m}(1-a^*)\right]\left(\frac{k_{eff}}{k_m}\right)^2-\left[2(1+2a^*)+\frac{k_f}{k_m}(1-4a^*)+9\left(\frac{k_f}{k_m}-1\right)v_f\right]\frac{k_{eff}}{k_m} \\ -\left[2(1-a^*)+\frac{k_f}{k_m}(1+2a^*)\right]=0 \tag{2.61}$$

where $a^*=\left(\frac{r_1}{r_2}\right)^3$.

For the particle embedded closely in the homogeneous medium of k_{eff}, Eq. (2.61) can be reduced by giving $a^*=1$ as follows:

$$(1-v_f)\frac{k_m-k_{eff}}{k_m+2k_{eff}}+v_f\frac{k_f-k_{eff}}{k_f+2k_{eff}}=0 \tag{2.62}$$

Eq. (2.62) is known as Bruggeman-Landauer self-consistent effective medium approximation (BL-SCEMA) [13].

CHAPTER 3
LITERATURE REVIEWS

Due to the continuing increase in electronic packing density, materials with high thermal conductivities are preferred to solve the heat dissipation problem [4]. Furthermore, these materials should include the other desired properties such as coefficients of thermal expansion matching those of substrates, low density, and low cost [3]. To meet all requirements, new materials have been developed by combining two or more constituents. These new materials are called composites that provide unique combinations of properties.

Polymer is an interesting material that can be used as matrix of composite because it possesses several desired properties such as light weight, chemical inertness, long service life, easy processing, and low cost [3, 39]. However, the thermal conductivity of polymer is low in the range of 0.15 – 0.25 W/m-K [42]. This causes a plastic part to not able to conduct heat to reduce the hot spots or to act as a heat sink for a thermally sensitive component [39]. By incorporating highly thermally conductive filler such as ceramic particles or metal particles in polymer, it leads to a polymer composite that possesses higher thermal conductivity than neat polymer and still preserves the original properties of neat polymer. Polymer composites have been used for several applications in electronic packaging such as printed circuit boards (PCBs), electrically/thermally conductive adhesives, encapsulations, thermal interface materials (TIMs), and electrical interconnections [3, 51]. Due to the needs of these diverse applications, many researchers have paid their attention on the improvement of the thermal conductivity of polymers [4, 6, 52-57]. Some important aspects of those works were briefly reviewed in this section.

The effect of filler content on the thermal conductivity was studied by Sofian *et al*. [56]. Metal powder filled high-density polyethylene composites were investigated experimentally in the range of filler content of 0-24 vol.%. The thermal conductivity of composites increased with the filler content. At low filler content, 0-16 vol.%, the particles were distributed homogeneously in the polymer matrix and did not interact

with each other. This led to the gradual increase of the thermal conductivity of composites. At higher filler content, the formation of agglomerates and conductive chains were occurred resulting in a rapid increase of thermal conductivity. However, the thermal conductivity of composite could decrease at very high filler content due to the agglomeration of filler and formation of voids [55].

Tekce *et al*. [57] investigated the effect of particle shape on thermal conductivity of copper reinforced polyamide. For a given filler loading, they discovered that copper particles in form of short fiber increased the thermal conductivity of composite higher than copper particles in form of spherical and plate. This fact was emphasized by Nurul and Mariatti [55] who indicated that polypropylene filled with cylindrical particles, i.e. carbon nanotube, had the thermal conductivity higher than polypropylene filled with spherical particles, i.e. synthetic diamond, boron nitride, and copper. They suggested that the high aspect ratio of filler particle facilitates the formation of bridges for phonon transformation.

The effect of particle size on thermal conductivity of epoxy-based composites filled with boron nitride was studied by Kochetove *et al*. [58]. Boron nitride with different average sizes, i.e. 70 nm (nanoparticles), 0.5 μm (submicron or mesoparticles), 1.5 μm and 5 μm (micron sized particles) were used in the experiment. The results showed that thermal conductivities of composites were nearly the same (0.234-0.264 W/m-K for 10 wt.% of boron nitride and 0.329-0.399 W/m-K for 20 wt.%) albeit the average particle size increased. They seggested that the filler content strongly dominated the thermal conductivity of composite more than the particle size. The similar results were observed by Han *et al*. [59]. Their works showed that there was no significant difference in the thermal conductivities of epoxy resin filled with different sizes of boron nitride particle. They suggested that the size of filler particle was not necessarily crucial to the thermal conductivity of the composites at low to moderate concentrations. Except for high concentration, polymer filled with smaller size particles could possess either higher thermal conductivity or lower thermal conductivity depending on which effect of conductive path formation or interfacial thermal resistance would be more influential [12, 60]. The distribution of particle size can be used to improve the thermal conductivity of composite. By using filler particles with

bimodal particle size distribution, Ishida and Rimdusit [4] succeeded in preparing a boron nitride-filled polybenzoxazine with a high thermal conductivity of 32.5 W/m-K at maximum filler loading of 78.5 vol.%. This high thermal conductivity was the result of the increase of particle packing density that provided the capability of forming conductive networks with low thermal resistance along the conductive paths.

The interfacial thermal resistance between matrix and nanoparticle plays the important role in thermal transport in the nanocomposites. The interface thermal resistance across the carbon nanotube matrix reported by Huxtable *et al*. [61] was about 8.3×10^{-8} m^2K/W. The understanding of the interface effect on the thermal behavior of the nanotube composites was presented in form of a model by Nan *et al*. [29]. They modified the Maxwell-Garnett-type effective medium approach (EMA) to consider the effect of interfacial thermal resistance in form of the equivalent thermal conductivities along transverse and longitudinal axes of a composite unit cell, i.e., a nanotube coated with a very thin interfacial thermal barrier layer. The model showed that a large interfacial thermal resistance across the nanotube-matrix interface caused a significant degradation in the thermal conductivity. In addition, there are other models that were developed to consider the effect of the interfacial thermal resistance [13, 31, 34, 42, 62]. Although the concept of the interfacial thermal resistance had been purposed by Kapitza [32] for a long time; however, the determination of the interfacial thermal resistance for each composite still has not been reported in a large number, partly because of the difficulties of such measurement related to the small size of the particles [63]. Most researches just presented the values of interfacial thermal resistance derived from fitting the experimental thermal conductivity with a theoretical model (indirect method for determination of the interfacial thermal resistance) [55, 62, 64]. To enhance the thermal transport of polymer composites, Fukushima *et al*. [65] showed that the interfacial thermal resistance can be reduced by the organic modifications of an inorganic surface of ceramic particles.

The basic models as described in section 2.4 generally take into account the effects of filler content, shape of filler particle, and the orientation of filler particle. Those models focused on the ideal case of perfect interface contact between filler particle and matrix. In case of polymer composites filled with highly conductive filler,

heat transfer at the interface is reduced due to thermal expansion mismatch and low adhesion between phases, and the influence of the interface is more important if the conductivity of the composite is high or filled with large amount of particles [63]. Recent theoretical models have been developed to include the effect of the interface in term of the interfacial conductance or interfacial thermal resistance [13, 31]. Some of interesting models were reviewed in this section.

Hasselman and Johnson [28] extended the classical work of Maxwell and Lord Rayleigh to consider the interfacial thermal resistance by modifying the boundary condition between the filler and the matrix [13, 31]. For composites filled with spherical particles at low filler content and uniform distribution, the equation was expressed as [13]

$$\frac{k_{eff}}{k_m} = \frac{2v_f\left(\frac{k_f}{k_m} - \frac{k_f}{rh_{int}} - 1\right) + \frac{k_f}{k_m} + \frac{2k_f}{rh_{int}} + 2}{v_f\left(1 - \frac{k_f}{k_m} + \frac{k_f}{rh_{int}}\right) + \frac{k_f}{k_m} + \frac{2k_f}{rh_{int}} + 2} \tag{3.1}$$

where r is the radius of spherical particle and h_{int} is the thermal interfacial conductance that is reciprocal of the thermal interfacial resistance R_{int}. In case of perfect interfaces or $\frac{1}{h_{int}} = 0$, Eq. (3.1) reduces to the MG equation (Eq. (2.49)).

Benveniste and Miloh [13] introduced a general approach to compute the effective thermal conductivity of composites with imperfect interfaces between constituents. This model was one of the first two models incorporating the effect of the interfacial thermal resistance on the effective thermal conductivity of the composite by modifying Maxwell's theory (another was Hasselman and Johnson model [28] as described previously). The method was based on the solution of the temperature field both interior and exterior at the particle surface because of a uniform heat flux at infinity. The temperature drop across the interface due to the interfacial thermal resistance was accounted for in term of the interfacial conductance (h_{int}). For spherical particles, the derived equation was [13]

$$\frac{k_{eff}}{k_m} = 1 - 3v_f \frac{1 - \frac{k_f}{k_m} + \frac{k_f}{rh_{int}}}{2 + \frac{k_f}{k_m} + \frac{2k_f}{rh_{int}}} \tag{3.2}$$

where r is the radius of the spherical particles.

Eq. (3.2) was a special form of Eq. (3.1) in case of vanishingly small v_f. Furthermore, for perfect interface between the constituents, Eq. (3.2) also reduces to the MG equation (Eq. (2.49)).

To extend the range of filler content, Benveniste [30] modified two micromechanical models, i.e., generalized self-consistent scheme and Mori Tanaka theory [66], to predict the effective thermal conductivity of particulate composites at filler content up to $v_f = \frac{\pi}{6}$ and including a thermal contact resistance at interphase boundaries. The two models resulted in the same closed-form expression for the effective thermal conductivity of composites filled with spherical particles as follows [30]:

$$\frac{k_{eff}}{k_m} = \frac{2(1 - v_f) + \frac{rh_B}{k_m}\left[1 + 2v_f + \frac{2k_m}{k_f}(1 - v_f)\right]}{(2 + v_f) + \frac{rh_B}{k_m}\left[1 - v_f + \frac{k_m}{k_f}(2 + v_f)\right]} \tag{3.3}$$

where h_B was the so-called "skin constant" that represented the effect of a thermal interfacial resistance in this model.

In case of the composites filled with high conductive particles, the concept of the Kapitza radius a_K was often used, which was defined as [34]

$$a_K = R_{int} k_m \tag{3.4}$$

The Kapitza radius is in principle the critical particle size and is usually used in form of the interfacial thermal resistance factor (α_K) as follows [34]:

$$\alpha_K = \frac{a_K}{r} \tag{3.5}$$

The dimensionless factor α_K is a measure of the interfacial thermal resistance. If $\alpha_K = 0$ or $r \gg a_K$, this means there is no interfacial thermal resistance; the conductive filler can improve the thermal conductivity of the composite to be higher than that of the matrix. In contrast, if r is smaller than a_K, the thermal conductivity of composites is lowered by adding the filler particles in the matrix even though the particles themselves possess a much higher intrinsic conductivity than the matrix. If the radius of the particles is equal to the Kapitza radius or $\alpha_K = 1$, the contribution of the interfacial thermal resistance is then exactly balanced by the much higher thermal conductivity of the particles [13].

Using the concept of the Kapitza radius, Eq. (3.1) can be rewritten as [34, 42]

$$\frac{k_{eff}}{k_m} = \frac{\left[k_f(1+2\alpha_K)+2k_m\right]+2v_f\left[k_f(1-\alpha_K)-k_m\right]}{\left[k_f(1+2\alpha_K)+2k_m\right]-v_f\left[k_f(1-\alpha_K)-k_m\right]} \tag{3.6}$$

Eq. (3.6) was also called “the modified MG equation” and can be reduced to MG equation (Eq. (2.49)) when the interfacial thermal resistance was neglected ($\alpha_K = 0$). Eq. (3.6) was valid only when the volume fraction of filler was sufficiently dilute [34].

Nan *et al*. [31] developed a more general formulation for the effective thermal conductivity of composites filled ellipsoidal particles based on multiple-scattering theory. This model contained the effects of particle size, shape, orientation distribution, volume fraction, and interfacial thermal resistance, but neglecting the effect of the interaction between particles. To include the effect of interface, they assumed that an ellipsoidal particle in the matrix was surrounded by interface layer of thickness δ and conductivity k_{int} as a composite unit cell. The interfacial thermal resistance was thought of as the limiting case of heat transport across bulk phase separated by a thin, poorly conducting interphase region, leading to the limit that $\delta \to 0$ and $k_{int} \to 0$. This interfacial thermal property was considered on a surface of zero thickness and defined as

$$R_{int} = \lim_{\substack{\delta \to 0 \\ k_{int} \to 0}} \left(\frac{\delta}{k_{int}}\right) \tag{3.7}$$

By this concept, the effective thermal conductivity ($k_{eff,ii}, i = 1,2,3$) was derived as along the materials axes X_i

$$k_{eff,11} = k_{eff,22} = k_m \frac{2 + v_f[\beta_{11}(1 - L_{11})(1 + \langle\cos^2\theta\rangle) + \beta_{33}(1 - L_{33})(1 - \langle\cos^2\theta\rangle)]}{2 - v_f[\beta_{11}L_{11}(1 + \langle\cos^2\theta\rangle) + \beta_{33}L_{33}(1 - \langle\cos^2\theta\rangle)]} \quad (3.8)$$

$$k_{eff,33} = k_m \frac{1 + v_f[\beta_{11}(1 - L_{11})(1 - \langle\cos^2\theta\rangle) + \beta_{33}(1 - L_{33})\langle\cos^2\theta\rangle]}{1 - v_f[\beta_{11}L_{11}(1 - \langle\cos^2\theta\rangle) + \beta_{33}L_{33}\langle\cos^2\theta\rangle]} \quad (3.9)$$

with

$$\beta_{ii} = \frac{k_{c,ii} - k_m}{k_m + L_{ii}(k_{c,ii} - k_m)} \quad (3.10)$$

$$\langle\cos^2\theta\rangle = \frac{\int \vartheta(\theta)\cos^2\theta \sin\theta \, d\theta}{\int \vartheta(\theta)\sin\theta \, d\theta} \quad (3.11)$$

where θ was the angle between the materials axis X_3 and the local particle axis X'_3, $\vartheta(\theta)$ was a distribution function describing ellipsoidal particle orientation and L_{ii} were geometrical factors dependent on the particle shape given by

$$L_{11} = L_{22} = \frac{a_r^2}{2(a_r^2 - 1)} - \frac{a_r}{2(a_r^2 - 1)^{1.5}}\cosh^{-1} a_r \qquad \text{for } a_r \geq 1 \quad (3.12a)$$

$$L_{11} = L_{22} = \frac{a_r^2}{2(a_r^2 - 1)} + \frac{a_r}{2(1 - a_r^2)^{1.5}}\cos^{-1} a_r \qquad \text{for } a_r \leq 1 \quad (3.12b)$$

$$L_{33} = 1 - 2L_{11} \quad (3.12c)$$

where $a_r = \frac{r_3}{r_1}$ was the aspect ratio of the ellipsoidal particle; r_1 and r_3 were radii of the ellipsoid along the X'_1 and X'_3 axes, respectively, and $a_r > 1$ and $a_r < 1$ for a prolate ($a_1 = a_2 < a_3$) and an oblate ($a_1 = a_2 > a_3$) ellipsoidal particle, respectively, $k_{eff,ii}$ was the effective thermal conductivity along the local axes of an ellipsoidal particle ($i = 1,2,3$) expressed as

$$k_{eff,ii} = \frac{k_f}{\left(1 + \frac{\left(2 + \frac{1}{a_r}\right)\alpha_K L_{ii} k_f}{k_m}\right)} \quad \text{for } a_r \geq 1 \tag{3.13a}$$

$$k_{eff,ii} = \frac{k_f}{\left(1 + \frac{(1 + 2a_r)\alpha_K L_{ii} k_f}{k_m}\right)} \quad \text{for } a_r \leq 1 \tag{3.13b}$$

Here the interfacial thermal resistance factor was defined by

$$\alpha_K = \frac{a_K}{a_1} \quad \text{for } a_r \geq 1 \tag{3.14a}$$

$$\alpha_K = \frac{a_K}{a_3} \quad \text{for } a_r \leq 1 \tag{3.14b}$$

When the ellipsoidal particles became spheres, $a_r = 1$, $L_{11} = L_{33} = \frac{1}{3}$, and $\langle \cos^2 \theta \rangle = \frac{1}{3}$, then Eq. (3.8) or (3.9) can revert back to modified MG equation (Eq. (3.6)).

For higher volume fraction of filler, Every *et al*. [27] developed a differential form of Eq. (3.6) based on Differential Effective Medium theory (DEM) or Bruggeman's integration embedding principle [43] to take into account the particle-particle interaction as follows:

$$dk = 3k \frac{dv\left[k_f(1 - \alpha_K) - k\right]}{(1 - v)\left[k_f(1 + 2\alpha_K) + 2k\right]} \tag{3.15}$$

where k is the thermal conductivity and v is the varying volume fraction of filler.

Integrating Eq. (3.15) with k from k_m to k_{eff}, and v from 0 to v_f, the effective thermal conductivity of composites was derived as

$$\left(1-v_f\right)^3=\left(\frac{k_m}{k_{eff}}\right)^{\frac{1+2\alpha_K}{1-\alpha_K}}\left(\frac{k_{eff}-k_f(1-\alpha_K)}{k_m-k_f(1-\alpha_K)}\right)^{\frac{3}{1-\alpha_K}} \tag{3.16}$$

If $\alpha_K=0$, negligible interfacial resistance, Eq. (3.16) reduces to Bruggeman's equation (Eq. (2.53)). Thus Eq. (3.16) was called that modified Bruggeman model.

Jiajun and Xiao-Su [34] introduced into the remodified MG equation with the effect of both interfacial thermal resistance and particle shape by combination of Hasselman's modification [28] and Hamiton's modification [18] as follows:

$$\frac{k_{eff}}{k_m}=\frac{(1+(n-1)\alpha_K)k_f+(n-1)k_m+(n-1)\left[k_f(1-\alpha_K)-k_m\right]v_f}{(1+(n-1)\alpha_K)k_f+(n-1)k_m-\left[k_f(1-\alpha_K)-k_m\right]v_f} \tag{3.17}$$

For a small volume fraction of filler, the differential form of Eq. (3.17) can be written as

$$dk=nk\frac{dv\left[k_f(1-\alpha_K)-k\right]}{(1-v)\left[k_f(1+(n-1)\alpha_K)+(n-1)k\right]} \tag{3.18}$$

Eq. (3.18) was integrated based on Bruggeman's integration embedding principle with v from 0 to v_f and k from k_m to k_{eff}. The final equation which took both the effects of interfacial thermal resistance and particle shapes into considerations was as follows:

$$\left(1-v_f\right)^n=\left(\frac{k_m}{k_{eff}}\right)^{\frac{1+n\alpha_K-\alpha_K}{1-\alpha_K}}\left(\frac{k_{eff}-k_f(1-\alpha_K)}{k_m-k_f(1-\alpha_K)}\right)^{\frac{n}{1-\alpha_K}} \tag{3.19}$$

Eq. (3.19) predicted the effective thermal conductivities that was in good agreement with the experimental data of polyimide filled with aluminum nitride powder in range of filler volume fraction less than 0.25, by using $\alpha_K = 0.117$ [34].

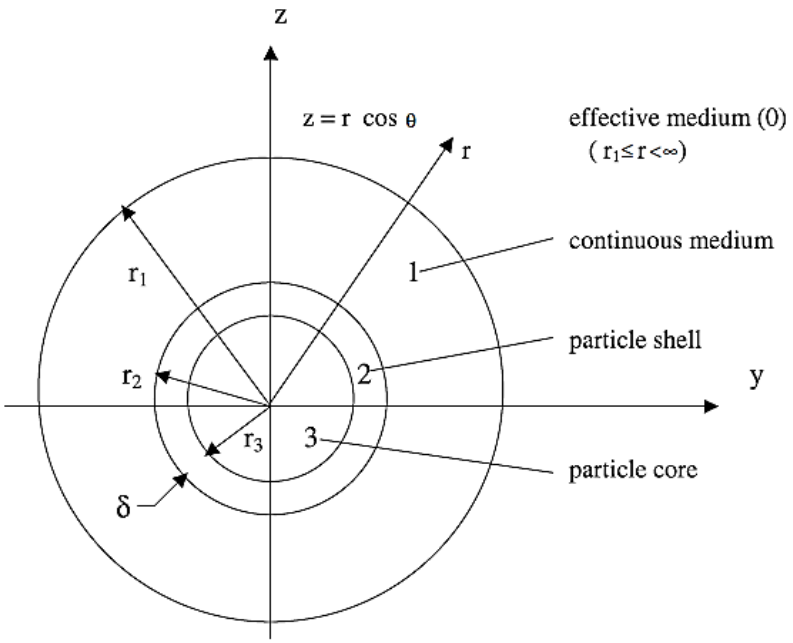

Figure 3.1 Geometry of cell for self-consistent field analysis of composite spheres randomly mixed into a continuum [67]

Felske [67] extended the self-consistent scheme to determine the effective thermal conductivity of composites containing randomly spherical particles and including the thermal interfacial resistance. The geometry of cell for self-consistent field analysis was modified by determining the core-shell sphere cell ($0 \leq r \leq r_1$) embedded in the effective medium ($r_1 \leq r < \infty$) as shown in Figure 3.1. An analytical solution was derived by determining the temperature distribution for each material and using the volume average of any property on the volume of the material. After performing algebraic manipulation, the effective thermal conductivity can be expressed as

$$\frac{k_{eff}}{k_m} = \frac{2(1-v_f)\Psi_2 + \beta_2\Theta_N}{(2+v_f)\Psi_2 + \beta_2\Theta_D} \tag{3.20}$$

with

$$\beta_2 = \frac{h_{21} r_2}{k_2} \tag{3.21}$$

$$\Psi_2 = (2 + v_{f3})k_{32} - 2(1 - v_{f3}) \tag{3.22}$$

$$\begin{aligned}\Theta_N = {} & (1 - v_f)[2(1 + 2v_{f3}) - 2(1 - v_{f3})k_{32}] \\ & + (1 + 2v_f)[(2 + v_{f3})k_{31} - 2(1 - v_{f3})k_{21}]\end{aligned} \tag{3.23}$$

$$\begin{aligned}\Theta_D = {} & (2 + v_f)[(1 + 2v_{f3}) - (1 - v_{f3})k_{32}] \\ & + (1 - 2v_f)[(2 + v_{f3})k_{31} - 2(1 - v_{f3})k_{21}]\end{aligned} \tag{3.24}$$

where $v_{f3} = \left(\frac{r_2}{r_3}\right)^3$, $v_{3f} = v_{f3}^{-1}$, h_{21} was the contact conductance at the interface between the sphere and the continuous medium, $k_{mn} = \frac{k_m}{k_n}$ where $m, n = 1,2,3$ was the thermal conductivity ratio where 1, 2, and 3 referred to continuous medium, particle shell, and particle core, respectively. For a special case, the composite sphere behaves as a uniform sphere when the shell and core have the same thermal conductivity ($k_3 = k_2$) leading to $k_{32} = 1$ and $k_{31} = k_{21}$. This makes Eq. (3.20) reduces to Eq. (3.3) according to the result of Benveniste [30].

It should be noted that the equations of the modified models usually reduced to the famous modified models, namely the modified Maxwell and the modified Bruggeman models, for the composite filled with spherical particles. Every *et al.* [27] plotted both models with the data of ZnS as a matrix and diamond particles as a filler. The plots of these models at different values of α_K were quite similar as shown in Figure 3.2 for the modified Maxwell model and Figure 3.3 for the modified Bruggeman model. The effective thermal conductivity decreased with increasing α_K that related to the interfacial thermal resistance. When α_K = 1, the effective thermal conductivity was the same as that of the matrix. This could be explained that the higher thermal conductivity of the particles was exactly balanced by the higher resistance of the

interfaces. For α_K < 1, the effective thermal conductivity was lower than that of the matrix, until α_K approached infinity the lowest effective thermal conductivity was obtained.

A comparison between the prediction by the modified Bruggeman model and the experimental data of ZnS/diamond cited from [27] was presented in Figure 3.4. It indicated that the modified Bruggeman model was in good agreement with the experimental data of ZnS filled with average particle size $\approx 2\ \mu$m of diamond. It should be noticed that this model cannot predict the effective thermal conductivity of ZnS filled with average particle size $\approx 0.25\ \mu$m of diamond due to the nonspherical shape of the diamond particles [27]. However, the effect of filler particle size was included into the model. It showed that the composite filled with smaller particles had the higher interfacial thermal resistance than the composite filled with larger particles.

As mentioned above, the effective interfacial thermal resistance can be included into the effective thermal conductivity model by using the concept of Kapitza radius. By this way, the effect of particle size was automatically incorporated in the model. All modified models presented above were based on the exact solution. No modified model based on the simplified solution has been presented so far.

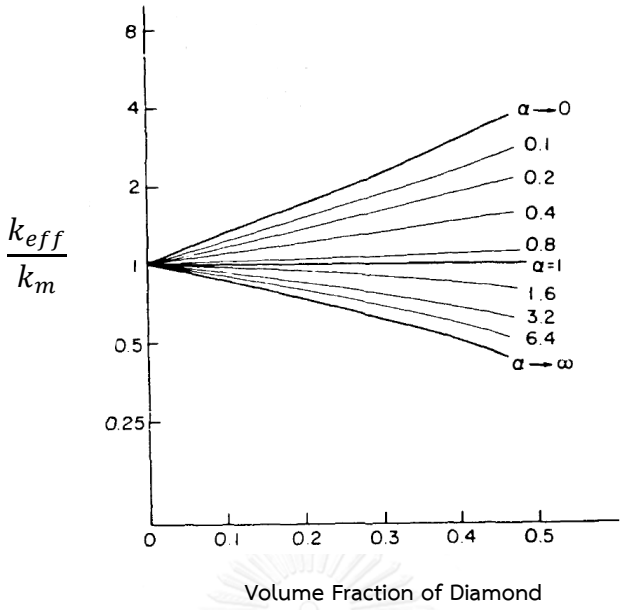

Figure 3.2 Relationship between the effective thermal conductivity and volume fraction of filler of ZnS/diamond predicted by the modified Maxwell model by varying α_K (adapted from [27])

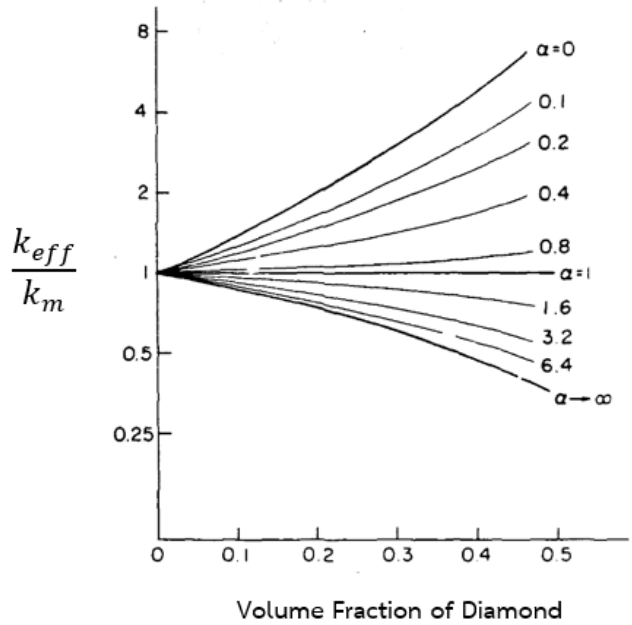

Figure 3.3 Relationship between the effective thermal conductivity and volume fraction of filler of ZnS/diamond predicted by the modified Bruggeman model by varying α_K (adapted from [27])

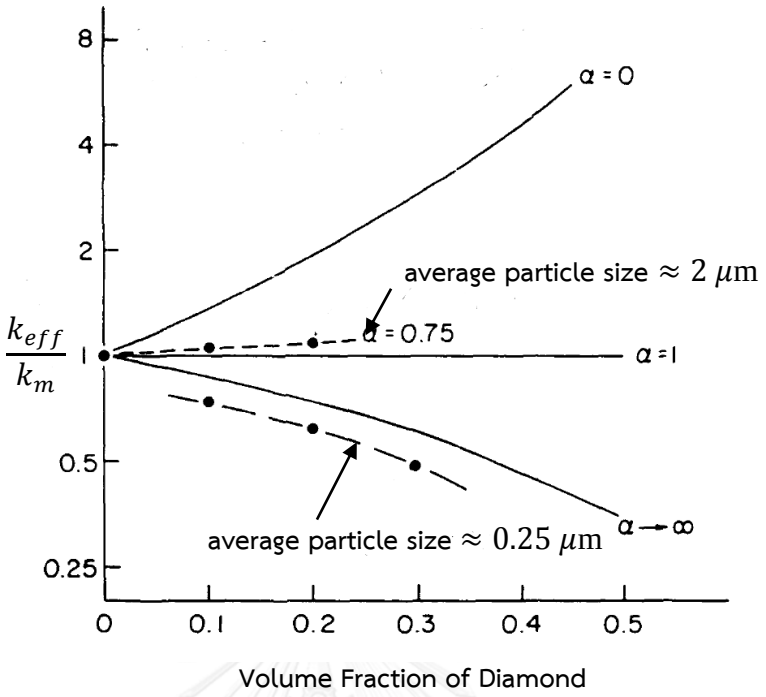

Figure 3.4 Comparison between the effective thermal conductivity predicted by the modified Bruggeman model and experimental data for ZnS/diamond (adapted from [27])

CHAPTER 4
MODELING

4.1 Effective Thermal Conductivity Model without the Interfacial Thermal Resistance

In this work, the effective thermal conductivity models were derive based on the simplified solution and the analogy to the electrical circuit. Composite composed of two materials, i.e., a polymer and a filler, was considered. In general, polymer is the matrix phase while filler is the dispersed phase. For simplification, the fillers were assumed as spherical particles that were homogeneously distributed and placed in the form of ordered periodic arrangement. By this way, the particles could be considered as being arranged similar to atoms in a crystal structure and the concept of unit cell analogous to crystallography could be applied [68]. Therefore, unit cell was defined as a representative volume element (RVE); a volume element which was small enough to show the microscopic structural details and large enough to represent the overall behavior of the composite [69]. In this work, three ideal arrangements, i.e. simple cubic (SC), body-centered cubic (BCC) and face-centered cubic (FCC), were chosen as RVE as shown in Figure 4.1.

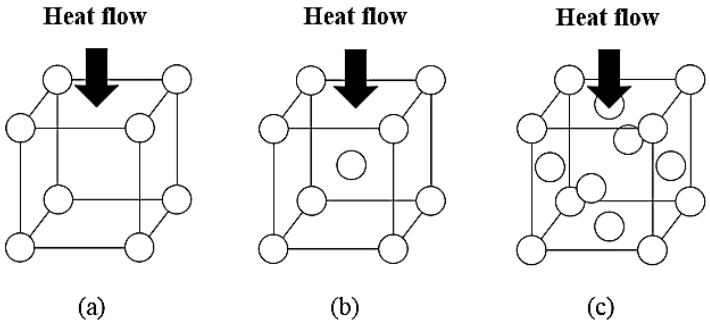

Figure 4.1 Representative volume element (RVE) in form of (a) simple cubic (SC), (b) body-centered cubic (BCC), and (c) face-centered cubic (FCC)

The side length of an element was defined as a. The radius and diameter of spherical particle were r and D, respectively. The volume of each spherical particle was $\frac{\pi D^3}{6}$ and the total volume of RVE was a^3. Thus the filler volume fraction can be expressed as

$$v_f = \frac{n_f \pi D^3}{6a^3} \tag{4.1}$$

where n_f is the number of spherical particles in a RVE.

For SC element, there is one spherical particle on each corner of the cube. Each particle is shared equally between eight adjacent cubes. Therefore, RVE contains in total one particle or $n_f = 1$. The filler volume fraction for SC element ($v_{f,\mathrm{SC}}$) was expressed as

$$v_{f,\mathrm{SC}} = \frac{\pi D^3}{6a^3} \tag{4.2}$$

For BCC element, there are one particle in the center and one spherical particle on each corner of the cube (one-eight contribution per a particle). Thus the total number of particle is equal to $n_f = 2$. The filler volume fraction for BCC element ($v_{f,\mathrm{BCC}}$) was expressed as

$$v_{f,\mathrm{BCC}} = \frac{\pi D^3}{3a^3} \tag{4.3}$$

For FCC element, there are one spherical particle on each face of the cube. Each gives exactly one half contribution. In addition, there are one particle on each corner of the cube similar to two cases above. Thus, the total number of particle is equal to $n_f = 4$. The filler volume fraction for FCC element ($v_{f,\mathrm{FCC}}$) was defined as

$$v_{f,\mathrm{FCC}} = \frac{2\pi D^3}{3a^3} \tag{4.4}$$

In this study, the effective thermal conductivity of nonlayered composite was modeled based on parallel-series arrangements of the thermal resistances. It was essential to assume that local thermal equilibrium existed over a RVE and heat transfer was occurred in one-dimension along x axis. The heat flow entered into the element from top of the cube as shown in Figure 4.1. Thermal interfacial resistance was neglected in this section. The mathematical model of each RVE depended on the filler loading and their distribution in polymer matrix [10]. Consequently, the heat transfer models of SC, BCC and FCC element were divided into eight cases by filler contents as shown in Figures 4.2, 4.3 and 4.4, respectively.

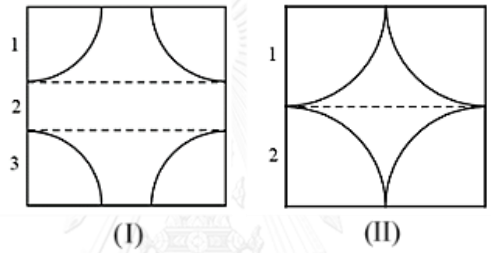

Figure 4.2 Side view of simple cubic element for polymer composites filled with filler volume fraction (I) < 0.524, and (II) 0.524

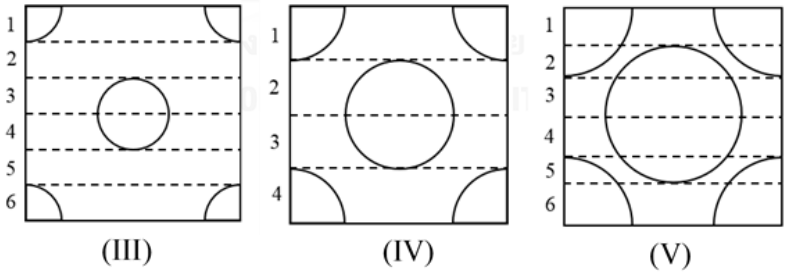

Figure 4.3 Side view of body-centered cubic element for polymer composites filled with filler volume fraction (III) < 0.131, (IV) 0.131, and (V) > 0.131

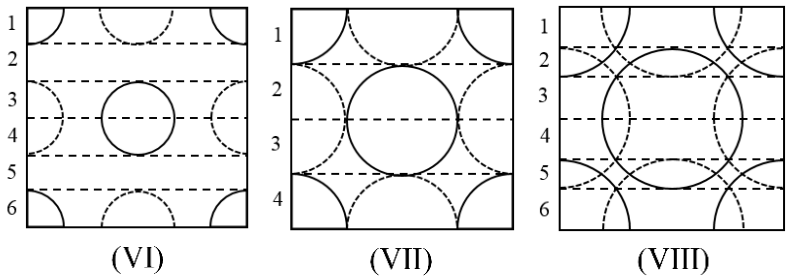

Figure 4.4 Side view of face-centered cubic element for polymer composites filled with filler volume fraction (VI) < 0.262, (VII) 0.262, and (VIII) > 0.262

4.1.1 Simple Cubic Model (SC1 Model)

4.1.1.1 Case I: SC1 Model with the Volume Fraction of Filler < 0.524

In case of SC element with filler volume fraction less than 0.524, the element was divided into three section as shown in Figure 4.5(a). Section 1 and 3 contain one-eighth of spherical particle on each corner and the rest is polymer matrix. Section 2 contains only polymer matrix. Thus, the thermal resistances of section 1 and 3 were considered as parallel arrangement of polymer matrix resistance and filler resistance, while the thermal resistance of section 2 comes from only the polymer matrix. Thermal resistances of each section are arranged in series as shown in Figure 4.5(b) where $R_{m,i}$ is the polymer matrix thermal resistance of section i and $R_{f,i}$ is the filler thermal resistance of section i and $i = 1,2,3$.

By the definition of series resistance (Eq. (2.32)), the total thermal resistance of this element is the addition of thermal resistances of each section.

$$R_{\Sigma} = R_1 + R_2 + R_3 \tag{4.5}$$

where R_1, R_2, and R_3 is the thermal resistance of section 1, 2, and 3, respectively.

Then the heat flow can be written as

$$Q = \frac{T_1 - T_2}{\frac{a}{Ak_{eff,\mathrm{SC1-1}}}} = \frac{T_1 - T_2}{R_1 + R_2 + R_3} \tag{4.6}$$

where $k_{eff,\mathrm{SC1-1}}$ is the effective thermal conductivity of case I of SC1 model and A is the area perpendicular to the heat flow.

(a) Physical model (b) Thermal circuit model

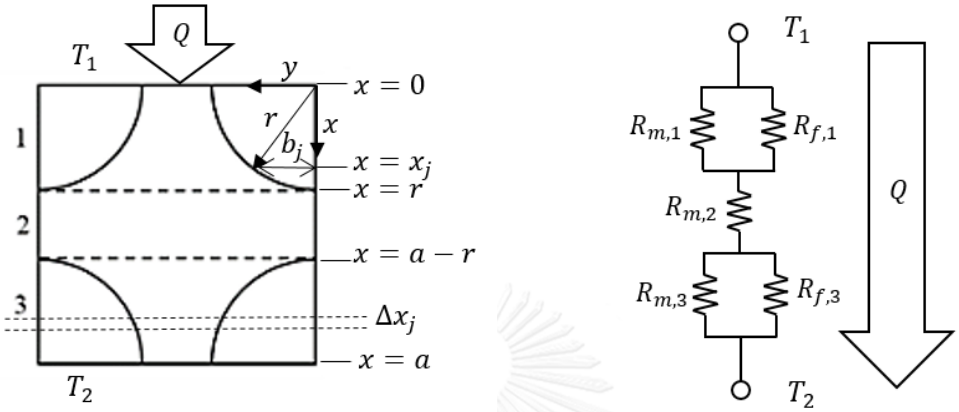

Figure 4.5 (a) Physical and (b) Thermal circuit model of simple cubic element with filler volume fraction < 0.524

Due to $A = a^2$, $k_{eff,\mathrm{SC1-1}}$ can be derived by rearranging Eq. (4.6) as

$$k_{eff,\mathrm{SC1-1}} = \frac{1}{a}\left(\frac{1}{R_1 + R_2 + R_3}\right) \tag{4.7}$$

Note that the thermal resistance of section 1 is equivalent to that of section 3, thus they were considered together. It can be imagined that the element can be divided into very thin layer j that its thickness is Δx_j, as shown in Figure 4.5(a). The resistance of a layer j is in parallel pattern of thermal resistances of polymer matrix resistance $R_{m,j}$ and filler resistance $R_{f,j}$. These layers j are arranged in series pattern. Therefore, the thermal resistances of section 1 and 3 can be written as

$$R_1 = R_3 = \sum_{j=0}^{r}\left(\frac{1}{R_{m,j}} + \frac{1}{R_{f,j}}\right)^{-1} \tag{4.8}$$

Because there are one fourth of a circle on each corner of the square plane (y, z) of layer *j*, thus there is one circle in each layer and then $R_{f,j}$ can be written as

$$R_{f,j} = \frac{\Delta x_j}{(\pi b_j^2) k_f} \tag{4.9}$$

where b_j is the radius of circle at $x = x_j$. By trigonometric relationship, it can be written as

$$b_j = \sqrt{r^2 - x_j^2} \tag{4.10}$$

The illustration of Eq. (4.10) is also shown in Figure 4.5.

The remaining area is of polymer matrix. Thus $R_{m,j}$ is expressed as

$$R_{m,j} = \frac{\Delta x_j}{(a^2 - \pi b_j^2) k_m} \tag{4.11}$$

Substituting Eq. (4.9), (4.10), and (4.11) into Eq. (4.8), it can be arranged in form of

$$R_1 = R_3 = \sum_{j=0}^{r} \frac{\Delta x_j}{a^2 k_m + \pi (k_f - k_m)(r^2 - x_j^2)} \tag{4.12}$$

When Δx_j approaches to zero, it can be written as

$$\begin{aligned} R_1 = R_3 &= \lim_{\Delta x_j \to 0} \sum_{j=0}^{r} \frac{\Delta x_j}{a^2 k_m + \pi (k_f - k_m)(r^2 - x_j^2)} \\ &= \int_0^r \frac{1}{a^2 k_m + \pi (k_f - k_m)(r^2 - x_j^2)} \, dx_j \end{aligned} \tag{4.13}$$

Before integrating, Eq. (4.13) can be further arranged as

$$R_1 = R_3 = \frac{1}{\pi(k_f - k_m)} \int_0^r \frac{1}{\left[\frac{k_m + \frac{\pi r^2}{a^2}(k_f - k_m)}{\frac{\pi}{a^2}(k_f - k_m)}\right] - x_j^2} dx_j$$

$$= \frac{1}{\pi(k_f - k_m)} \int_0^r \frac{1}{\left\{\left(\frac{a^2}{\pi}\right)\left(\frac{\pi r^2}{a^2}\right)\left[\frac{a^2}{\pi r^2}\left(\frac{k_m}{k_f - k_m}\right) + 1\right]\right\} - x_j^2} dx_j$$

$$= \frac{1}{\pi(k_f - k_m)} \int_0^r \frac{1}{\left\{r^2\left[\frac{a^2}{\pi r^2}\left(\frac{k_m}{k_f - k_m}\right) + 1\right]\right\} - x_j^2} dx_j \quad (4.14)$$

From Eq. (4.2), the length of RVE for this case can be written as

$$a = \left(\frac{4\pi r^3}{3v_f}\right)^{\frac{1}{3}} \quad (4.15)$$

Substituting Eq. (4.15) into Eq. (4.14), it goes to be

$$R_1 = R_3 = \frac{1}{\pi(k_f - k_m)} \int_0^r \frac{1}{\left\{r^2\left[\left(\frac{4\pi r^3}{3v_f}\right)^{\frac{2}{3}}\left(\frac{1}{\pi r^2}\right)\left(\frac{k_m}{k_f - k_m}\right) + 1\right]\right\} - x_j^2} dx_j$$

$$= \frac{1}{\pi(k_f - k_m)} \int_0^r \frac{1}{\left\{r^2\left[\left(\frac{16}{9\pi v_f^2}\right)^{\frac{1}{3}}\left(\frac{k_m}{k_f - k_m}\right) + 1\right]\right\} - x_j^2} dx_j$$

$$= \frac{1}{\pi(k_f - k_m)} \int_0^r \frac{1}{\left[r\sqrt{\gamma_{SC1} + 1}\right]^2 - x_j^2} dx_j \quad (4.16)$$

where γ_{SC1} is expressed as

$$\gamma_{SC1} = \left(\frac{16}{9\pi v_f^2}\right)^{\frac{1}{3}} \left(\frac{k_m}{k_f - k_m}\right) \tag{4.17}$$

Integrating Eq. (4.16), the thermal resistances of section 1 or 3 can be written as

$$R_1 = R_3 = \left(\frac{1}{2\pi r\left(k_f - k_m\right)}\right)\left(\frac{1}{\sqrt{\gamma_{SC1}+1}} \ln \frac{\sqrt{\gamma_{SC1}+1}+1}{\sqrt{\gamma_{SC1}+1}-1}\right) \tag{4.18}$$

Considering section 2, thermal resistance of this section is expressed as

$$R_2 = \frac{(a-r)-r}{a^2 k_m} = \frac{a-2r}{a^2 k_m} \tag{4.19}$$

Then Eq. (4.18) and (4.19) are substituted into Eq. (4.7) as

$$k_{eff,SC1-1} = \frac{1}{a}\left(\frac{1}{\frac{a-2r}{a^2 k_m} + 2\left(\frac{1}{2\pi r\left(k_f - k_m\right)}\right)\left(\frac{1}{\sqrt{\gamma_{SC1}+1}} \ln \frac{\sqrt{\gamma_{SC1}+1}+1}{\sqrt{\gamma_{SC1}+1}-1}\right)}\right) \tag{4.20}$$

Dividing Eq. (4.20) by k_m, the ratio of $k_{eff,SC1-1}$ and k_m can be derived as

$$\frac{k_{eff,SC1-1}}{k_m} = \frac{1}{a k_m}\left(\frac{1}{\frac{a-2r}{a^2 k_m} + 2\left(\frac{1}{2\pi r\left(k_f - k_m\right)}\right)\left(\frac{1}{\sqrt{\gamma_{SC1}+1}} \ln \frac{\sqrt{\gamma_{SC1}+1}+1}{\sqrt{\gamma_{SC1}+1}-1}\right)}\right)$$

$$= \frac{1}{1 - \frac{2r}{a} + \left(\frac{ak_m}{\pi r(k_f - k_m)}\right)\left(\frac{1}{\sqrt{\gamma_{SC1}+1}} \ln \frac{\sqrt{\gamma_{SC1}+1}+1}{\sqrt{\gamma_{SC1}+1}-1}\right)}$$

$$= \frac{1}{1 - \frac{2r}{2r\left(\frac{\pi}{6v_f}\right)^{\frac{1}{3}}} + \left(\frac{4\pi r^3}{3v_f}\right)^{\frac{1}{3}}\left(\frac{1}{\pi r}\right)\left(\frac{k_m}{k_f - k_m}\right)\left(\frac{1}{\sqrt{\gamma_{SC1}+1}} \ln \frac{\sqrt{\gamma_{SC1}+1}+1}{\sqrt{\gamma_{SC1}+1}-1}\right)}$$

$$= \frac{1}{1 - \left(\frac{6v_f}{\pi}\right)^{\frac{1}{3}} + \left(\frac{4}{3\pi^2 v_f}\right)^{\frac{1}{3}}\left(\frac{k_m}{k_f - k_m}\right)\left(\frac{1}{\sqrt{\gamma_{SC1}+1}} \ln \frac{\sqrt{\gamma_{SC1}+1}+1}{\sqrt{\gamma_{SC1}+1}-1}\right)}$$

$$= \frac{1}{1 - \left(\frac{6v_f}{\pi}\right)^{\frac{1}{3}} + \frac{1}{2}\left(\frac{6v_f}{\pi}\right)^{\frac{1}{3}}\left(\frac{16}{9\pi v_f^2}\right)^{\frac{1}{3}}\left(\frac{k_m}{k_f - k_m}\right)\left(\frac{1}{\sqrt{\gamma_{SC1}+1}} \ln \frac{\sqrt{\gamma_{SC1}+1}+1}{\sqrt{\gamma_{SC1}+1}-1}\right)}$$

$$\frac{k_{eff,SC1-1}}{k_m} = \frac{1}{1 - \left(\frac{6v_f}{\pi}\right)^{\frac{1}{3}}\left[1 - \frac{\gamma_{SC1}}{2\sqrt{\gamma_{SC1}+1}} \ln \frac{\sqrt{\gamma_{SC1}+1}+1}{\sqrt{\gamma_{SC1}+1}-1}\right]} \quad (4.21)$$

Eq. (4.21) is the thermal conductivity model for spherical inclusions as stated in [37].

4.1.1.2 Case II: SC1 Model with the Volume Fraction of Filler = 0.524

In contrast to the previous case, there are no neat polymer layer in this case because each spherical particle touches each other. The value of 0.524 is the maximum packing fraction in case of simple cubic element. The element was divided into two sections as shown in Figure 4.6(a). Sections 1 and 2 contain one-eighth of spherical particle on each corner. The thermal resistances of sections 1 and 2 were considered as parallel arrangement of polymer matrix resistance and filler resistance. Thermal resistance of each section was arranged in series as shown in Figure 4.6(b).

By the definition of series resistance (Eq. (2.32)), the total thermal resistance of this element is the addition of thermal resistances of each section.

$$R_{\Sigma} = R_1 + R_2 \tag{4.22}$$

where R_1 and R_2 is the thermal resistances of sections 1 and 2, respectively.

Then the heat flow can be expressed as

$$Q = \frac{T_1 - T_2}{\frac{a}{Ak_{eff,\mathrm{SC1-2}}}} = \frac{T_1 - T_2}{R_1 + R_2} \tag{4.23}$$

where $k_{eff,\mathrm{SC1-2}}$ is the effective thermal conductivity of case II of SC1 model and $A = a^2$ is the area perpendicular to the heat flow.

Rearranging Eq. (4.23), $k_{eff,\mathrm{SC1-2}}$ can be given as

$$k_{eff,\mathrm{SC1-2}} = \frac{1}{a}\left(\frac{1}{R_1 + R_2}\right) \tag{4.24}$$

Note that the thermal resistance of section 1 is equivalent to that of section 2, thus they were considered together. The element was divided into very thin layer j that its thickness is Δx_j, as shown in Figure 4.6(a). The resistance of a layer j is parallel resistance due to polymer matrix resistance $R_{m,j}$ and filler resistance $R_{f,j}$. These layers are arranged in series pattern. Therefore, the thermal resistances of sections 1 and 2 can be written as

$$R_1 = R_2 = \sum_{j=0}^{r}\left(\frac{1}{R_{m,j}} + \frac{1}{R_{f,j}}\right)^{-1} \tag{4.25}$$

(a) Physical model (b) Thermal circuit model

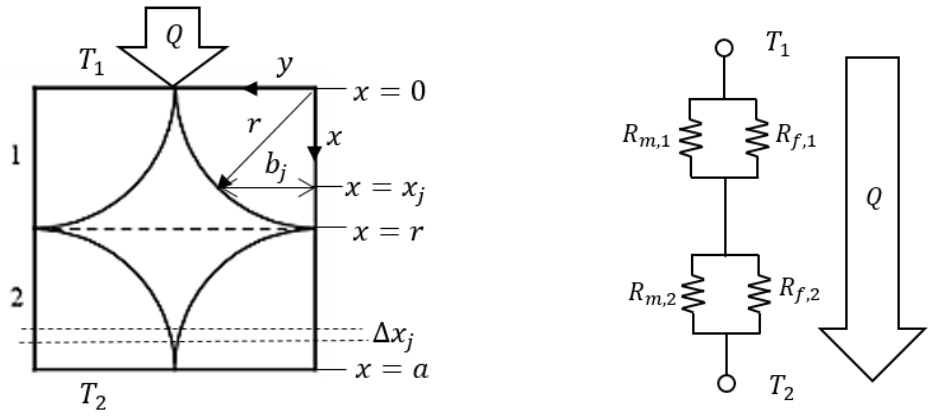

Figure 4.6 (a) Physical and (b) Thermal circuit model of simple cubic element with filler volume fraction equal to 0.524

Because there are one fourth of a circle on each corner of the square plane (y, z) of layer *j*, thus there is one circle in each layer and then $R_{f,j}$ is similar to Eq. (4.9) and $R_{m,j}$ is also similar to Eq. (4.11).

Substituting Eq. (4.9), (4.10) and (4.11) into Eq. (4.25), it leads to

$$R_1 = R_2 = \sum_{j=0}^{r} \frac{\Delta x_j}{a^2 k_m + \pi(k_f - k_m)(r^2 - x_j^2)} \tag{4.26}$$

When Δx_j approaches to zero, it can be written as

$$R_1 = R_2 = \lim_{\Delta x_j \to 0} \sum_{j=0}^{r} \frac{\Delta x_j}{a^2 k_m + \pi(k_f - k_m)(r^2 - x_j^2)}$$

$$= \int_0^r \frac{1}{a^2 k_m + \pi(k_f - k_m)(r^2 - x_j^2)} dx_j \tag{4.27}$$

Eq. (4.27) can be further arranged and it gave the same result with Eq. (4.14). Here, that equation was written again as

$$R_1 = R_2 = \frac{1}{\pi\left(k_f - k_m\right)} \int_0^r \frac{1}{\left\{r^2\left[\frac{a^2}{\pi r^2}\left(\frac{k_m}{k_f - k_m}\right) + 1\right]\right\} - x_j^2} dx_j \tag{4.28}$$

Substituting Eq. (4.15) into Eq. (4.28), it led to the result similar to Eq. (4.16).

$$R_1 = R_2 = \frac{1}{\pi\left(k_f - k_m\right)} \int_0^r \frac{1}{\left[r\sqrt{\gamma_{\mathrm{SC1}} + 1}\right]^2 - x_j^2} dx_j \tag{4.29}$$

where γ_{SC1} is expressed as

$$\gamma_{\mathrm{SC1}} = \left(\frac{16}{9\pi v_f^2}\right)^{\frac{1}{3}} \left(\frac{k_m}{k_f - k_m}\right) \tag{4.30}$$

Integrating Eq. (4.29), the thermal resistance of sectiosn 1 or 2 can be written as

$$R_1 = R_2 = \left(\frac{1}{2\pi r\left(k_f - k_m\right)}\right)\left(\frac{1}{\sqrt{\gamma_{\mathrm{SC1}} + 1}} \ln \frac{\sqrt{\gamma_{\mathrm{SC1}} + 1} + 1}{\sqrt{\gamma_{\mathrm{SC1}} + 1} - 1}\right) \tag{4.31}$$

Then Eq. (4.31) was substituted into Eq. (4.24) as

$$k_{eff,\mathrm{SC1-2}} = \frac{1}{a}\left(\frac{1}{2\left(\frac{1}{2\pi r\left(k_f - k_m\right)}\right)\left(\frac{1}{\sqrt{\gamma_{\mathrm{SC1}} + 1}} \ln \frac{\sqrt{\gamma_{\mathrm{SC1}} + 1} + 1}{\sqrt{\gamma_{\mathrm{SC1}} + 1} - 1}\right)}\right) \tag{4.32}$$

Dividing Eq. (4.20) by k_m, the ratio of $k_{eff,\mathrm{SC1-2}}$ and k_m can be derived as

$$\frac{k_{eff,\mathrm{SC1-2}}}{k_m} = \frac{1}{ak_m}\left(\frac{1}{2\left(\frac{1}{2\pi r\left(k_f - k_m\right)}\right)\left(\frac{1}{\sqrt{\gamma_{\mathrm{SC1}}+1}}\ln\frac{\sqrt{\gamma_{\mathrm{SC1}}+1}+1}{\sqrt{\gamma_{\mathrm{SC1}}+1}-1}\right)}\right)$$

$$= \frac{1}{\left(\frac{ak_m}{\pi r\left(k_f - k_m\right)}\right)\left(\frac{1}{\sqrt{\gamma_{\mathrm{SC1}}+1}}\ln\frac{\sqrt{\gamma_{\mathrm{SC1}}+1}+1}{\sqrt{\gamma_{\mathrm{SC1}}+1}-1}\right)}$$

$$= \frac{1}{\left(\frac{4\pi r^3}{3v_f}\right)^{\frac{1}{3}}\left(\frac{1}{\pi r}\right)\left(\frac{k_m}{k_f - k_m}\right)\left(\frac{1}{\sqrt{\gamma_{\mathrm{SC1}}+1}}\ln\frac{\sqrt{\gamma_{\mathrm{SC1}}+1}+1}{\sqrt{\gamma_{\mathrm{SC1}}+1}-1}\right)}$$

$$= \frac{1}{\left(\frac{4}{3\pi^2 v_f}\right)^{\frac{1}{3}}\left(\frac{k_m}{k_f - k_m}\right)\left(\frac{1}{\sqrt{\gamma_{\mathrm{SC1}}+1}}\ln\frac{\sqrt{\gamma_{\mathrm{SC1}}+1}+1}{\sqrt{\gamma_{\mathrm{SC1}}+1}-1}\right)}$$

$$= \frac{1}{\frac{1}{2}\left(\frac{6v_f}{\pi}\right)^{\frac{1}{3}}\left(\frac{16}{9\pi v_f^2}\right)^{\frac{1}{3}}\left(\frac{k_m}{k_f - k_m}\right)\left(\frac{1}{\sqrt{\gamma_{\mathrm{SC1}}+1}}\ln\frac{\sqrt{\gamma_{\mathrm{SC1}}+1}+1}{\sqrt{\gamma_{\mathrm{SC1}}+1}-1}\right)}$$

$$\frac{k_{eff,\mathrm{SC1-2}}}{k_m} = \frac{1}{\left(\frac{6v_f}{\pi}\right)^{\frac{1}{3}}\left[\frac{\gamma_{\mathrm{SC1}}}{2\sqrt{\gamma_{\mathrm{SC1}}+1}}\ln\frac{\sqrt{\gamma_{\mathrm{SC1}}+1}+1}{\sqrt{\gamma_{\mathrm{SC1}}+1}-1}\right]} \tag{4.33}$$

Eq. (4.33) is different from Eq. (4.21) due to the absence of the neat polymer layer in the RVE. Eq. (4.33) predicts the effective thermal conductivity of the composite when filler network is formed by the contact of spherical particles which are ideally arranged in form of simple cubic structure.

4.1.2 Body-centered Cubic Model (BCC1 Model)

4.1.2.1 Case III: BCC1 Model with the Volume Fraction of Filler < 0.131

In case of BCC element with filler volume fraction less than 0.131, the element was divided into six sections as shown in Figure 4.7(a). Sections 1 and 6 contain one-eighth of spherical particle on each corner and the rest is polymer matrix. Sections 2 and 5 contain neat polymer matrix. Sections 3 and 4 contain half of spherical particle in the center. The thermal resistances of sections 1, 3, 4, and 6 were considered as parallel arrangement of polymer matrix resistance and filler resistance, while the thermal resistances of section 2 and 5 come from only the polymer matrix. Thermal resistance of each section was arranged in series as shown in Figure 4.7(b) where $R_{m,i}$ is the polymer matrix thermal resistance of section i and $R_{f,i}$ is the filler thermal resistance of section i, $i = 1, 2, 3, 4, 5, 6$.

By the definition of series resistance (Eq. (2.32)), the total thermal resistance of this element is the addition of thermal resistances of each section.

$$R_{\Sigma} = R_1 + R_2 + R_3 + R_4 + R_5 + R_6 \tag{4.34}$$

where R_i is the thermal resistance of section i.

Then the heat flow can be written as

$$Q = \frac{T_1 - T_2}{\frac{a}{Ak_{eff,\mathrm{BCC1-1}}}} = \frac{T_1 - T_2}{R_1 + R_2 + R_3 + R_4 + R_5 + R_6} \tag{4.35}$$

where $k_{eff,\mathrm{BCC1-1}}$ is the effective thermal conductivity of case III of BCC1 model, and A is the area perpendicular to the heat flow.

Due to $A = a^2$, $k_{eff,\mathrm{BCC1-1}}$ can be derived by rearranging Eq. (4.35) as

$$k_{eff,\mathrm{BCC1-1}} = \frac{1}{a}\left(\frac{1}{R_1 + R_2 + R_3 + R_4 + R_5 + R_6}\right) \tag{4.36}$$

Note that the thermal resistance of section 1 is equivalent to that of sections 3, 4, and 6, thus they were considered together. It can be imagined that the element was divided into very thin layer j that its thickness is Δx_j, as shown in Figure 4.7(a). The resistance of a layer j is parallel resistances due to polymer matrix resistance $R_{m,j}$ and filler resistance $R_{f,j}$. These layers are arranged in series pattern. Therefore, the thermal resistances of sections 1, 3, 4, and 6 can be written as

$$R_1 = R_3 = R_4 = R_6 = \sum_{j=0}^{r} \left(\frac{1}{R_{m,j}} + \frac{1}{R_{f,j}} \right)^{-1} \tag{4.37}$$

(a) Physical model (b) Thermal circuit model

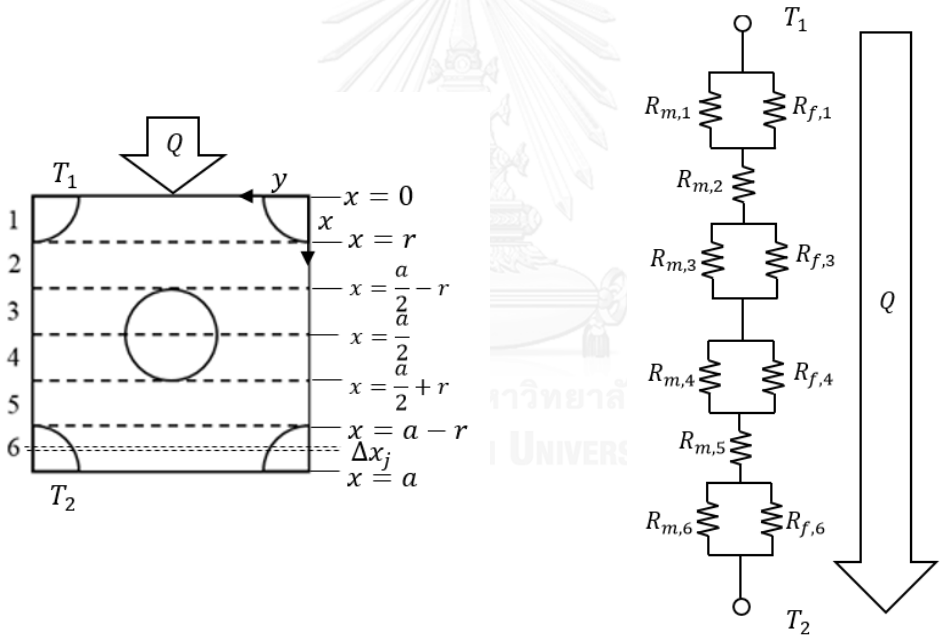

Figure 4.7 (a) Physical and (b) Thermal circuit model of body-centered cubic element with filler volume fraction < 0.131

Because there is one fourth of a circle on each corner of the square plane (y, z) in sections 1 and 6 and there is a circle on center of the square plane (y, z) in sections 3 and 4, thus there is one circle in each layer and then $R_{f,j}$ can be written as

$$R_{f,j} = \frac{\Delta x_j}{(\pi b_j^2) k_f} \tag{4.38}$$

where b_j is the radius of circle at $x = x_j$ as defined in Eq. (4.10).

The remaining area is of polymer matrix. Thus $R_{m,j}$ is expressed as

$$R_{m,j} = \frac{\Delta x_j}{(a^2 - \pi b_j^2) k_m} \tag{4.39}$$

Substituting Eq. (4.38) and (4.39) into Eq. (4.37), it can be rearranged as

$$R_1 = R_3 = R_4 = R_6 = \sum_{j=0}^{r} \frac{\Delta x_j}{a^2 k_m + \pi (k_f - k_m)(r^2 - x_j^2)} \tag{4.40}$$

When Δx_j approaches zero, it can be written as

$$\begin{aligned} R_1 = R_3 = R_4 = R_6 &= \lim_{\Delta x_j \to 0} \sum_{j=0}^{r} \frac{\Delta x_j}{a^2 k_m + \pi (k_f - k_m)(r^2 - x_j^2)} \\ &= \int_0^r \frac{1}{a^2 k_m + \pi (k_f - k_m)(r^2 - x_j^2)} dx_j \end{aligned} \tag{4.41}$$

Before integrating, Eq. (4.41) can be further arranged as

$$\begin{aligned} R_1 = R_3 = R_4 = R_6 &= \frac{1}{\pi (k_f - k_m)} \int_0^r \frac{1}{\left[\frac{k_m + \frac{\pi r^2}{a^2}(k_f - k_m)}{\frac{\pi}{a^2}(k_f - k_m)} \right] - x_j^2} dx_j \\ &= \frac{1}{\pi (k_f - k_m)} \int_0^r \frac{1}{\left\{ \left(\frac{a^2}{\pi} \right) \left(\frac{\pi r^2}{a^2} \right) \left[\frac{a^2}{\pi r^2} \left(\frac{k_m}{k_f - k_m} \right) + 1 \right] \right\} - x_j^2} dx_j \end{aligned}$$

$$= \frac{1}{\pi\left(k_f - k_m\right)} \int_0^r \frac{1}{\left\{r^2\left[\frac{a^2}{\pi r^2}\left(\frac{k_m}{k_f - k_m}\right) + 1\right]\right\} - x_j^2} dx_j \tag{4.42}$$

From Eq. (4.3), the length of RVE for BCC can be written in form of

$$a = \left(\frac{8\pi r^3}{3v_f}\right)^{\frac{1}{3}} \tag{4.43}$$

Substituting Eq. (4.43) into Eq. (4.42), it goes to be

$$R_1 = R_3 = R_4 = R_6 = \frac{1}{\pi\left(k_f - k_m\right)} \int_0^r \frac{1}{\left\{r^2\left[\left(\frac{8\pi r^3}{3v_f}\right)^{\frac{2}{3}}\left(\frac{1}{\pi r^2}\right)\left(\frac{k_m}{k_f - k_m}\right) + 1\right]\right\} - x_j^2} dx_j$$

$$= \frac{1}{\pi\left(k_f - k_m\right)} \int_0^r \frac{1}{\left\{r^2\left[\left(\frac{64}{9\pi v_f^2}\right)^{\frac{1}{3}}\left(\frac{k_m}{k_f - k_m}\right) + 1\right]\right\} - x_j^2} dx_j$$

$$= \frac{1}{\pi\left(k_f - k_m\right)} \int_0^r \frac{1}{\left[r\sqrt{\gamma_{\mathrm{BCC1}} + 1}\right]^2 - x_j^2} dx_j \tag{4.44}$$

where γ_{BCC1} is expressed as

$$\gamma_{\mathrm{BCC1}} = \left(\frac{64}{9\pi v_f^2}\right)^{\frac{1}{3}}\left(\frac{k_m}{k_f - k_m}\right) \tag{4.45}$$

Integrating Eq. (4.44), the thermal resistances of these sections can be written as

$$R_1 = R_3 = R_4 = R_6 = \left(\frac{1}{2\pi r\left(k_f - k_m\right)}\right)\left(\frac{1}{\sqrt{\gamma_{\mathrm{BCC1}} + 1}} \ln \frac{\sqrt{\gamma_{\mathrm{BCC1}} + 1} + 1}{\sqrt{\gamma_{\mathrm{BCC1}} + 1} - 1}\right) \tag{4.46}$$

Considering sections 2 and 5, thermal resistance is expressed as

$$R_2 = R_5 = \frac{\left(\frac{a}{2} - r\right) - r}{a^2 k_m} = \frac{\frac{a}{2} - 2r}{a^2 k_m} \tag{4.47}$$

Then Eq. (4.46) and (4.47) are substituted into Eq. (4.36) as

$$k_{eff,\mathrm{BCC1-1}} = \frac{1}{a}\left(\frac{1}{2\left(\frac{\frac{a}{2} - 2r}{a^2 k_m}\right) + 4\left(\frac{1}{2\pi r\left(k_f - k_m\right)}\right)\left(\frac{1}{\sqrt{\gamma_{\mathrm{BCC1}} + 1}} \ln \frac{\sqrt{\gamma_{\mathrm{BCC1}} + 1} + 1}{\sqrt{\gamma_{\mathrm{BCC1}} + 1} - 1}\right)}\right) \tag{4.48}$$

Dividing Eq. (4.48) by k_m, the ratio of $k_{eff,\mathrm{BCC1-1}}$ and k_m can be derived as

$$\frac{k_{eff,\mathrm{BCC1-1}}}{k_m} = \frac{1}{a k_m}\left(\frac{1}{\frac{a - 4r}{a^2 k_m} + 4\left(\frac{1}{2\pi r\left(k_f - k_m\right)}\right)\left(\frac{1}{\sqrt{\gamma_{\mathrm{BCC1}} + 1}} \ln \frac{\sqrt{\gamma_{\mathrm{BCC1}} + 1} + 1}{\sqrt{\gamma_{\mathrm{BCC1}} + 1} - 1}\right)}\right)$$

$$= \frac{1}{1 - \frac{4r}{a} + 2\left(\frac{a k_m}{\pi r\left(k_f - k_m\right)}\right)\left(\frac{1}{\sqrt{\gamma_{\mathrm{BCC1}} + 1}} \ln \frac{\sqrt{\gamma_{\mathrm{BCC1}} + 1} + 1}{\sqrt{\gamma_{\mathrm{BCC1}} + 1} - 1}\right)}$$

$$= \frac{1}{1 - \frac{4r}{2r\left(\frac{\pi}{3v_f}\right)^{\frac{1}{3}}} + 2\left(\frac{8\pi r^3}{3v_f}\right)^{\frac{1}{3}}\left(\frac{1}{\pi r}\right)\left(\frac{k_m}{k_f - k_m}\right)\left(\frac{1}{\sqrt{\gamma_{\mathrm{BCC1}} + 1}} \ln \frac{\sqrt{\gamma_{\mathrm{BCC1}} + 1} + 1}{\sqrt{\gamma_{\mathrm{BCC1}} + 1} - 1}\right)}$$

$$= \frac{1}{1 - 2\left(\frac{3v_f}{\pi}\right)^{\frac{1}{3}} + 2\left(\frac{8}{3\pi^2 v_f}\right)^{\frac{1}{3}}\left(\frac{k_m}{k_f - k_m}\right)\left(\frac{1}{\sqrt{\gamma_{\mathrm{BCC1}} + 1}} \ln \frac{\sqrt{\gamma_{\mathrm{BCC1}} + 1} + 1}{\sqrt{\gamma_{\mathrm{BCC1}} + 1} - 1}\right)}$$

$$= \frac{1}{1 - 2\left(\frac{3v_f}{\pi}\right)^{\frac{1}{3}} + \frac{2}{2}\left(\frac{3v_f}{\pi}\right)^{\frac{1}{3}}\left(\frac{64}{9\pi v_f^2}\right)^{\frac{1}{3}}\left(\frac{k_m}{k_f - k_m}\right)\left(\frac{1}{\sqrt{\gamma_{\mathrm{BCC1}} + 1}}\ln\frac{\sqrt{\gamma_{\mathrm{BCC1}} + 1} + 1}{\sqrt{\gamma_{\mathrm{BCC1}} + 1} - 1}\right)}$$

$$\frac{k_{eff,\mathrm{BCC1-1}}}{k_m} = \frac{1}{1 - \left(\frac{24v_f}{\pi}\right)^{\frac{1}{3}}\left[1 - \frac{\gamma_{\mathrm{BCC1}}}{2\sqrt{\gamma_{\mathrm{BCC1}} + 1}}\ln\frac{\sqrt{\gamma_{\mathrm{BCC1}} + 1} + 1}{\sqrt{\gamma_{\mathrm{BCC1}} + 1} - 1}\right]} \tag{4.49}$$

4.1.2.2 Case IV: BCC1 Model with the Volume Fraction of Filler = 0.131

In case of BCC element with filler volume fraction equal to 0.131, the element was divided into four sections as shown in Figure 4.8(a). Sections 1 and 4 contain one-eighth of spherical particle on each corner and the rest is polymer matrix. Sections 2 and 3 contain half of a spherical particle on center of each section. The thermal resistances of each section were considered as parallel arrangement of polymer matrix resistance and filler resistance. Thermal resistances of each section were arranged in series as shown in Figure 4.8(b) where $R_{m,i}$ is the polymer matrix thermal resistance of section i and $R_{f,i}$ is the filler thermal resistance of section i, $i = 1, 2, 3, 4$.

By the definition of series resistance (Eq. (2.32)), the total thermal resistance of this element is the addition of thermal resistances of each section.

$$R_\Sigma = R_1 + R_2 + R_3 + R_4 \tag{4.50}$$

where R_i is the thermal resistance of section i.

Then the heat flow can be written as

$$Q = \frac{T_1 - T_2}{\frac{a}{Ak_{eff,\mathrm{BCC1-2}}}} = \frac{T_1 - T_2}{R_1 + R_2 + R_3 + R_4} \tag{4.51}$$

where $k_{eff,\mathrm{BCC1-2}}$ is the effective thermal conductivity of case IV of BCC1-2 and A is the area perpendicular to the heat flow.

Due to $A = a^2$, $k_{eff,\mathrm{BCC1-2}}$ can be derived by rearranging Eq. (4.51) as

$$k_{eff,\mathrm{BCC1-2}} = \frac{1}{a}\left(\frac{1}{R_1 + R_2 + R_3 + R_4}\right) \tag{4.52}$$

Note that the thermal resistances of every sections are equal, thus they were considered together. It can be imagined that the element is divided into very thin layer *j* that its thickness is Δx_j, as shown in Figure 4.8(a). The resistance of a layer *j* is parallel resistance due to polymer matrix resistance $R_{m,j}$ and filler resistance $R_{f,j}$. These layers arrange in series pattern. Therefore, the thermal resistances of sections 1, 2, 3, and 4 can be written as

$$R_1 = R_2 = R_3 = R_4 = \sum_{j=0}^{r}\left(\frac{1}{R_{m,j}} + \frac{1}{R_{f,j}}\right)^{-1} \tag{4.53}$$

Because there is one circle in each layer, then $R_{f,j}$ can be written as

$$R_{f,j} = \frac{\Delta x_j}{(\pi b_j^2)k_f} \tag{4.54}$$

where b_j is the radius of circle at $x = x_j$ as defined in Eq. (4.10).

(a) Physical model (b) Thermal circuit model

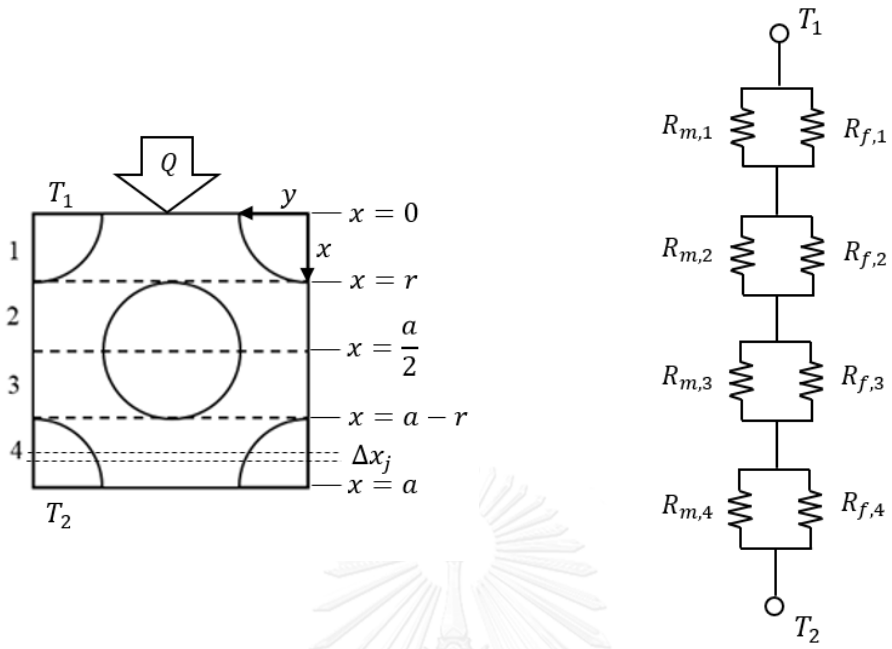

Figure 4.8 (a) Physical and (b) Thermal circuit model of body-centered cubic element with filler volume fraction = 0.131

The remaining area is of polymer matrix. Thus $R_{m,j}$ is expressed as

$$R_{m,j} = \frac{\Delta x_j}{\left(a^2 - \pi b_j^2\right) k_m} \tag{4.55}$$

Substituting Eq. (4.54) and (4.55) into Eq. (4.53), it can be rearranged as

$$R_1 = R_2 = R_3 = R_4 = \sum_{j=0}^{r} \frac{\Delta x_j}{a^2 k_m + \pi\left(k_f - k_m\right)\left(r^2 - x_j^2\right)} \tag{4.56}$$

When Δx_j approaches zero, it can be written as

$$R_1 = R_2 = R_3 = R_4 = \lim_{\Delta x_j \to 0} \sum_{j=0}^{r} \frac{\Delta x_j}{a^2 k_m + \pi(k_f - k_m)(r^2 - x_j^2)}$$

$$= \int_0^r \frac{1}{a^2 k_m + \pi(k_f - k_m)(r^2 - x_j^2)} dx_j \tag{4.57}$$

Before integrating, Eq. (4.57) can be further arranged as

$$R_1 = R_2 = R_3 = R_4 = \frac{1}{\pi(k_f - k_m)} \int_0^r \frac{1}{\left[\frac{k_m + \frac{\pi r^2}{a^2}(k_f - k_m)}{\frac{\pi}{a^2}(k_f - k_m)}\right] - x_j^2} dx_j$$

$$= \frac{1}{\pi(k_f - k_m)} \int_0^r \frac{1}{\left\{\left(\frac{a^2}{\pi}\right)\left(\frac{\pi r^2}{a^2}\right)\left[\frac{a^2}{\pi r^2}\left(\frac{k_m}{k_f - k_m}\right) + 1\right]\right\} - x_j^2} dx_j$$

$$= \frac{1}{\pi(k_f - k_m)} \int_0^r \frac{1}{\left\{r^2\left[\frac{a^2}{\pi r^2}\left(\frac{k_m}{k_f - k_m}\right) + 1\right]\right\} - x_j^2} dx_j \tag{4.58}$$

Substituting Eq. (4.43) into Eq. (4.58), it goes to be

$$R_1 = R_2 = R_3 = R_4 = \frac{1}{\pi(k_f - k_m)} \int_0^r \frac{1}{\left\{r^2\left[\left(\frac{8\pi r^3}{3v_f}\right)^{\frac{2}{3}}\left(\frac{1}{\pi r^2}\right)\left(\frac{k_m}{k_f - k_m}\right) + 1\right]\right\} - x_j^2} dx_j$$

$$= \frac{1}{\pi(k_f - k_m)} \int_0^r \frac{1}{\left\{r^2\left[\left(\frac{64}{9\pi v_f^2}\right)^{\frac{1}{3}}\left(\frac{k_m}{k_f - k_m}\right) + 1\right]\right\} - x_j^2} dx_j$$

$$= \frac{1}{\pi(k_f - k_m)} \int_0^r \frac{1}{\left[r\sqrt{\gamma_{\mathrm{BCC1}} + 1}\right]^2 - x_j^2} dx_j \tag{4.59}$$

where γ_{BCC1} is expressed as

$$\gamma_{\mathrm{BCC1}} = \left(\frac{64}{9\pi v_f^2}\right)^{\frac{1}{3}}\left(\frac{k_m}{k_f - k_m}\right) \tag{4.60}$$

Integrating Eq. (4.44), the thermal resistance of these sections can be written as

$$\begin{aligned} R_1 = R_2 = R_3 = R_4 \\ = \left(\frac{1}{2\pi r\left(k_f - k_m\right)}\right)\left(\frac{1}{\sqrt{\gamma_{\mathrm{BCC1}} + 1}} \ln \frac{\sqrt{\gamma_{\mathrm{BCC1}} + 1} + 1}{\sqrt{\gamma_{\mathrm{BCC1}} + 1} - 1}\right) \end{aligned} \tag{4.61}$$

Then Eq. (4.61) is substituted into Eq. (4.52) as

$$k_{eff,\mathrm{BCC1-2}} = \frac{1}{a}\left(\frac{1}{4\left(\frac{1}{2\pi r\left(k_f - k_m\right)}\right)\left(\frac{1}{\sqrt{\gamma_{\mathrm{BCC1}} + 1}} \ln \frac{\sqrt{\gamma_{\mathrm{BCC1}} + 1} + 1}{\sqrt{\gamma_{\mathrm{BCC1}} + 1} - 1}\right)}\right) \tag{4.62}$$

Dividing Eq. (4.62) by k_m, the ratio of $k_{eff,\mathrm{BCC1-2}}$ and k_m can be derived as

$$\frac{k_{eff,\mathrm{BCC1-2}}}{k_m} = \frac{1}{ak_m}\left(\frac{1}{4\left(\frac{1}{2\pi r\left(k_f - k_m\right)}\right)\left(\frac{1}{\sqrt{\gamma_{\mathrm{BCC1}} + 1}} \ln \frac{\sqrt{\gamma_{\mathrm{BCC1}} + 1} + 1}{\sqrt{\gamma_{\mathrm{BCC1}} + 1} - 1}\right)}\right)$$

$$= \frac{1}{2\left(\frac{ak_m}{\pi r\left(k_f - k_m\right)}\right)\left(\frac{1}{\sqrt{\gamma_{\mathrm{BCC1}} + 1}} \ln \frac{\sqrt{\gamma_{\mathrm{BCC1}} + 1} + 1}{\sqrt{\gamma_{\mathrm{BCC1}} + 1} - 1}\right)}$$

$$= \frac{1}{2\left(\frac{8\pi r^3}{3v_f}\right)^{\frac{1}{3}}\left(\frac{1}{\pi r}\right)\left(\frac{k_m}{k_f - k_m}\right)\left(\frac{1}{\sqrt{\gamma_{\mathrm{BCC1}} + 1}} \ln \frac{\sqrt{\gamma_{\mathrm{BCC1}} + 1} + 1}{\sqrt{\gamma_{\mathrm{BCC1}} + 1} - 1}\right)}$$

$$= \frac{1}{2\left(\frac{8}{3\pi^2 v_f}\right)^{\frac{1}{3}}\left(\frac{k_m}{k_f - k_m}\right)\left(\frac{1}{\sqrt{\gamma_{\mathrm{BCC1}}+1}}\ln\frac{\sqrt{\gamma_{\mathrm{BCC1}}+1}+1}{\sqrt{\gamma_{\mathrm{BCC1}}+1}-1}\right)}$$

$$= \frac{1}{\frac{2}{2}\left(\frac{3v_f}{\pi}\right)^{\frac{1}{3}}\left(\frac{64}{9\pi v_f^2}\right)^{\frac{1}{3}}\left(\frac{k_m}{k_f - k_m}\right)\left(\frac{1}{\sqrt{\gamma_{\mathrm{BCC1}}+1}}\ln\frac{\sqrt{\gamma_{\mathrm{BCC1}}+1}+1}{\sqrt{\gamma_{\mathrm{BCC1}}+1}-1}\right)}$$

$$\frac{k_{eff,\mathrm{BCC1-2}}}{k_m} = \frac{1}{\left(\frac{24v_f}{\pi}\right)^{\frac{1}{3}}\left(\frac{\gamma_{\mathrm{BCC1}}}{2\sqrt{\gamma_{\mathrm{BCC1}}+1}}\ln\frac{\sqrt{\gamma_{\mathrm{BCC1}}+1}+1}{\sqrt{\gamma_{\mathrm{BCC1}}+1}-1}\right)} \quad (4.63)$$

4.1.2.3 Case V: BCC1 Model with the Volume Fraction of Filler > 0.131

In case of BCC element with filler volume fraction more than 0.131, the element was divided into six sections as shown in Figure 4.9(a). Sections 1 and 6 contain some segment of spherical particle on each corner and the rest is polymer matrix. Sections 2 and 5 contain some segment of spherical particle on each corner and center. Sections 3 and 4 contain some segment of spherical particle on center. The thermal resistances of every sections were considered as parallel arrangement of polymer matrix resistance and filler resistance. Thermal resistance of each section was arranged in series as shown in Figure 4.9(b) where $R_{m,i}$ is the polymer matrix thermal resistance of section i and $R_{f,i}$ is the filler thermal resistance of section i, $i = 1, 2, 3, 4, 5, 6$.

From the definition of series resistance (Eq. (2.32)), the total thermal resistance of this element is the addition of thermal resistances of each section.

$$R_{\Sigma} = R_1 + R_2 + R_3 + R_4 + R_5 + R_6 \quad (4.64)$$

where R_i is the thermal resistance of section i.

Then the heat flow can be written as

$$Q = \frac{T_1 - T_2}{\frac{a}{Ak_{eff,\mathrm{BCC1-3}}}} = \frac{T_1 - T_2}{R_1 + R_2 + R_3 + R_4 + R_5 + R_6} \tag{4.65}$$

where $k_{eff,\mathrm{BCC1-3}}$ is the effective thermal conductivity of case V of BCC1 model, and A is the area perpendicular to the heat flow.

Due to $A = a^2$, $k_{eff,\mathrm{BCC1-3}}$ can be derived by rearranging Eq. (4.65) as

$$k_{eff,\mathrm{BCC1-3}} = \frac{1}{a}\left(\frac{1}{R_1 + R_2 + R_3 + R_4 + R_5 + R_6}\right) \tag{4.66}$$

It is worth to note that the thermal resistance of section 1 is equivalent to that of section 6, the thermal resistance of section 2 is equivalent to that of section 5, and the thermal resistance of section 3 is equivalent to that of section 4. Each section will be considered separately.

It can be imagined that the element is divided into very thin layer *j* that its thickness is Δx_j, as shown in Figure 4.9(a). The resistance of a layer *j* is parallel resistances due to polymer matrix resistance $R_{m,j}$ and filler resistance $R_{f,j}$. These layers arrange in series pattern. Therefore, the thermal resistance of each section can be written as

$$R_i = \sum_{j=0}^{n}\left(\frac{1}{R_{m,j}} + \frac{1}{R_{f,j}}\right)^{-1} \tag{4.67}$$

where subscript j is the layer number.

For sections 1 and 6, because there is one fourth of a circle on each corner of the square plane (y, z), thus there is one circle in each layer and then $R_{f,j}$ can be written as

$$R_{f,j} = \frac{\Delta x_j}{\left(\pi b_j^2\right) k_f} \tag{4.68}$$

where b_j is the radius of circle at $x = x_j$ as defined in Eq. (4.10).

(a) Physical model (b) Thermal circuit model

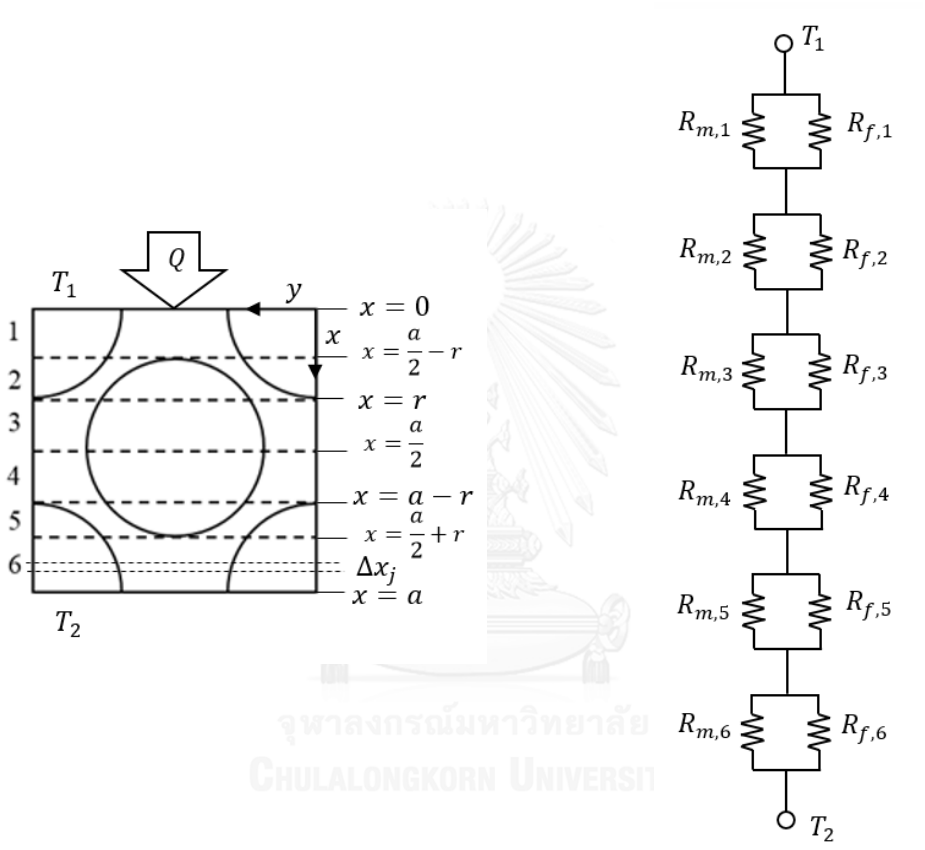

Figure 4.9 (a) Physical and (b) Thermal circuit model of body-centered cubic element with filler volume fraction > 0.131

The remaining area is of polymer matrix. Thus $R_{m,j}$ is expressed as

$$R_{m,j} = \frac{\Delta x_j}{\left(a^2 - \pi b_j^2\right)k_m} \tag{4.69}$$

Substituting Eq. (4.68) and (4.69) into Eq. (4.67), it can be arranged in form of

$$R_1 = R_6 = \sum_{j=0}^{\frac{a}{2}-r} \frac{\Delta x_j}{a^2 k_m + \pi\left(k_f - k_m\right)\left(r^2 - x_j^2\right)} \tag{4.70}$$

When Δx_j approaches to zero, it can be written as

$$\begin{aligned} R_1 = R_6 &= \lim_{\Delta x_j \to 0} \sum_{j=0}^{\frac{a}{2}-r} \frac{\Delta x_j}{a^2 k_m + \pi\left(k_f - k_m\right)\left(r^2 - x_j^2\right)} \\ &= \int_0^{\frac{a}{2}-r} \frac{1}{a^2 k_m + \pi\left(k_f - k_m\right)\left(r^2 - x_j^2\right)} dx_j \end{aligned} \tag{4.71}$$

Before integrating, Eq. (4.71) can be further arranged as

$$\begin{aligned} R_1 = R_6 &= \frac{1}{\pi\left(k_f - k_m\right)} \int_0^{\frac{a}{2}-r} \frac{1}{\left[\frac{k_m + \frac{\pi r^2}{a^2}\left(k_f - k_m\right)}{\frac{\pi}{a^2}\left(k_f - k_m\right)}\right] - x_j^2} dx_j \\ &= \frac{1}{\pi\left(k_f - k_m\right)} \int_0^{\frac{a}{2}-r} \frac{1}{\left\{\left(\frac{a^2}{\pi}\right)\left(\frac{\pi r^2}{a^2}\right)\left[\frac{a^2}{\pi r^2}\left(\frac{k_m}{k_f - k_m}\right) + 1\right]\right\} - x_j^2} dx_j \\ &= \frac{1}{\pi\left(k_f - k_m\right)} \int_0^{\frac{a}{2}-r} \frac{1}{\left\{r^2\left[\frac{a^2}{\pi r^2}\left(\frac{k_m}{k_f - k_m}\right) + 1\right]\right\} - x_j^2} dx_j \end{aligned} \tag{4.72}$$

Substituting Eq. (4.43) into Eq. (4.72), it leads to

$$R_1 = R_6 = \frac{1}{\pi\left(k_f - k_m\right)} \int_0^{\frac{a}{2}-r} \frac{1}{\left\{ r^2 \left[\left(\frac{8\pi r^3}{3v_f} \right)^{\frac{2}{3}} \left(\frac{1}{\pi r^2} \right) \left(\frac{k_m}{k_f - k_m} \right) + 1 \right] \right\} - x_j^2} dx_j$$

$$= \frac{1}{\pi\left(k_f - k_m\right)} \int_0^{\frac{a}{2}-r} \frac{1}{\left\{ r^2 \left[\left(\frac{64}{9\pi v_f^2} \right)^{\frac{1}{3}} \left(\frac{k_m}{k_f - k_m} \right) + 1 \right] \right\} - x_j^2} dx_j$$

$$= \frac{1}{\pi\left(k_f - k_m\right)} \int_0^{\frac{a}{2}-r} \frac{1}{\left[r\sqrt{\gamma_{\mathrm{BCC1}} + 1} \right]^2 - x_j^2} dx_j \tag{4.73}$$

where γ_{BCC1} is expressed as

$$\gamma_{\mathrm{BCC1}} = \left(\frac{64}{9\pi v_f^2} \right)^{\frac{1}{3}} \left(\frac{k_m}{k_f - k_m} \right) \tag{4.74}$$

Integrating Eq. (4.73), the thermal resistances of sections 1 and 6 can be written as

$$R_1 = R_6 = \left(\frac{1}{2\pi r\left(k_f - k_m\right)} \right) \left(\frac{1}{\sqrt{\gamma_{\mathrm{BCC1}} + 1}} \ln \frac{\sqrt{\gamma_{\mathrm{BCC1}} + 1} + \beta_{\mathrm{BCC1}}}{\sqrt{\gamma_{\mathrm{BCC1}} + 1} - \beta_{\mathrm{BCC1}}} \right) \tag{4.75}$$

where β_{BCC1} is defined as

$$\beta_{\mathrm{BCC1}} = \left(\frac{\pi}{3v_f} \right)^{\frac{1}{3}} - 1 \tag{4.76}$$

For sections 2 and 5, there are one fourth of a circle on each corner and one circle on center of the square plane (y, z), thus there is two circle in each layer and then $R_{f,j}$ can be written as

$$R_{f,j} = \frac{\Delta x_j}{\left(\pi b_j^2 + \pi d_j^2\right) k_f} \tag{4.77}$$

where b_j is the radius of circle at $x = x_j$ as defined in Eq. (4.10) and d_j is the radius of circle at $x = x_j$ as follows

$$d_j = \sqrt{r^2 - \left(\frac{a}{2} - x_j\right)^2} \tag{4.78}$$

The illustration of Eq. (4.78) is shown as Figure 4.10.

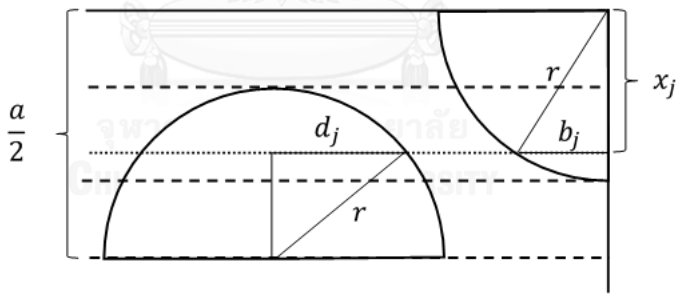

Figure 4.10 Radius of two spherical particles on plane (y, z) in section 2 of body-centered cubic element with filler volume fraction > 0.131

The remaining area is of polymer matrix. Thus $R_{m,j}$ is expressed as

$$R_{m,j} = \frac{\Delta x_j}{\left(a^2 - \pi b_j^2 - \pi d_j^2\right)k_m} \tag{4.79}$$

Substituting Eq. (4.77) and (4.79) into Eq. (4.67), thermal resistances of sections 2 and 5 can be written as

$$R_2 = R_5 = \sum_{j=\frac{a}{2}-r}^{r} \frac{\Delta x_j}{-2\pi(k_f - k_m)x_j^2 + a\pi(k_f - k_m)x_j + k_m a^2 + 2\pi r^2(k_f - k_m) - \frac{\pi a^2}{4}(k_f - k_m)}$$

$$= \frac{1}{\pi(k_f - k_m)} \sum_{j=\frac{a}{2}-r}^{r} \frac{\Delta x_j}{-2x_j^2 + ax_j + \frac{k_m a^2}{\pi(k_f - k_m)} + 2r^2 - \frac{a^2}{4}} \tag{4.80}$$

When Δx_j approaches zero, it can be written as

$$R_2 = R_5 = \lim_{\Delta x_j \to 0} \frac{1}{\pi(k_f - k_m)} \sum_{j=\frac{a}{2}-r}^{r} \frac{\Delta x_j}{-2x_j^2 + ax_j + \frac{k_m a^2}{\pi(k_f - k_m)} + 2r^2 - \frac{a^2}{4}}$$

$$= \frac{1}{\pi(k_f - k_m)} \int_{\frac{a}{2}-r}^{r} \frac{1}{-2x_j^2 + ax_j + \frac{k_m a^2}{\pi(k_f - k_m)} + 2r^2 - \frac{a^2}{4}} dx_j \tag{4.81}$$

Before integrating, Eq. (4.81) can be further arranged as

$$R_2 = R_5 = \frac{1}{\pi(k_f - k_m)} \int_{\frac{a}{2}-r}^{r} \frac{1}{-2x_j^2 + ax_j + \frac{k_m a^2}{\pi(k_f - k_m)} + 2r^2 - \frac{a^2}{4}} dx_j$$

$$= \frac{1}{\pi(k_f - k_m)} \int_{\frac{a}{2}-r}^{r} \frac{1}{-2x_j^2 + ax_j + \left\{\left(\frac{a^2}{\pi}\right)\left(\frac{\pi r^2}{a^2}\right)\left[\frac{a^2}{\pi r^2}\left(\frac{k_m}{k_f - k_m}\right) - \frac{a^2}{4r^2} + 2\right]\right\}} dx_j$$

$$= \frac{1}{\pi(k_f - k_m)} \int_{\frac{a}{2}-r}^{r} \frac{1}{-2x_j^2 + ax_j + \left\{ r^2 \left[\frac{a^2}{\pi r^2} \left(\frac{k_m}{k_f - k_m} \right) - \frac{a^2}{4r^2} + 2 \right] \right\}} dx_j \tag{4.82}$$

Substituting Eq. (4.43) into Eq. (4.82), it leads to

$$R_2 = R_5 = \frac{1}{\pi(k_f - k_m)} \int_{\frac{a}{2}-r}^{r} \frac{1}{-2x_j^2 + ax_j + \left\{ r^2 \left[\left(\frac{8\pi r^3}{3v_f} \right)^{\frac{2}{3}} \left(\frac{1}{\pi r^2} \right) \left(\frac{k_m}{k_f - k_m} \right) - \left(\frac{8\pi r^3}{3v_f} \right)^{\frac{2}{3}} \left(\frac{1}{4r^2} \right) + 2 \right] \right\}} dx_j$$

$$= \frac{1}{\pi(k_f - k_m)} \int_{\frac{a}{2}-r}^{r} \frac{1}{-2x_j^2 + ax_j + \left\{ r^2 \left[\left(\frac{64}{9\pi v_f^2} \right)^{\frac{1}{3}} \left(\frac{k_m}{k_f - k_m} \right) - \left(\frac{\pi}{3v_f} \right)^{\frac{2}{3}} + 2 \right] \right\}} dx_j$$

$$= \frac{1}{\pi(k_f - k_m)} \int_{\frac{a}{2}-r}^{r} \frac{1}{-2x_j^2 + ax_j + \left\{ r^2 \left[\gamma_{\mathrm{BCC1}} - \left(\frac{\pi}{3v_f} \right)^{\frac{2}{3}} + 2 \right] \right\}} dx_j \tag{4.83}$$

where γ_{BCC1} is defined as Eq. (4.74).

Integrating Eq. (4.83), the thermal resistances of sections 2 and 5 can be written as

$$R_2 = R_5 = \left(\frac{1}{\pi r(k_f - k_m)} \right) \left(\frac{2}{\sqrt{4 + 2\gamma_{\mathrm{BCC1}} - \left(\frac{\pi}{3v_f} \right)^{\frac{2}{3}}}} \ln \frac{2 - \left(\frac{\pi}{3v_f} \right)^{\frac{1}{3}} + \sqrt{4 + 2\gamma_{\mathrm{BCC1}} - \left(\frac{\pi}{3v_f} \right)^{\frac{2}{3}}}}{2 - \left(\frac{\pi}{3v_f} \right)^{\frac{1}{3}} - \sqrt{4 + 2\gamma_{\mathrm{BCC1}} - \left(\frac{\pi}{3v_f} \right)^{\frac{2}{3}}}} \right)$$

$$R_2 = R_5 = \left(\frac{1}{\pi r(k_f - k_m)} \right) \left(\frac{2}{\delta_{\mathrm{BCC1}}} \ln \frac{1 - \beta_{\mathrm{BCC1}} + \delta_{\mathrm{BCC1}}}{1 - \beta_{\mathrm{BCC1}} - \delta_{\mathrm{BCC1}}} \right) \tag{4.84}$$

where β_{BCC1} is defined as Eq. (4.76) and δ_{BCC1} is expressed as

$$\delta_{\mathrm{BCC1}} = \sqrt{4 + 2\gamma_{\mathrm{BCC1}} - \left(\frac{\pi}{3v_f}\right)^{\frac{2}{3}}} = \sqrt{4 + 2\gamma_{\mathrm{BCC1}} - (\beta_{\mathrm{BCC1}} + 1)^2} \tag{4.85}$$

For sections 3 and 4, there is one circle on center in each layer of the square plane (y, z) and then $R_{f,j}$ can be written as

$$R_{f,j} = \frac{\Delta x_j}{(\pi d_j^2) k_f} \tag{4.86}$$

where d_j is the radius of circle at $x = x_j$ as defined in Eq. (4.78).

The remaining area is of polymer matrix. Thus $R_{m,j}$ is expressed as

$$R_{m,j} = \frac{\Delta x_j}{(a^2 - \pi d_j^2) k_m} \tag{4.87}$$

Substituting Eq. (4.86) and (4.87) into Eq. (4.67), it can be arranged as

$$R_3 = R_4 = \sum_{j=r}^{\frac{a}{2}} \frac{\Delta x_j}{a^2 k_m + \pi(k_f - k_m)\left(r^2 - \left(\frac{a}{2} - x_j\right)^2\right)} \tag{4.88}$$

When Δx_j approaches zero, it can be written as

$$\begin{aligned} R_3 = R_4 &= \lim_{\Delta x_j \to 0} \sum_{j=r}^{\frac{a}{2}} \frac{\Delta x_j}{a^2 k_m + \pi(k_f - k_m)\left(r^2 - \left(\frac{a}{2} - x_j\right)^2\right)} \\ &= \int_r^{\frac{a}{2}} \frac{1}{a^2 k_m + \pi(k_f - k_m)\left(r^2 - \left(\frac{a}{2} - x_j\right)^2\right)} dx_j \end{aligned} \tag{4.89}$$

Before integrating, Eq. (4.89) can be further arranged as

$$R_3 = R_4 = \frac{1}{\pi(k_f - k_m)} \int_r^{\frac{a}{2}} \frac{1}{\left[\frac{k_m + \frac{\pi r^2}{a^2}(k_f - k_m)}{\frac{\pi}{a^2}(k_f - k_m)}\right] - \left(\frac{a}{2} - x_j\right)^2} dx_j$$

$$= \frac{1}{\pi(k_f - k_m)} \int_r^{\frac{a}{2}} \frac{1}{\left\{\left(\frac{a^2}{\pi}\right)\left(\frac{\pi r^2}{a^2}\right)\left[\frac{a^2}{\pi r^2}\left(\frac{k_m}{k_f - k_m}\right) + 1\right]\right\} - \left(\frac{a}{2} - x_j\right)^2} dx_j$$

$$= \frac{1}{\pi(k_f - k_m)} \int_r^{\frac{a}{2}} \frac{1}{\left\{r^2\left[\frac{a^2}{\pi r^2}\left(\frac{k_m}{k_f - k_m}\right) + 1\right]\right\} - \left(\frac{a}{2} - x_j\right)^2} dx_j \quad (4.90)$$

Substituting Eq. (4.43) into Eq. (4.90), it led to

$$R_3 = R_4 = \frac{1}{\pi(k_f - k_m)} \int_r^{\frac{a}{2}} \frac{1}{\left\{r^2\left[\left(\frac{8\pi r^3}{3v_f}\right)^{\frac{2}{3}}\left(\frac{1}{\pi r^2}\right)\left(\frac{k_m}{k_f - k_m}\right) + 1\right]\right\} - \left(\frac{a}{2} - x_j\right)^2} dx_j$$

$$= \frac{1}{\pi(k_f - k_m)} \int_r^{\frac{a}{2}} \frac{1}{\left\{r^2\left[\left(\frac{64}{9\pi v_f^2}\right)^{\frac{1}{3}}\left(\frac{k_m}{k_f - k_m}\right) + 1\right]\right\} - \left(\frac{a}{2} - x_j\right)^2} dx_j$$

$$= \frac{1}{\pi(k_f - k_m)} \int_r^{\frac{a}{2}} \frac{1}{\left[r\sqrt{\gamma_{\mathrm{BCC1}} + 1}\right]^2 - \left(\frac{a}{2} - x_j\right)^2} dx_j \quad (4.91)$$

where γ_{BCC1} is expressed as Eq. (4.74).

Integrating Eq. (4.91), the thermal resistances of sections 3 and 4 can be written as

$$R_3 = R_4 = \left(\frac{1}{2\pi r(k_f - k_m)}\right)\left(\frac{1}{\sqrt{\gamma_{\mathrm{BCC1}} + 1}} \ln \frac{\sqrt{\gamma_{\mathrm{BCC1}} + 1} + \beta_{\mathrm{BCC1}}}{\sqrt{\gamma_{\mathrm{BCC1}} + 1} - \beta_{\mathrm{BCC1}}}\right) \quad (4.92)$$

where $\boldsymbol{\beta_{\mathrm{BCC1}}}$ is defined as Eq. (4.76).

Then Eq. (4.75), (4.84), and (4.92) are substituted into Eq. (4.66) as

$$k_{eff,\mathrm{BCC1-3}} = \frac{1}{a}\left\{\frac{1}{2\left(\frac{1}{\pi r\left(k_f - k_m\right)}\right)\left[\left(\frac{2}{\delta_{\mathrm{BCC1}}}\ln\frac{1-\beta_{\mathrm{BCC1}}+\delta_{\mathrm{BCC1}}}{1-\beta_{\mathrm{BCC1}}-\delta_{\mathrm{BCC1}}}\right)+\left(\frac{1}{\sqrt{\gamma_{\mathrm{BCC1}}+1}}\ln\frac{\sqrt{\gamma_{\mathrm{BCC1}}+1}+\beta_{\mathrm{BCC1}}}{\sqrt{\gamma_{\mathrm{BCC1}}+1}-\beta_{\mathrm{BCC1}}}\right)\right]}\right\}$$

$$\frac{k_{eff,\mathrm{BCC1-3}}}{k_m} = \frac{1}{ak_m}\left\{\frac{1}{2\left(\frac{1}{\pi r\left(k_f - k_m\right)}\right)\left[\left(\frac{2}{\delta_{\mathrm{BCC1}}}\ln\frac{1-\beta_{\mathrm{BCC1}}+\delta_{\mathrm{BCC1}}}{1-\beta_{\mathrm{BCC1}}-\delta_{\mathrm{BCC1}}}\right)+\left(\frac{1}{\sqrt{\gamma_{\mathrm{BCC1}}+1}}\ln\frac{\sqrt{\gamma_{\mathrm{BCC1}}+1}+\beta_{\mathrm{BCC1}}}{\sqrt{\gamma_{\mathrm{BCC1}}+1}-\beta_{\mathrm{BCC1}}}\right)\right]}\right\}$$

$$= \frac{1}{2\left(\frac{ak_m}{\pi r\left(k_f - k_m\right)}\right)\left[\left(\frac{2}{\delta_{\mathrm{BCC1}}}\ln\frac{1-\beta_{\mathrm{BCC1}}+\delta_{\mathrm{BCC1}}}{1-\beta_{\mathrm{BCC1}}-\delta_{\mathrm{BCC1}}}\right)+\left(\frac{1}{\sqrt{\gamma_{\mathrm{BCC1}}+1}}\ln\frac{\sqrt{\gamma_{\mathrm{BCC1}}+1}+\beta_{\mathrm{BCC1}}}{\sqrt{\gamma_{\mathrm{BCC1}}+1}-\beta_{\mathrm{BCC1}}}\right)\right]}$$

$$= \frac{1}{2\left(\frac{8\pi r^3}{3v_f}\right)^{\frac{1}{3}}\left(\frac{1}{\pi r}\right)\left(\frac{k_m}{k_f - k_m}\right)\left[\left(\frac{2}{\delta_{\mathrm{BCC1}}}\ln\frac{1-\beta_{\mathrm{BCC1}}+\delta_{\mathrm{BCC1}}}{1-\beta_{\mathrm{BCC1}}-\delta_{\mathrm{BCC1}}}\right)+\left(\frac{1}{\sqrt{\gamma_{\mathrm{BCC1}}+1}}\ln\frac{\sqrt{\gamma_{\mathrm{BCC1}}+1}+\beta_{\mathrm{BCC1}}}{\sqrt{\gamma_{\mathrm{BCC1}}+1}-\beta_{\mathrm{BCC1}}}\right)\right]}$$

$$= \frac{1}{2\left(\frac{8}{3\pi^2 v_f}\right)^{\frac{1}{3}}\left(\frac{k_m}{k_f - k_m}\right)\left[\left(\frac{2}{\delta_{\mathrm{BCC1}}}\ln\frac{1-\beta_{\mathrm{BCC1}}+\delta_{\mathrm{BCC1}}}{1-\beta_{\mathrm{BCC1}}-\delta_{\mathrm{BCC1}}}\right)+\left(\frac{1}{\sqrt{\gamma_{\mathrm{BCC1}}+1}}\ln\frac{\sqrt{\gamma_{\mathrm{BCC1}}+1}+\beta_{\mathrm{BCC1}}}{\sqrt{\gamma_{\mathrm{BCC1}}+1}-\beta_{\mathrm{BCC1}}}\right)\right]}$$

$$= \frac{1}{\left(\frac{3v_f}{\pi}\right)^{\frac{1}{3}}\left(\frac{64}{9\pi v_f^2}\right)^{\frac{1}{3}}\left(\frac{k_m}{k_f - k_m}\right)\left[\left(\frac{2}{\delta_{\mathrm{BCC1}}}\ln\frac{1-\beta_{\mathrm{BCC1}}+\delta_{\mathrm{BCC1}}}{1-\beta_{\mathrm{BCC1}}-\delta_{\mathrm{BCC1}}}\right)+\left(\frac{1}{\sqrt{\gamma_{\mathrm{BCC1}}+1}}\ln\frac{\sqrt{\gamma_{\mathrm{BCC1}}+1}+\beta_{\mathrm{BCC1}}}{\sqrt{\gamma_{\mathrm{BCC1}}+1}-\beta_{\mathrm{BCC1}}}\right)\right]}$$

$$\frac{k_{eff,\mathrm{BCC1-3}}}{k_m} = \frac{1}{\left(\frac{3v_f}{\pi}\right)^{\frac{1}{3}}\left[\left(\frac{2\gamma_{\mathrm{BCC1}}}{\delta_{\mathrm{BCC1}}}\ln\frac{1-\beta_{\mathrm{BCC1}}+\delta_{\mathrm{BCC1}}}{1-\beta_{\mathrm{BCC1}}-\delta_{\mathrm{BCC1}}}\right)+\left(\frac{\gamma_{\mathrm{BCC1}}}{\sqrt{\gamma_{\mathrm{BCC1}}+1}}\ln\frac{\sqrt{\gamma_{\mathrm{BCC1}}+1}+\beta_{\mathrm{BCC1}}}{\sqrt{\gamma_{\mathrm{BCC1}}+1}-\beta_{\mathrm{BCC1}}}\right)\right]} \quad (4.93)$$

Finally, the ratio of $\boldsymbol{k_{eff,\mathrm{BCC1-3}}}$ and $\boldsymbol{k_m}$ is derived as shown in Eq. (4.93).

4.1.3 Face-centered Cubic Model (FCC1 Model)

4.1.3.1 Case VI: FCC1 Model with the Volume Fraction of Filler < 0.262

In case of FCC element with filler volume fraction less than 0.262, the element was divided into six sections as shown in Figure 4.11(a). Sections 1, 3, 4 and 6 contain one-eighth of spherical particle on each corner and half of spherical particle on center. Sections 2 and 5 contain neat polymer matrix. The thermal resistances of sections 1, 3, 4, and 6 were considered as parallel arrangement of polymer matrix resistance and filler resistance, while the thermal resistance of sections 2 and 5 come from only the polymer matrix. Thermal resistances of each section is arranged in series as shown in Figure 4.11(b) where $R_{m,i}$ is the polymer matrix thermal resistance of section i and $R_{f,i}$ is the filler thermal resistance of section i, $i = 1, 2, 3, 4, 5, 6$.

By the definition of series resistance (Eq. (2.32)), the total thermal resistance of this element (R_{Σ}) is the addition of thermal resistances of each section.

$$R_{\Sigma} = R_1 + R_2 + R_3 + R_4 + R_5 + R_6 \tag{4.94}$$

where R_i is the thermal resistance of section i.

Then the heat flow can be written as

$$Q = \frac{T_1 - T_2}{\frac{a}{Ak_{eff,\mathrm{FCC1-1}}}} = \frac{T_1 - T_2}{R_1 + R_2 + R_3 + R_4 + R_5 + R_6} \tag{4.95}$$

where $k_{eff,\mathrm{FCC1-1}}$ is the effective thermal conductivity of case VI of FCC1 model and A is the area perpendicular to the heat flow.

Due to $A = a^2$, $k_{eff,\mathrm{FCC1-1}}$ can be derived by rearranging Eq. (4.95) as

$$k_{eff,\mathrm{FCC1-1}} = \frac{1}{a}\left(\frac{1}{R_1 + R_2 + R_3 + R_4 + R_5 + R_6}\right) \tag{4.96}$$

(a) Physical model (b) Thermal circuit model

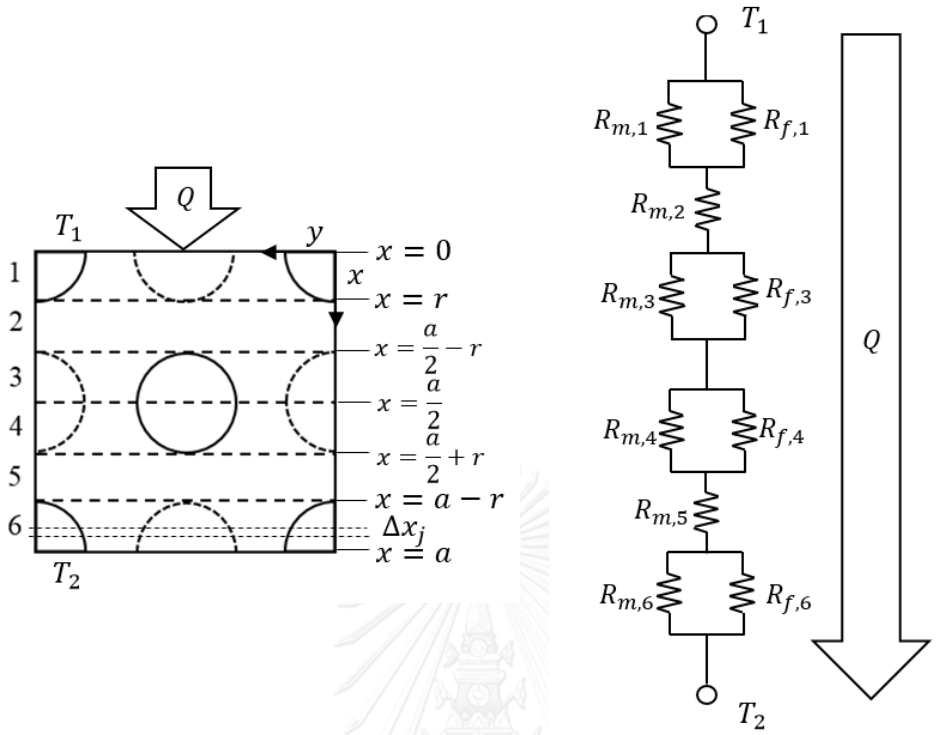

Figure 4.11 (a) Physical and (b) Thermal circuit model of face-centered cubic element with filler volume fraction < 0.262

Note that the thermal resistance of section 1 is equivalent to that of sections 3, 4, and 6, thus they were considered together. It can be imagined that the element is divided into very thin layer *j* that its thickness is Δx_j, as shown in Figure 4.11(a). The resistance of a layer *j* is parallel resistances due to polymer matrix resistance $R_{m,j}$ and filler resistance $R_{f,j}$. These layers arrange in series pattern. Therefore, the thermal resistances of sections 1, 3, 4, and 6 can be written as

$$R_1 = R_3 = R_4 = R_6 = \sum_{j=0}^{r} \left(\frac{1}{R_{m,j}} + \frac{1}{R_{f,j}} \right)^{-1} \tag{4.97}$$

Because there is one fourth of a circle on each corner and one circle on center of the square plane (y, z) in these sections, thus there is two circles in each layer and then $R_{f,j}$ can be written as

$$R_{f,j} = \frac{\Delta x_j}{\left(2\pi b_j^2\right)k_f} \tag{4.98}$$

where b_j is the radius of circle at $x = x_j$ as defined in Eq. (4.10).

The remaining area is of polymer matrix. Thus $R_{m,j}$ is expressed as

$$R_{m,j} = \frac{\Delta x_j}{\left(a^2 - 2\pi b_j^2\right)k_m} \tag{4.99}$$

Substituting Eq. (4.98) and (4.99) into Eq. (4.97), it can be arranged as

$$R_1 = R_3 = R_4 = R_6 = \sum_{j=0}^{r} \frac{\Delta x_j}{a^2 k_m + 2\pi\left(k_f - k_m\right)\left(r^2 - x_j^2\right)} \tag{4.100}$$

When Δx_j approaches zero, it can be written as

$$\begin{aligned} R_1 = R_3 = R_4 = R_6 &= \lim_{\Delta x_j \to 0} \sum_{j=0}^{r} \frac{\Delta x_j}{a^2 k_m + 2\pi\left(k_f - k_m\right)\left(r^2 - x_j^2\right)} \\ &= \int_0^r \frac{1}{a^2 k_m + 2\pi\left(k_f - k_m\right)\left(r^2 - x_j^2\right)} dx_j \end{aligned} \tag{4.101}$$

Eq. (4.101) can be further arranged as

$$\begin{aligned} R_1 = R_3 = R_4 = R_6 &= \frac{1}{2\pi\left(k_f - k_m\right)} \int_0^r \frac{1}{\left[\dfrac{k_m + \dfrac{2\pi r^2}{a^2}\left(k_f - k_m\right)}{\dfrac{2\pi}{a^2}\left(k_f - k_m\right)}\right] - x_j^2} dx_j \\ &= \frac{1}{2\pi\left(k_f - k_m\right)} \int_0^r \frac{1}{\left\{\left(\dfrac{a^2}{\pi}\right)\left(\dfrac{\pi r^2}{a^2}\right)\left[\dfrac{a^2}{2\pi r^2}\left(\dfrac{k_m}{k_f - k_m}\right) + 1\right]\right\} - x_j^2} dx_j \end{aligned}$$

$$= \frac{1}{2\pi\left(k_f - k_m\right)} \int_0^r \frac{1}{\left\{r^2\left[\frac{a^2}{2\pi r^2}\left(\frac{k_m}{k_f - k_m}\right) + 1\right]\right\} - x_j^2} dx_j \tag{4.102}$$

From Eq. (4.4), the length of RVE for FCC can be written in form of

$$a = \left(\frac{16\pi r^3}{3v_f}\right)^{\frac{1}{3}} \tag{4.103}$$

Substituting Eq. (4.103) into Eq. (4.102), it goes to be

$$R_1 = R_3 = R_4 = R_6 = \frac{1}{2\pi\left(k_f - k_m\right)} \int_0^r \frac{1}{\left\{r^2\left[\left(\frac{16\pi r^3}{3v_f}\right)^{\frac{2}{3}}\left(\frac{1}{2\pi r^2}\right)\left(\frac{k_m}{k_f - k_m}\right) + 1\right]\right\} - x_j^2} dx_j$$

$$= \frac{1}{2\pi\left(k_f - k_m\right)} \int_0^r \frac{1}{\left\{r^2\left[\left(\frac{32}{9\pi v_f^2}\right)^{\frac{1}{3}}\left(\frac{k_m}{k_f - k_m}\right) + 1\right]\right\} - x_j^2} dx_j$$

$$= \frac{1}{2\pi\left(k_f - k_m\right)} \int_0^r \frac{1}{\left[r\sqrt{\gamma_{\mathrm{FCC1}} + 1}\right]^2 - x_j^2} dx_j \tag{4.104}$$

where γ_{FCC1} is expressed as

$$\gamma_{\mathrm{FCC1}} = \left(\frac{32}{9\pi v_f^2}\right)^{\frac{1}{3}}\left(\frac{k_m}{k_f - k_m}\right) \tag{4.105}$$

Integrating Eq. (4.104), the thermal resistance of these sections can be written as

$$R_1 = R_3 = R_4 = R_6 = \left(\frac{1}{4\pi r\left(k_f - k_m\right)}\right)\left(\frac{1}{\sqrt{\gamma_{\mathrm{FCC1}} + 1}} \ln \frac{\sqrt{\gamma_{\mathrm{FCC1}} + 1} + 1}{\sqrt{\gamma_{\mathrm{FCC1}} + 1} - 1}\right) \tag{4.106}$$

Considering sections 2 and 5, thermal resistances are expressed as

$$R_2 = R_5 = \frac{\left(\frac{a}{2} - r\right) - r}{a^2 k_m} = \frac{\frac{a}{2} - 2r}{a^2 k_m} \tag{4.107}$$

Then Eq. (4.106) and (4.107) are substituted into Eq. (4.96) as

$$k_{eff,\mathrm{FCC1-1}} = \frac{1}{a}\left(\frac{1}{2\left(\frac{\frac{a}{2} - 2r}{a^2 k_m}\right) + 4\left(\frac{1}{4\pi r\left(k_f - k_m\right)}\right)\left(\frac{1}{\sqrt{\gamma_{\mathrm{FCC1}} + 1}} \ln \frac{\sqrt{\gamma_{\mathrm{FCC1}} + 1} + 1}{\sqrt{\gamma_{\mathrm{FCC1}} + 1} - 1}\right)}\right) \tag{4.108}$$

Dividing Eq. (4.108) by k_m, the ratio of $k_{eff,\mathrm{FCC1-1}}$ and k_m can be derived as

$$\frac{k_{eff,\mathrm{FCC1-1}}}{k_m} = \frac{1}{ak_m}\left(\frac{1}{\frac{a - 4r}{a^2 k_m} + 4\left(\frac{1}{4\pi r\left(k_f - k_m\right)}\right)\left(\frac{1}{\sqrt{\gamma_{\mathrm{FCC1}} + 1}} \ln \frac{\sqrt{\gamma_{\mathrm{FCC1}} + 1} + 1}{\sqrt{\gamma_{\mathrm{FCC1}} + 1} - 1}\right)}\right)$$

$$= \frac{1}{1 - \frac{4r}{a} + \left(\frac{ak_m}{\pi r\left(k_f - k_m\right)}\right)\left(\frac{1}{\sqrt{\gamma_{\mathrm{FCC1}} + 1}} \ln \frac{\sqrt{\gamma_{\mathrm{FCC1}} + 1} + 1}{\sqrt{\gamma_{\mathrm{FCC1}} + 1} - 1}\right)}$$

$$= \frac{1}{1 - \frac{4r}{2r\left(\frac{2\pi}{3v_f}\right)^{\frac{1}{3}}} + \left(\frac{16\pi r^3}{3v_f}\right)^{\frac{1}{3}}\left(\frac{1}{\pi r}\right)\left(\frac{k_m}{k_f - k_m}\right)\left(\frac{1}{\sqrt{\gamma_{\mathrm{FCC1}} + 1}} \ln \frac{\sqrt{\gamma_{\mathrm{FCC1}} + 1} + 1}{\sqrt{\gamma_{\mathrm{FCC1}} + 1} - 1}\right)}$$

$$= \frac{1}{1 - 2\left(\frac{3v_f}{2\pi}\right)^{\frac{1}{3}} + \left(\frac{16}{3\pi^2 v_f}\right)^{\frac{1}{3}}\left(\frac{k_m}{k_f - k_m}\right)\left(\frac{1}{\sqrt{\gamma_{\mathrm{FCC1}} + 1}} \ln \frac{\sqrt{\gamma_{\mathrm{FCC1}} + 1} + 1}{\sqrt{\gamma_{\mathrm{FCC1}} + 1} - 1}\right)}$$

$$= \frac{1}{1 - 2\left(\frac{3v_f}{2\pi}\right)^{\frac{1}{3}} + \left(\frac{3v_f}{2\pi}\right)^{\frac{1}{3}}\left(\frac{32}{9\pi v_f^2}\right)^{\frac{1}{3}}\left(\frac{k_m}{k_f - k_m}\right)\left(\frac{1}{\sqrt{\gamma_{\text{FCC1}} + 1}}\ln\frac{\sqrt{\gamma_{\text{FCC1}} + 1} + 1}{\sqrt{\gamma_{\text{FCC1}} + 1} - 1}\right)}$$

$$\frac{k_{eff,\text{FCC1}-1}}{k_m} = \frac{1}{1 - \left(\frac{12v_f}{\pi}\right)^{\frac{1}{3}}\left[1 - \frac{\gamma_{\text{FCC1}}}{2\sqrt{\gamma_{\text{FCC1}} + 1}}\ln\frac{\sqrt{\gamma_{\text{FCC1}} + 1} + 1}{\sqrt{\gamma_{\text{FCC1}} + 1} - 1}\right]} \quad (4.109)$$

4.1.3.2 Case VII: FCC1 Model with the Volume Fraction of Filler = 0.262

In case of BCC element with filler volume fraction equal to 0.262, the element was divided into four sections as shown in Figure 4.12(a). Every sections contain one-eighth of spherical particle on each corner and half of a spherical particle on center of each section. The thermal resistances of each section were considered as parallel arrangement of polymer matrix resistance and filler resistance. Thermal resistance of each section was arranged in series as shown in Figure 4.12(b) where $R_{m,i}$ is the polymer matrix thermal resistance of section i and $R_{f,i}$ is the filler thermal resistance of section i, $i = 1, 2, 3, 4$.

By the definition of series resistance (Eq. (2.32)), the total thermal resistance of this element is the addition of thermal resistances of each section.

$$R_\Sigma = R_1 + R_2 + R_3 + R_4 \quad (4.110)$$

where R_i is the thermal resistance of section i.

Then the heat flow can be written as

$$Q = \frac{T_1 - T_2}{\frac{a}{Ak_{eff,\text{FCC1}-2}}} = \frac{T_1 - T_2}{R_1 + R_2 + R_3 + R_4} \quad (4.111)$$

where $k_{eff,\mathrm{FCC1-2}}$ is the effective thermal conductivity of case VII of FCC1 model and A is the area perpendicular to the heat flow.

Due to $A = a^2$, $k_{eff,\mathrm{FCC1-2}}$ can be derived by rearranging Eq. (4.101) as

$$k_{eff,\mathrm{FCC1-2}} = \frac{1}{a}\left(\frac{1}{R_1 + R_2 + R_3 + R_4}\right) \tag{4.112}$$

Note that the thermal resistances of every sections are equal, thus they were considered together. It can be imagined that the element is divided into very thin layer j that its thickness is Δx_j, as shown in Figure 4.12(a). The resistance of a layer j is parallel resistance due to polymer matrix resistance $R_{m,j}$ and filler resistance $R_{f,j}$. These layers arrange in series pattern. Therefore, the thermal resistances of sections 1, 2, 3, and 4 can be written as

$$R_1 = R_2 = R_3 = R_4 = \sum_{j=0}^{r}\left(\frac{1}{R_{m,j}} + \frac{1}{R_{f,j}}\right)^{-1} \tag{4.113}$$

Because there are two circles in each layer, then $R_{f,j}$ can be written as

$$R_{f,j} = \frac{\Delta x_j}{\left(2\pi b_j^2\right)k_f} \tag{4.114}$$

where b_j is the radius of circle at $x = x_j$ as defined in Eq. (4.10).

(a) Physical model (b) Thermal circuit model

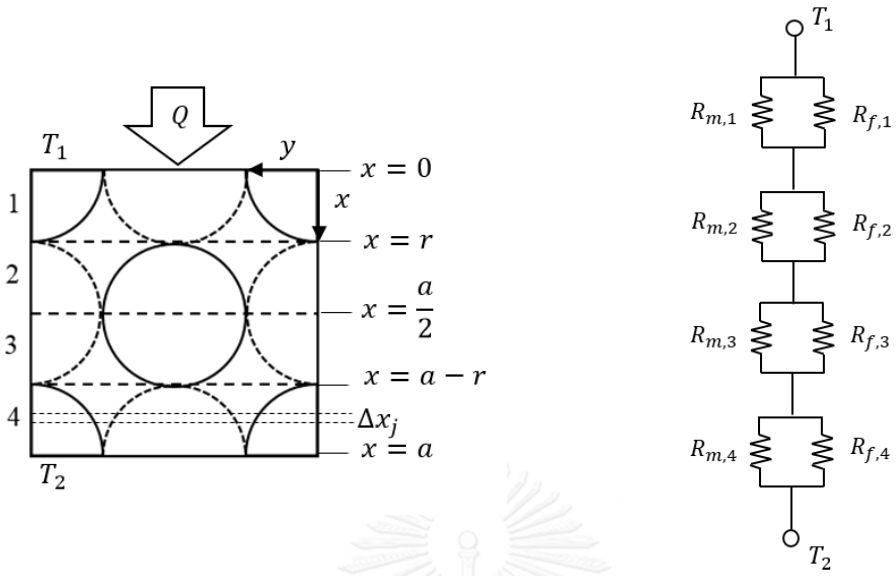

Figure 4.12 (a) Physical and (b) Thermal circuit model of face-centered cubic element with filler volume fraction = 0.262

The remaining area is of polymer matrix. Thus $R_{m,j}$ is expressed as

$$R_{m,j} = \frac{\Delta x_j}{\left(a^2 - 2\pi b_j^2\right)k_m} \tag{4.115}$$

Substituting Eq. (4.114) and (4.115) into Eq. (4.113), it can be arranged as

$$R_1 = R_2 = R_3 = R_4 = \sum_{j=0}^{r} \frac{\Delta x_j}{a^2 k_m + 2\pi\left(k_f - k_m\right)\left(r^2 - x_j^2\right)} \tag{4.116}$$

When Δx_j approaches zero, it can be written as

$$R_1 = R_2 = R_3 = R_4 = \lim_{\Delta x_j \to 0} \sum_{j=0}^{r} \frac{\Delta x_j}{a^2 k_m + 2\pi\left(k_f - k_m\right)\left(r^2 - x_j^2\right)}$$

$$= \int_0^r \frac{1}{a^2 k_m + 2\pi(k_f - k_m)(r^2 - x_j^2)} dx_j \tag{4.117}$$

Before integrating, Eq. (4.117) can be further arranged as

$$R_1 = R_2 = R_3 = R_4 = \frac{1}{2\pi(k_f - k_m)} \int_0^r \frac{1}{\left[\frac{k_m + \frac{2\pi r^2}{a^2}(k_f - k_m)}{\frac{2\pi}{a^2}(k_f - k_m)}\right] - x_j^2} dx_j$$

$$= \frac{1}{2\pi(k_f - k_m)} \int_0^r \frac{1}{\left\{\left(\frac{a^2}{\pi}\right)\left(\frac{\pi r^2}{a^2}\right)\left[\frac{a^2}{2\pi r^2}\left(\frac{k_m}{k_f - k_m}\right) + 1\right]\right\} - x_j^2} dx_j$$

$$= \frac{1}{2\pi(k_f - k_m)} \int_0^r \frac{1}{\left\{r^2\left[\frac{a^2}{2\pi r^2}\left(\frac{k_m}{k_f - k_m}\right) + 1\right]\right\} - x_j^2} dx_j \tag{4.118}$$

Substituting Eq. (4.103) into Eq. (4.118), it goes to be

$$R_1 = R_2 = R_3 = R_4 = \frac{1}{2\pi(k_f - k_m)} \int_0^r \frac{1}{\left\{r^2\left[\left(\frac{16\pi r^3}{3v_f}\right)^{\frac{2}{3}}\left(\frac{1}{2\pi r^2}\right)\left(\frac{k_m}{k_f - k_m}\right) + 1\right]\right\} - x_j^2} dx_j$$

$$= \frac{1}{2\pi(k_f - k_m)} \int_0^r \frac{1}{\left\{r^2\left[\left(\frac{32}{9\pi v_f^2}\right)^{\frac{1}{3}}\left(\frac{k_m}{k_f - k_m}\right) + 1\right]\right\} - x_j^2} dx_j$$

$$= \frac{1}{2\pi(k_f - k_m)} \int_0^r \frac{1}{\left[r\sqrt{\gamma_{\mathrm{FCC1}} + 1}\right]^2 - x_j^2} dx_j \tag{4.119}$$

where γ_{FCC1} is expressed as

$$\gamma_{\mathrm{FCC1}} = \left(\frac{32}{9\pi v_f^2}\right)^{\frac{1}{3}}\left(\frac{k_m}{k_f - k_m}\right) \tag{4.120}$$

Integrating Eq. (4.119), the thermal resistances of these sections can be written as

$$R_1 = R_2 = R_3 = R_4 = \left(\frac{1}{4\pi r\left(k_f - k_m\right)}\right)\left(\frac{1}{\sqrt{\gamma_{\mathrm{FCC1}}+1}}\ln\frac{\sqrt{\gamma_{\mathrm{FCC1}}+1}+1}{\sqrt{\gamma_{\mathrm{FCC1}}+1}-1}\right) \tag{4.121}$$

Then Eq. (4.121) is substituted into Eq. (4.112) as

$$k_{eff,\mathrm{FCC1-2}} = \frac{1}{a}\left(\frac{1}{4\left(\frac{1}{4\pi r\left(k_f - k_m\right)}\right)\left(\frac{1}{\sqrt{\gamma_{\mathrm{FCC1}}+1}}\ln\frac{\sqrt{\gamma_{\mathrm{FCC1}}+1}+1}{\sqrt{\gamma_{\mathrm{FCC1}}+1}-1}\right)}\right) \tag{4.122}$$

Dividing Eq. (4.122) by k_m, the ratio of $k_{eff,\mathrm{FCC1-2}}$ and k_m can be derived as

$$\frac{k_{eff,\mathrm{FCC1-2}}}{k_m} = \frac{1}{ak_m}\left(\frac{1}{4\left(\frac{1}{4\pi r\left(k_f - k_m\right)}\right)\left(\frac{1}{\sqrt{\gamma_{\mathrm{FCC1}}+1}}\ln\frac{\sqrt{\gamma_{\mathrm{FCC1}}+1}+1}{\sqrt{\gamma_{\mathrm{FCC1}}+1}-1}\right)}\right)$$

$$= \frac{1}{\left(\frac{ak_m}{\pi r\left(k_f - k_m\right)}\right)\left(\frac{1}{\sqrt{\gamma_{\mathrm{FCC1}}+1}}\ln\frac{\sqrt{\gamma_{\mathrm{FCC1}}+1}+1}{\sqrt{\gamma_{\mathrm{FCC1}}+1}-1}\right)}$$

$$= \frac{1}{\left(\frac{16\pi r^3}{3v_f}\right)^{\frac{1}{3}}\left(\frac{1}{\pi r}\right)\left(\frac{k_m}{k_f - k_m}\right)\left(\frac{1}{\sqrt{\gamma_{\mathrm{FCC1}}+1}}\ln\frac{\sqrt{\gamma_{\mathrm{FCC1}}+1}+1}{\sqrt{\gamma_{\mathrm{FCC1}}+1}-1}\right)}$$

$$= \frac{1}{\left(\frac{16}{3\pi^2 v_f}\right)^{\frac{1}{3}}\left(\frac{k_m}{k_f - k_m}\right)\left(\frac{1}{\sqrt{\gamma_{\mathrm{FCC1}}+1}}\ln\frac{\sqrt{\gamma_{\mathrm{FCC1}}+1}+1}{\sqrt{\gamma_{\mathrm{FCC1}}+1}-1}\right)}$$

$$= \frac{1}{\left(\frac{3v_f}{2\pi}\right)^{\frac{1}{3}}\left(\frac{32}{9\pi v_f^2}\right)^{\frac{1}{3}}\left(\frac{k_m}{k_f - k_m}\right)\left(\frac{1}{\sqrt{\gamma_{\mathrm{FCC1}}+1}}\ln\frac{\sqrt{\gamma_{\mathrm{FCC1}}+1}+1}{\sqrt{\gamma_{\mathrm{FCC1}}+1}-1}\right)}$$

$$\frac{k_{eff,\mathrm{FCC1-2}}}{k_m} = \frac{1}{\left(\frac{12v_f}{\pi}\right)^{\frac{1}{3}}\left(\frac{\gamma_{\mathrm{FCC1}}}{2\sqrt{\gamma_{\mathrm{FCC1}}+1}}\ln\frac{\sqrt{\gamma_{\mathrm{FCC1}}+1}+1}{\sqrt{\gamma_{\mathrm{FCC1}}+1}-1}\right)} \quad (4.123)$$

4.1.3.3 Case VIII: FCC1 Model with the Volume Fraction of Filler > 0.262

In case of BCC element with filler volume fraction more than 0.262, the element was divided into six sections as shown in Figure 4.13(a). Sections 1 and 6 contain some segment of spherical particle on each corner and center. Sections 2 and 5 contain some segment of spherical particle on each corner, edge, and center. Sections 3 and 4 contain some segment of spherical particle on each edge. The thermal resistances of every sections were considered as parallel arrangement of polymer matrix resistance and filler resistance. Thermal resistances of each section were arranged in series as shown in Figure 4.13(b) where $R_{m,i}$ is the polymer matrix thermal resistance of section i and $R_{f,i}$ is the filler thermal resistance of section i, i = 1, 2, 3, 4, 5, 6.

By the definition of series resistance (Eq. (2.32)), the total thermal resistance of this element is the addition of thermal resistances of each section.

$$R_{\Sigma} = R_1 + R_2 + R_3 + R_4 + R_5 + R_6 \quad (4.124)$$

where R_i is the thermal resistance of section i.

Then the heat flow can be written as

$$Q = \frac{T_1 - T_2}{\frac{a}{Ak_{eff,\mathrm{FCC1-3}}}} = \frac{T_1 - T_2}{R_1 + R_2 + R_3 + R_4 + R_5 + R_6} \quad (4.125)$$

where $k_{eff,\mathrm{FCC1-3}}$ is the effective thermal conductivity for case VIII of FCC1 model and A is the area perpendicular to the heat flow.

Due to $A = a^2$, $k_{eff,\mathrm{FCC1-3}}$ can be derived by rearranging Eq. (4.125) as

$$k_{eff,\mathrm{FCC1-3}} = \frac{1}{a}\left(\frac{1}{R_1 + R_2 + R_3 + R_4 + R_5 + R_6}\right) \tag{4.126}$$

It is worth to note that the thermal resistance of section 1 is equivalent to that of sections 3, 4, and 6, and the thermal resistance of section 2 is equivalent to that of section 5.

It can be imagined that the element is divided into very thin layer *j* that its thickness is Δx_j, as shown in Figure 4.13(a). The resistance of a layer *j* is parallel resistances due to polymer matrix resistance $R_{m,j}$ and filler resistance $R_{f,j}$. These layers arrange in series pattern. Therefore, the thermal resistance of each section can be written as

$$R_i = \sum_{j=0}^{n}\left(\frac{1}{R_{m,j}} + \frac{1}{R_{f,j}}\right)^{-1} \tag{4.127}$$

For sections 1, 3, 4, and 6, because there is one fourth of a circle on each corner and one circle on center of the square plane (y, z), thus there is one circle in each layer and then $R_{f,j}$ can be written as

$$R_{f,j} = \frac{\Delta x_j}{\left(2\pi b_j^2\right)k_f} \tag{4.128}$$

where b_j is the radius of circle at $x = x_j$ as defined in Eq. (4.10).

(a) Physical model (b) Thermal circuit model

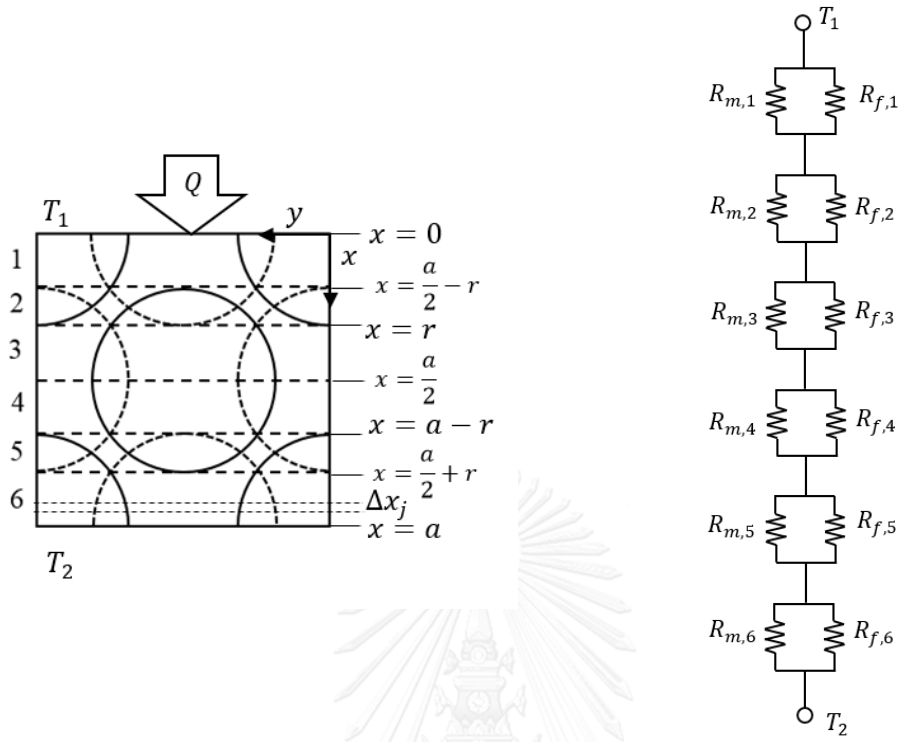

Figure 4.13 (a) Physical and (b) Thermal circuit model of face-centered cubic element with filler volume fraction > 0.262

The remaining area is of polymer matrix. Thus $R_{m,j}$ is expressed as

$$R_{m,j} = \frac{\Delta x_j}{\left(a^2 - 2\pi b_j^2\right)k_m} \tag{4.129}$$

Substituting Eq. (4.128) and (4.129) into Eq. (4.127), it can be arranged as

$$R_1 = R_3 = R_4 = R_6 = \sum_{j=0}^{\frac{a}{2}-r} \frac{\Delta x_j}{a^2 k_m + 2\pi\left(k_f - k_m\right)\left(r^2 - x_j^2\right)} \tag{4.130}$$

When Δx_j approaches to zero, it can be written as

$$R_1 = R_3 = R_4 = R_6 = \lim_{\Delta x_j \to 0} \sum_{j=0}^{\frac{a}{2}-r} \frac{\Delta x_j}{a^2 k_m + 2\pi(k_f - k_m)(r^2 - x_j^2)}$$
$$= \int_0^{\frac{a}{2}-r} \frac{1}{a^2 k_m + 2\pi(k_f - k_m)(r^2 - x_j^2)} dx_j \quad (4.131)$$

Before integrating, Eq. (4.131) can be further arranged as

$$R_1 = R_3 = R_4 = R_6 = \frac{1}{2\pi(k_f - k_m)} \int_0^{\frac{a}{2}-r} \frac{1}{\left[\frac{k_m + \frac{2\pi r^2}{a^2}(k_f - k_m)}{\frac{2\pi}{a^2}(k_f - k_m)}\right] - x_j^2} dx_j$$
$$= \frac{1}{2\pi(k_f - k_m)} \int_0^{\frac{a}{2}-r} \frac{1}{\left\{\left(\frac{a^2}{\pi}\right)\left(\frac{\pi r^2}{a^2}\right)\left[\frac{a^2}{2\pi r^2}\left(\frac{k_m}{k_f - k_m}\right) + 1\right]\right\} - x_j^2} dx_j$$
$$= \frac{1}{2\pi(k_f - k_m)} \int_0^{\frac{a}{2}-r} \frac{1}{\left\{r^2\left[\frac{a^2}{2\pi r^2}\left(\frac{k_m}{k_f - k_m}\right) + 1\right]\right\} - x_j^2} dx_j \quad (4.132)$$

Substituting Eq. (4.103) into Eq. (4.132), it led to

$$R_1 = R_3 = R_4 = R_6 = \frac{1}{2\pi(k_f - k_m)} \int_0^{\frac{a}{2}-r} \frac{1}{\left\{r^2\left[\left(\frac{16\pi r^3}{3v_f}\right)^{\frac{2}{3}}\left(\frac{1}{2\pi r^2}\right)\left(\frac{k_m}{k_f - k_m}\right) + 1\right]\right\} - x_j^2} dx_j$$
$$= \frac{1}{2\pi(k_f - k_m)} \int_0^{\frac{a}{2}-r} \frac{1}{\left\{r^2\left[\left(\frac{32}{9\pi v_f^2}\right)^{\frac{1}{3}}\left(\frac{k_m}{k_f - k_m}\right) + 1\right]\right\} - x_j^2} dx_j$$
$$= \frac{1}{2\pi(k_f - k_m)} \int_0^{\frac{a}{2}-r} \frac{1}{\left[r\sqrt{\gamma_{\mathrm{FCC1}} + 1}\right]^2 - x_j^2} dx_j \quad (4.133)$$

where γ_{FCC1} is expressed as

$$\gamma_{\mathrm{FCC1}} = \left(\frac{32}{9\pi v_f^2}\right)^{\frac{1}{3}}\left(\frac{k_m}{k_f - k_m}\right) \tag{4.134}$$

Integrating Eq. (4.133), the thermal resistances of sections 1, 3, 4 and 6 can be written as

$$R_1 = R_3 = R_4 = R_6 = \left(\frac{1}{4\pi r\left(k_f - k_m\right)}\right)\left(\frac{1}{\sqrt{\gamma_{\mathrm{FCC1}} + 1}}\ln\frac{\sqrt{\gamma_{\mathrm{FCC1}} + 1} + \beta_{\mathrm{FCC1}}}{\sqrt{\gamma_{\mathrm{FCC1}} + 1} - \beta_{\mathrm{FCC1}}}\right) \tag{4.135}$$

where β_{FCC1} is defined as

$$\beta_{\mathrm{FCC1}} = \left(\frac{2\pi}{3v_f}\right)^{\frac{1}{3}} - 1 \tag{4.136}$$

For sections 2 and 5, there are one fourth of a circle on each corner, one circle on center, and half of circle on each edge of the square plane (y, z), thus there are four circles in each layer and then $R_{f,j}$ can be written as

$$R_{f,j} = \frac{\Delta x_j}{\left(2\pi b_j^2 + 2\pi d_j^2\right)k_f} \tag{4.137}$$

where b_j is the radius of circle at $x = x_j$ as defined in Eq. (4.10) and d_j is the radius of circle at $x = x_j$ as defined in Eq. (4.78).

The remaining area is of polymer matrix. Thus $R_{m,j}$ is expressed as

$$R_{m,j} = \frac{\Delta x_j}{\left(a^2 - 2\pi b_j^2 - 2\pi d_j^2\right)k_m} \tag{4.138}$$

Substituting Eq. (4.137) and (4.138) into Eq. (4.127), thermal resistances of sections 2 and 5 can be written as

$$R_2 = R_5 = \sum_{j=\frac{a}{2}-r}^{r} \frac{\Delta x_j}{-4\pi(k_f - k_m)x_j^2 + 2a\pi(k_f - k_m)x_j + k_m a^2 + 4\pi r^2(k_f - k_m) - \frac{\pi a^2}{2}(k_f - k_m)}$$

$$= \frac{1}{2\pi(k_f - k_m)} \sum_{j=\frac{a}{2}-r}^{r} \frac{\Delta x_j}{-2x_j^2 + ax_j + \frac{k_m a^2}{2\pi(k_f - k_m)} + 2r^2 - \frac{a^2}{4}} \qquad (4.139)$$

When Δx_j approaches zero, it can be written as

$$R_2 = R_5 = \lim_{\Delta x_j \to 0} \frac{1}{2\pi(k_f - k_m)} \sum_{j=\frac{a}{2}-r}^{r} \frac{\Delta x_j}{-2x_j^2 + ax_j + \frac{k_m a^2}{2\pi(k_f - k_m)} + 2r^2 - \frac{a^2}{4}}$$

$$= \frac{1}{2\pi(k_f - k_m)} \int_{\frac{a}{2}-r}^{r} \frac{1}{-2x_j^2 + ax_j + \frac{k_m a^2}{2\pi(k_f - k_m)} + 2r^2 - \frac{a^2}{4}} dx_j \qquad (4.140)$$

Before integrating, Eq. (4.140) can be further arranged as

$$R_2 = R_5 = \frac{1}{2\pi(k_f - k_m)} \int_{\frac{a}{2}-r}^{r} \frac{1}{-2x_j^2 + ax_j + \frac{k_m a^2}{2\pi(k_f - k_m)} + 2r^2 - \frac{a^2}{4}} dx_j$$

$$= \frac{1}{2\pi(k_f - k_m)} \int_{\frac{a}{2}-r}^{r} \frac{1}{-2x_j^2 + ax_j + \left\{\left(\frac{a^2}{\pi}\right)\left(\frac{\pi r^2}{a^2}\right)\left[\frac{a^2}{2\pi r^2}\left(\frac{k_m}{k_f - k_m}\right) - \frac{a^2}{4r^2} + 2\right]\right\}} dx_j$$

$$= \frac{1}{2\pi(k_f - k_m)} \int_{\frac{a}{2}-r}^{r} \frac{1}{-2x_j^2 + ax_j + \left\{r^2\left[\frac{a^2}{2\pi r^2}\left(\frac{k_m}{k_f - k_m}\right) - \frac{a^2}{4r^2} + 2\right]\right\}} dx_j \qquad (4.141)$$

Substituting Eq. (4.103) into Eq. (4.141), it led to

$$R_2 = R_5 = \frac{1}{2\pi(k_f - k_m)} \int_{\frac{a}{2}-r}^{r} \frac{1}{-2x_j^2 + ax_j + \left\{ r^2 \left[\left(\frac{16\pi r^3}{3v_f} \right)^{\frac{2}{3}} \left(\frac{1}{2\pi r^2} \right) \left(\frac{k_m}{k_f - k_m} \right) - \left(\frac{16\pi r^3}{3v_f} \right)^{\frac{2}{3}} \left(\frac{1}{4r^2} \right) + 2 \right] \right\}} dx_j$$

$$= \frac{1}{2\pi(k_f - k_m)} \int_{\frac{a}{2}-r}^{r} \frac{1}{-2x_j^2 + ax_j + \left\{ r^2 \left[\left(\frac{32}{9\pi v_f^2} \right)^{\frac{1}{3}} \left(\frac{k_m}{k_f - k_m} \right) - \left(\frac{2\pi}{3v_f} \right)^{\frac{2}{3}} + 2 \right] \right\}} dx_j$$

$$= \frac{1}{2\pi(k_f - k_m)} \int_{\frac{a}{2}-r}^{r} \frac{1}{-2x_j^2 + ax_j + \left\{ r^2 \left[\gamma_{\mathrm{FCC1}} - \left(\frac{2\pi}{3v_f} \right)^{\frac{2}{3}} + 2 \right] \right\}} dx_j \qquad (4.142)$$

where γ_{BCC1} is defined as Eq. (4.134).

Integrating Eq. (4.142), the thermal resistances of sections 2 and 5 can be written as

$$R_2 = R_5 = \left(\frac{1}{\pi r(k_f - k_m)} \right) \left(\frac{1}{\sqrt{4 + 2\gamma_{\mathrm{FCC1}} - \left(\frac{2\pi}{3v_f} \right)^{\frac{2}{3}}}} \ln \frac{2 - \left(\frac{2\pi}{3v_f} \right)^{\frac{1}{3}} + \sqrt{4 + 2\gamma_{\mathrm{FCC1}} - \left(\frac{2\pi}{3v_f} \right)^{\frac{2}{3}}}}{2 - \left(\frac{2\pi}{3v_f} \right)^{\frac{1}{3}} - \sqrt{4 + 2\gamma_{\mathrm{FCC1}} - \left(\frac{2\pi}{3v_f} \right)^{\frac{2}{3}}}} \right)$$

$$R_2 = R_5 = \left(\frac{1}{\pi r(k_f - k_m)} \right) \left(\frac{1}{\delta_{\mathrm{FCC1}}} \ln \frac{1 - \beta_{\mathrm{FCC1}} + \delta_{\mathrm{FCC1}}}{1 - \beta_{\mathrm{FCC1}} - \delta_{\mathrm{FCC1}}} \right) \qquad (4.143)$$

where β_{FCC1} is defined as Eq. (4.136) and δ_{FCC1} is expressed as

$$\delta_{\mathrm{FCC1}} = \sqrt{4 + 2\gamma_{\mathrm{FCC1}} - \left(\frac{2\pi}{3v_f} \right)^{\frac{2}{3}}} = \sqrt{4 + 2\gamma_{\mathrm{FCC1}} - (\beta_{\mathrm{FCC1}} + 1)^2} \qquad (4.144)$$

Then Eq. (4.135) and (4.143) are substituted into Eq. (4.126) as

$$k_{eff,\mathrm{FCC1-3}} = \frac{1}{a}\left\{\frac{1}{\left(\frac{1}{\pi r(k_f-k_m)}\right)\left[\left(\frac{2}{\delta_{\mathrm{FCC1}}}\ln\frac{1-\beta_{\mathrm{FCC1}}+\delta_{\mathrm{FCC1}}}{1-\beta_{\mathrm{FCC1}}-\delta_{\mathrm{FCC1}}}\right)+\left(\frac{1}{\sqrt{\gamma_{\mathrm{FCC1}}+1}}\ln\frac{\sqrt{\gamma_{\mathrm{FCC1}}+1}+\beta_{\mathrm{FCC1}}}{\sqrt{\gamma_{\mathrm{FCC1}}+1}-\beta_{\mathrm{FCC1}}}\right)\right]}\right\}$$

$$\frac{k_{eff,\mathrm{FCC1-3}}}{k_m} = \frac{1}{ak_m}\left\{\frac{1}{\left(\frac{1}{\pi r(k_f-k_m)}\right)\left[\left(\frac{2}{\delta_{\mathrm{FCC1}}}\ln\frac{1-\beta_{\mathrm{FCC1}}+\delta_{\mathrm{FCC1}}}{1-\beta_{\mathrm{FCC1}}-\delta_{\mathrm{FCC1}}}\right)+\left(\frac{1}{\sqrt{\gamma_{\mathrm{FCC1}}+1}}\ln\frac{\sqrt{\gamma_{\mathrm{FCC1}}+1}+\beta_{\mathrm{FCC1}}}{\sqrt{\gamma_{\mathrm{FCC1}}+1}-\beta_{\mathrm{FCC1}}}\right)\right]}\right\}$$

$$= \frac{1}{\left(\frac{ak_m}{\pi r(k_f-k_m)}\right)\left[\left(\frac{2}{\delta_{\mathrm{FCC1}}}\ln\frac{1-\beta_{\mathrm{FCC1}}+\delta_{\mathrm{FCC1}}}{1-\beta_{\mathrm{FCC1}}-\delta_{\mathrm{FCC1}}}\right)+\left(\frac{1}{\sqrt{\gamma_{\mathrm{FCC1}}+1}}\ln\frac{\sqrt{\gamma_{\mathrm{FCC1}}+1}+\beta_{\mathrm{FCC1}}}{\sqrt{\gamma_{\mathrm{FCC1}}+1}-\beta_{\mathrm{FCC1}}}\right)\right]}$$

$$= \frac{1}{\left(\frac{16\pi r^3}{3v_f}\right)^{\frac{1}{3}}\left(\frac{1}{\pi r}\right)\left(\frac{k_m}{k_f-k_m}\right)\left[\left(\frac{2}{\delta_{\mathrm{FCC1}}}\ln\frac{1-\beta_{\mathrm{FCC1}}+\delta_{\mathrm{FCC1}}}{1-\beta_{\mathrm{FCC1}}-\delta_{\mathrm{FCC1}}}\right)+\left(\frac{1}{\sqrt{\gamma_{\mathrm{FCC1}}+1}}\ln\frac{\sqrt{\gamma_{\mathrm{FCC1}}+1}+\beta_{\mathrm{FCC1}}}{\sqrt{\gamma_{\mathrm{FCC1}}+1}-\beta_{\mathrm{FCC1}}}\right)\right]}$$

$$= \frac{1}{\left(\frac{16}{3\pi^2 v_f}\right)^{\frac{1}{3}}\left(\frac{k_m}{k_f-k_m}\right)\left[\left(\frac{2}{\delta_{\mathrm{FCC1}}}\ln\frac{1-\beta_{\mathrm{FCC1}}+\delta_{\mathrm{FCC1}}}{1-\beta_{\mathrm{FCC1}}-\delta_{\mathrm{FCC1}}}\right)+\left(\frac{1}{\sqrt{\gamma_{\mathrm{FCC1}}+1}}\ln\frac{\sqrt{\gamma_{\mathrm{FCC1}}+1}+\beta_{\mathrm{FCC1}}}{\sqrt{\gamma_{\mathrm{FCC1}}+1}-\beta_{\mathrm{FCC1}}}\right)\right]}$$

$$= \frac{1}{\left(\frac{3v_f}{2\pi}\right)^{\frac{1}{3}}\left(\frac{32}{9\pi v_f^2}\right)^{\frac{1}{3}}\left(\frac{k_m}{k_f-k_m}\right)\left[\left(\frac{2}{\delta_{\mathrm{FCC1}}}\ln\frac{1-\beta_{\mathrm{FCC1}}+\delta_{\mathrm{FCC1}}}{1-\beta_{\mathrm{FCC1}}-\delta_{\mathrm{FCC1}}}\right)+\left(\frac{1}{\sqrt{\gamma_{\mathrm{FCC1}}+1}}\ln\frac{\sqrt{\gamma_{\mathrm{FCC1}}+1}+\beta_{\mathrm{FCC1}}}{\sqrt{\gamma_{\mathrm{FCC1}}+1}-\beta_{\mathrm{FCC1}}}\right)\right]}$$

$$\frac{k_{eff,\mathrm{FCC1-3}}}{k_m} = \frac{1}{\left(\frac{3v_f}{2\pi}\right)^{\frac{1}{3}}\left[\left(\frac{2\gamma_{\mathrm{FCC1}}}{\delta_{\mathrm{FCC1}}}\ln\frac{1-\beta_{\mathrm{FCC1}}+\delta_{\mathrm{FCC1}}}{1-\beta_{\mathrm{FCC1}}-\delta_{\mathrm{FCC1}}}\right)+\left(\frac{\gamma_{\mathrm{FCC1}}}{\sqrt{\gamma_{\mathrm{FCC1}}+1}}\ln\frac{\sqrt{\gamma_{\mathrm{FCC1}}+1}+\beta_{\mathrm{FCC1}}}{\sqrt{\gamma_{\mathrm{FCC1}}+1}-\beta_{\mathrm{FCC1}}}\right)\right]} \quad (4.145)$$

4.2 Effective Thermal Conductivity Model with the Interfacial Thermal Resistance

Effective thermal conductivity models in section 4.1 were modified to include the effect of interfacial thermal resistance. In general, the presence of the interfacial thermal resistance causes the temperature discontinuity at the interface between matrix and filler as shown in Figure 4.14. This makes the temperature not a linear distribution along the x axis. In order to comply with the assumption that the heat flow is unidirectional and the temperature distribution along x axis is linear, the concept of the cubic element included the interfacial layer were introduced in this work.

The temperature along x axis of a composite is modeled as shown in Figure 4.14(a). The temperature immediately drops at the interface between matrix and filler phase due to the interfacial thermal resistance. Since the heat flux along the x axis is constant, the interfacial thermal resistance in this case can be expressed by the definition in Eq. (2.38) as

$$R_{int} = \frac{\Delta T}{q} = \frac{\Delta T}{k_m \frac{\Delta T}{\Delta l}} \tag{4.146}$$

where ΔT is the temperature difference at the interface and Δl is the thickness of an imaginative interfacial layer material.

Eq. (4.146) can be rearranged as

$$R_{int} = \frac{\Delta l}{k_m} \tag{4.147}$$

Eq. (4.147) is in accordance with the concept of Kapitza radius (Eq. (3.4)) and Δl is equal to a_K. This means that the effect of the temperature discontinuity at the interface can be compensated by a layer of a matrix material that has a thickness of a_K as shown in Figure 4.14(b). This layer is called the “interfacial layer" and has a thickness equal to the Kapitza radius a_K. It should be noted that the interfacial layer is just an idealized layer and non-existent.

(a)

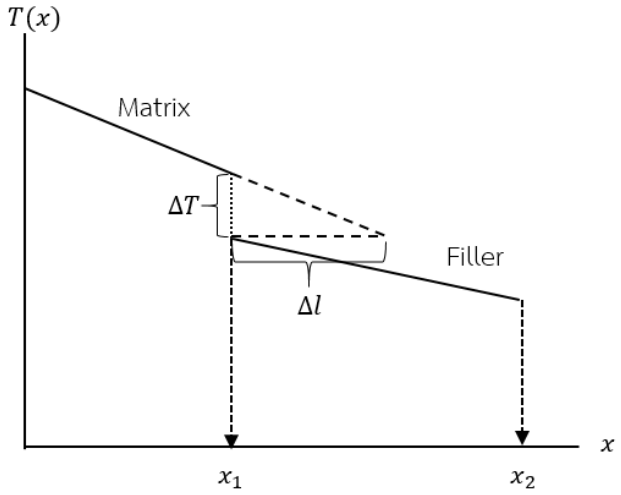

(b)

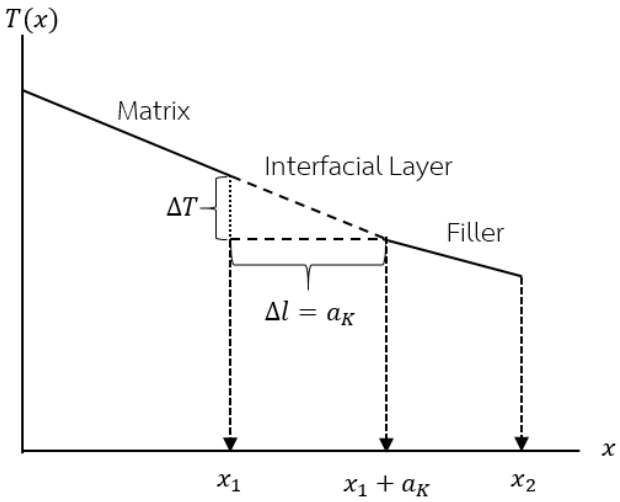

Figure 4.14 The simple scheme of temperature along x axis of a composite (a) and with the interfacial layer (b)

In the previous section, each cubic RVE has the side length of a and the total volume of RVE is equal to

$$V = V_m + V_f = a^3 \tag{4.148}$$

where V_m and V_f are volume of matrix and filler, respectively. Since the filler particle is spherical, the volume of filler can be written as

$$V_f = \frac{4n_f \pi r^3}{3} \tag{4.149}$$

It was assumed that each spherical particle is surrounded by an interfacial layer as shown in Figure 4.15. In this case, the radius of spherical particle with the interfacial layer or effective filler particle (r') is smaller than that without the interfacial layer (r). This means that the volume of filler was reduced due to the presence of interfacial thermal resistance while the volume of matrix was defined as a constant. The volume of RVE with the interfacial layer can be written as

$$V = V_m + V_K + V_f' = a^3 \tag{4.150}$$

where V_K is the volume of interfacial layer and V_f' is the volume of effective filler particle (i.e. volume of filler less the volume of interfacial layer).

The value of a for RVE with the interfacial layer can be calculated by

$$a = \left(\frac{4n_f \pi (r')^3}{3v_f'}\right)^{\frac{1}{3}} \tag{4.151}$$

where v_f' is the volume fraction of effective filler particle .

The volume of filler with the interfacial layer can be defined as

$$\begin{aligned} V_f' &= \frac{4n_f \pi (r')^3}{3} \\ &= \frac{4n_f \pi (r - a_K)^3}{3} \\ &= \frac{4n_f \pi r^3}{3}\left(1 - \frac{a_K}{r}\right)^3 \end{aligned} \tag{4.152}$$

From Eq. (4.149), Eq. (4.152) can be further simplified as

$$V_f' = \varepsilon_K V_f \tag{4.153}$$

where ε_K is the effective volume factor defined as

$$\varepsilon_K = \left(1 - \frac{a_K}{r}\right)^3 = (1 - \alpha_K)^3 = \left(\frac{r'}{r}\right)^3 \tag{4.154}$$

and α_K is the interfacial thermal resistance factor as defined in Eq. (3.5) (see chapter 3).

Dividing Eq. (4.153) by V, Eq. (4.153) can be written in term of volume fraction as

$$v_f' = \varepsilon_K v_f \tag{4.155}$$

By the way, the volume of interfacial layer is the volume of spherical shell and can be defined as

$$\begin{aligned} V_K &= \frac{4n_f\pi r^3}{3} - \frac{4n_f\pi (r')^3}{3} \\ &= \frac{4n_f\pi}{3}[r^3 - (r')^3] \\ &= \frac{4n_f\pi r^3}{3}\left[1 - \left(\frac{r - a_K}{r}\right)^3\right] \\ &= \frac{4n_f\pi r^3}{3}\left[1 - \left(1 - \frac{a_K}{r}\right)^3\right] \end{aligned} \tag{4.156}$$

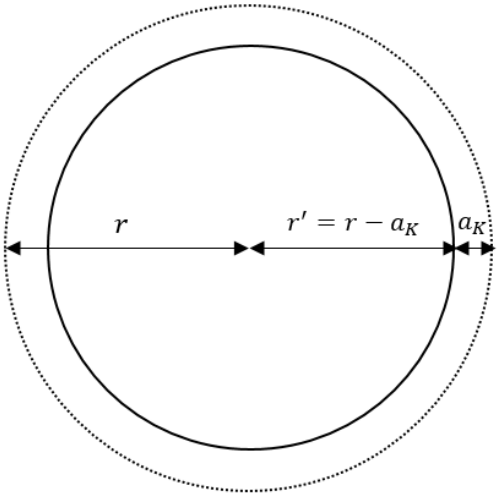

Figure 4.15 A spherical surrounded by an interfacial layer

From Eq. (4.149) and Eq. (4.154), Eq. (4.156) can be written as

$$V_K = (1 - \varepsilon_K)V_f \tag{4.157}$$

Dividing Eq. (4.157) by V, Eq. (4.157) can be written in term of volume fraction as

$$v_K = (1 - \varepsilon_K)v_f = v_f - v_f' \tag{4.158}$$

where v_K is the volume fraction of the interfacial layer.

From Eq. (4.154), it can be referred that the value of effective volume factor ε_K is always in the range of 0 – 1. Therefore, Eq. (4.155) gives the volume fraction of effective filler particle is only ε_K times of the original volume fraction when the interfacial layer was included. In case of $\varepsilon_K = 1$, the effect of interfacial thermal resistance is neglected ($a_K = 0$). In contrast, for $\varepsilon_K = 0$, this means the contribution of the interfacial thermal resistance is exactly balanced by the thermal conductivity of the filler particles. Since the interfacial layer is the imaginary layer which is built from the matrix phase according to Kapitza radius concept (Eq. (3.4)), thus its properties are

similar to the matrix. This leads to an easy way to include the effect of the interfacial thermal resistance into the models derived in previous section. In addition, it should be noted that the effect of the radius of particle is also included by this way.

4.2.1 SC Model with the Interfacial Thermal Resistance Layer (SC2)

SC model was chosen as a model to be modified by including the interfacial layer because this model predicted the effective thermal conductivity closer to the experimental data and showed more appropriate behavior of predictive curve than the other models in section 4.1.

It is assumed that there is the presence of the interfacial layer in simple cubic element at filler volume fraction lower than 0.524. Under this maximum filler volume fraction, it is expected that the filler particles have a uniform distribution and not touching each other. The physical model of simple cubic element with the interfacial layer was shown in Figure 4.16. It was noted that this physical model is similar with the physical model of simple cubic element without the interfacial layer (Figure 4.5(a)). Therefore, the thermal circuit model of this element is still the same with that of simple cubic element without the interfacial layer (Figure 4.5(b)). This was a result of the similarity of the interfacial layer and matrix.

The total thermal resistance of this element is the same as Eq. (4.5) and can be rewritten as

$$R_{\Sigma} = R_1 + R_2 + R_3 \tag{4.159}$$

The effective thermal conductivity can be written as

$$k_{eff,\mathrm{SC2}} = \frac{1}{a}\left(\frac{1}{R_1 + R_2 + R_3}\right) \tag{4.160}$$

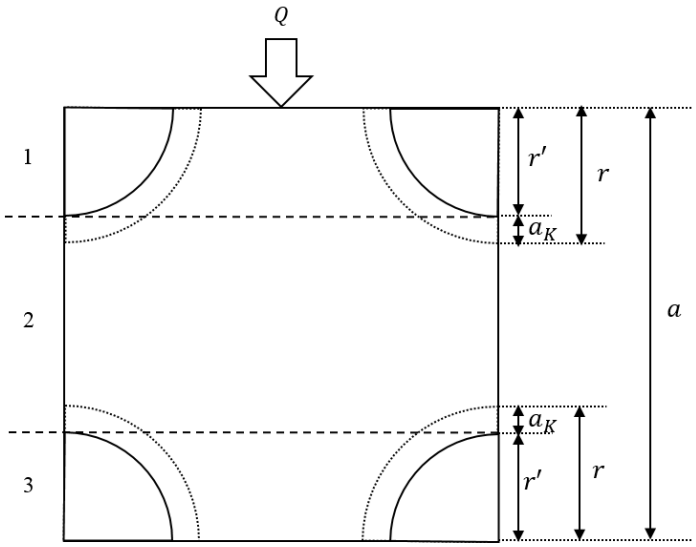

Figure 4.16 Physical model of simple cubic element with the interfacial layer

The thermal resistance of section 1 and 3 can be expressed by substituting r' instead of r in Eq. (4.14) as follows:

$$R_1 = R_3 = \frac{1}{\pi\left(k_f - k_m\right)} \int_0^{r'} \frac{1}{\left\{(r')^2 \left[\frac{(a)^2}{\pi(r')^2}\left(\frac{k_m}{k_f - k_m}\right) + 1\right]\right\} - x_j^2} dx_j \qquad (4.161)$$

Substituting Eq. (4.151) where $n_f = 1$ and Eq. (4.155) into Eq. (4.161) and rearranging, This led to

$$R_1 = R_3 = \frac{1}{\pi\left(k_f - k_m\right)} \int_0^{r'} \frac{1}{\left\{(r')^2 \left[\left(\frac{4\pi(r')^3}{3v_f'}\right)^{\frac{2}{3}}\left(\frac{1}{\pi(r')^2}\right)\left(\frac{k_m}{k_f - k_m}\right) + 1\right]\right\} - x_j^2} dx_j$$

$$= \frac{1}{\pi\left(k_f - k_m\right)} \int_0^{r'} \frac{1}{\left\{(r')^2 \left[\varepsilon_K^{-\frac{2}{3}}\left(\frac{16}{9\pi v_f^2}\right)^{\frac{1}{3}}\left(\frac{k_m}{k_f - k_m}\right) + 1\right]\right\} - x_j^2} dx_j$$

$$= \frac{1}{\pi\left(k_f - k_m\right)} \int_0^{r'} \frac{1}{\left[r'\sqrt{\varepsilon_K^{-\frac{2}{3}}\gamma_{\mathrm{SC1}} + 1}\right]^2 - x_j^2} dx_j \tag{4.162}$$

where γ_{SC1} is expressed in Eq. (4.17).

Integrating Eq. (4.162), the thermal resistance of section 1 or 3 can be written as

$$R_1 = R_3 = \left(\frac{1}{2\pi r'\left(k_f - k_m\right)}\right)\left(\frac{1}{\sqrt{\varepsilon_K^{-\frac{2}{3}}\gamma_{\mathrm{SC1}} + 1}} \ln \frac{\sqrt{\varepsilon_K^{-\frac{2}{3}}\gamma_{\mathrm{SC1}} + 1} + 1}{\sqrt{\varepsilon_K^{-\frac{2}{3}}\gamma_{\mathrm{SC1}} + 1} - 1}\right) \tag{4.163}$$

Considering section 2, thermal resistance of this section is expressed as

$$R_2 = \frac{(a - r') - r'}{a^2 k_m} = \frac{a - 2r'}{a^2 k_m} \tag{4.164}$$

Then Eq. (4.163) and (4.164) are substituted into Eq. (4.160) as

$$k_{eff,\mathrm{SC2}} = \frac{1}{a}\left(\frac{1}{\frac{a - 2r'}{a^2 k_m} + 2\left(\frac{1}{2\pi r'\left(k_f - k_m\right)}\right)\left(\frac{1}{\sqrt{\varepsilon_K^{-\frac{2}{3}}\gamma_{\mathrm{SC1}} + 1}} \ln \frac{\sqrt{\varepsilon_K^{-\frac{2}{3}}\gamma_{\mathrm{SC1}} + 1} + 1}{\sqrt{\varepsilon_K^{-\frac{2}{3}}\gamma_{\mathrm{SC1}} + 1} - 1}\right)}\right) \tag{4.165}$$

Dividing Eq. (4.165) by k_m, the ratio of $k_{eff,\mathrm{SC2}}$ and k_m can be derived as

$$\frac{k_{eff,\mathrm{SC2}}}{k_m}=\frac{1}{ak_m}\left(\frac{1}{\dfrac{a-2r'}{a^2k_m}+2\left(\dfrac{1}{2\pi r'\left(k_f-k_m\right)}\right)\left(\dfrac{1}{\sqrt{\varepsilon_K^{-\frac{2}{3}}\gamma_{\mathrm{SC1}}+1}}\ln\dfrac{\sqrt{\varepsilon_K^{-\frac{2}{3}}\gamma_{\mathrm{SC1}}+1}+1}{\sqrt{\varepsilon_K^{-\frac{2}{3}}\gamma_{\mathrm{SC1}}+1}-1}\right)}\right)$$

$$=\frac{1}{1-\dfrac{2r'}{a}+\left(\dfrac{ak_m}{\pi r'\left(k_f-k_m\right)}\right)\left(\dfrac{1}{\sqrt{\varepsilon_K^{-\frac{2}{3}}\gamma_{\mathrm{SC1}}+1}}\ln\dfrac{\sqrt{\varepsilon_K^{-\frac{2}{3}}\gamma_{\mathrm{SC1}}+1}+1}{\sqrt{\varepsilon_K^{-\frac{2}{3}}\gamma_{\mathrm{SC1}}+1}-1}\right)}$$

$$=\frac{1}{1-\dfrac{2r'}{2r'\left(\dfrac{\pi}{6v_f'}\right)^{\frac{1}{3}}}+\left(\dfrac{4\pi(r')^3}{3v_f'}\right)^{\frac{1}{3}}\left(\dfrac{1}{\pi r'}\right)\left(\dfrac{k_m}{k_f-k_m}\right)\left(\dfrac{1}{\sqrt{\varepsilon_K^{-\frac{2}{3}}\gamma_{\mathrm{SC1}}+1}}\ln\dfrac{\sqrt{\varepsilon_K^{-\frac{2}{3}}\gamma_{\mathrm{SC1}}+1}+1}{\sqrt{\varepsilon_K^{-\frac{2}{3}}\gamma_{\mathrm{SC1}}+1}-1}\right)}$$

$$=\frac{1}{1-\left(\dfrac{6v_f'}{\pi}\right)^{\frac{1}{3}}+\left(\dfrac{4}{3\pi^2v_f'}\right)^{\frac{1}{3}}\left(\dfrac{k_m}{k_f-k_m}\right)\left(\dfrac{1}{\sqrt{\varepsilon_K^{-\frac{2}{3}}\gamma_{\mathrm{SC1}}+1}}\ln\dfrac{\sqrt{\varepsilon_K^{-\frac{2}{3}}\gamma_{\mathrm{SC1}}+1}+1}{\sqrt{\varepsilon_K^{-\frac{2}{3}}\gamma_{\mathrm{SC1}}+1}-1}\right)}$$

$$=\frac{1}{1-\left(\dfrac{6v_f'}{\pi}\right)^{\frac{1}{3}}+\dfrac{1}{2}\left(\dfrac{6v_f'}{\pi}\right)^{\frac{1}{3}}\left(\dfrac{16}{9\pi\left(v_f'\right)^2}\right)^{\frac{1}{3}}\left(\dfrac{k_m}{k_f-k_m}\right)\left(\dfrac{1}{\sqrt{\varepsilon_K^{-\frac{2}{3}}\gamma_{\mathrm{SC1}}+1}}\ln\dfrac{\sqrt{\varepsilon_K^{-\frac{2}{3}}\gamma_{\mathrm{SC1}}+1}+1}{\sqrt{\varepsilon_K^{-\frac{2}{3}}\gamma_{\mathrm{SC1}}+1}-1}\right)}$$

$$\frac{k_{eff,\mathrm{SC2}}}{k_m}=\frac{1}{1-\left(\dfrac{6\varepsilon_K v_f}{\pi}\right)^{\frac{1}{3}}\left[1-\dfrac{\varepsilon_K^{-\frac{2}{3}}\gamma_{\mathrm{SC1}}}{2\sqrt{\varepsilon_K^{-\frac{2}{3}}\gamma_{\mathrm{SC1}}+1}}\ln\dfrac{\sqrt{\varepsilon_K^{-\frac{2}{3}}\gamma_{\mathrm{SC1}}+1}+1}{\sqrt{\varepsilon_K^{-\frac{2}{3}}\gamma_{\mathrm{SC1}}+1}-1}\right]} \tag{4.166}$$

where ε_K is defined in Eq. (4.154).

All models derived in this work were summarized in Table 4.1.

Table 4.1 List of equations for the effective thermal conductivity prediction

Model	Case	Restriction	Equation
SC1	I	- $v_f < 0.524$ - No effect of the interfacial thermal resistance	$\frac{k_{eff,\mathrm{SC1-1}}}{k_m} = \frac{1}{1-\left(\frac{6v_f}{\pi}\right)^{\frac{1}{3}}\left[1-\frac{\gamma_{\mathrm{SC1}}}{2\sqrt{\gamma_{\mathrm{SC1}}+1}}\ln\frac{\sqrt{\gamma_{\mathrm{SC1}}+1}+1}{\sqrt{\gamma_{\mathrm{SC1}}+1}-1}\right]}$ where $\gamma_{\mathrm{SC1}} = \left(\frac{16}{9\pi v_f^2}\right)^{\frac{1}{3}}\left(\frac{k_m}{k_f-k_m}\right)$
	II	- $v_f = 0.524$ - No effect of the interfacial thermal resistance	$\frac{k_{eff,\mathrm{SC1-2}}}{k_m} = \frac{1}{\left(\frac{6v_f}{\pi}\right)^{\frac{1}{3}}\left[\frac{\gamma_{\mathrm{SC1}}}{2\sqrt{\gamma_{\mathrm{SC1}}+1}}\ln\frac{\sqrt{\gamma_{\mathrm{SC1}}+1}+1}{\sqrt{\gamma_{\mathrm{SC1}}+1}-1}\right]}$
BCC1	III	- $v_f < 0.131$ - No effect of the interfacial thermal resistance	$\frac{k_{eff,\mathrm{BCC1-1}}}{k_m} = \frac{1}{1-\left(\frac{24v_f}{\pi}\right)^{\frac{1}{3}}\left[1-\frac{\gamma_{\mathrm{BCC1}}}{2\sqrt{\gamma_{\mathrm{BCC1}}+1}}\ln\frac{\sqrt{\gamma_{\mathrm{BCC1}}+1}+1}{\sqrt{\gamma_{\mathrm{BCC1}}+1}-1}\right]}$ where $\gamma_{\mathrm{BCC1}} = \left(\frac{64}{9\pi v_f^2}\right)^{\frac{1}{3}}\left(\frac{k_m}{k_f-k_m}\right)$

Table 4.1 List of equations for the effective thermal conductivity prediction (continued from previous)

Model	Case	Restriction	Equation
BCC1	IV	- $v_f = 0.131$ - No effect of the interfacial thermal resistance	$\frac{k_{eff,\mathrm{BCC1-2}}}{k_m} = \frac{1}{\left(\frac{24v_f}{\pi}\right)^{\frac{1}{3}}\left(\frac{\gamma_{\mathrm{BCC1}}}{2\sqrt{\gamma_{\mathrm{BCC1}}+1}}\ln\frac{\sqrt{\gamma_{\mathrm{BCC1}}+1}+1}{\sqrt{\gamma_{\mathrm{BCC1}}+1}-1}\right)}$
	V	- $0.68 \geq v_f > 0.131$ - No effect of the interfacial thermal resistance	$\frac{k_{eff,\mathrm{BCC1-3}}}{k_m} = \frac{1}{\left(\frac{3v_f}{\pi}\right)^{\frac{1}{3}}\left[\left(\frac{2\gamma_{\mathrm{BCC1}}}{\delta_{\mathrm{BCC1}}}\ln\frac{1-\beta_{\mathrm{BCC1}}+\delta_{\mathrm{BCC1}}}{1-\beta_{\mathrm{BCC1}}-\delta_{\mathrm{BCC1}}}\right)+\left(\frac{\gamma_{\mathrm{BCC1}}}{\sqrt{\gamma_{\mathrm{BCC1}}+1}}\ln\frac{\sqrt{\gamma_{\mathrm{BCC1}}+1}+\beta_{\mathrm{BCC1}}}{\sqrt{\gamma_{\mathrm{BCC1}}+1}-\beta_{\mathrm{BCC1}}}\right)\right]}$ where $\beta_{\mathrm{BCC1}} = \left(\frac{\pi}{3v_f}\right)^{\frac{1}{3}} - 1,$ $\delta_{\mathrm{BCC1}} = \sqrt{4+2\gamma_{\mathrm{BCC1}}-(\beta_{\mathrm{BCC1}}+1)^2}$
FCC1	VI	- $v_f < 0.262$ - No interfacial the thermal resistance	$\frac{k_{eff,\mathrm{FCC1-1}}}{k_m} = \frac{1}{1-\left(\frac{12v_f}{\pi}\right)^{\frac{1}{3}}\left[1-\frac{\gamma_{\mathrm{FCC1}}}{2\sqrt{\gamma_{\mathrm{FCC1}}+1}}\ln\frac{\sqrt{\gamma_{\mathrm{FCC1}}+1}+1}{\sqrt{\gamma_{\mathrm{FCC1}}+1}-1}\right]}$ where $\gamma_{\mathrm{FCC1}} = \left(\frac{32}{9\pi v_f^2}\right)^{\frac{1}{3}}\left(\frac{k_m}{k_f-k_m}\right)$

Table 4.1 List of equations for the effective thermal conductivity prediction (continued from previous)

Model	Case	Restriction	Equation
FCC1	VII	- $v_f = 0.262$ - No interfacial the thermal resistance	$\frac{k_{eff,\mathrm{FCC1-2}}}{k_m} = \frac{1}{\left(\frac{12v_f}{\pi}\right)^{\frac{1}{3}}\left(\frac{\gamma_{\mathrm{FCC1}}}{2\sqrt{\gamma_{\mathrm{FCC1}}+1}}\ln\frac{\sqrt{\gamma_{\mathrm{FCC1}}+1}+1}{\sqrt{\gamma_{\mathrm{FCC1}}+1}-1}\right)}$
	VIII	- $0.741 \geq v_f > 0.262$ - No effect of the interfacial thermal resistance	$\frac{k_{eff,\mathrm{FCC1-3}}}{k_m} = \frac{1}{\left(\frac{3v_f}{2\pi}\right)^{\frac{1}{3}}\left[\left(\frac{2\gamma_{\mathrm{FCC1}}}{\delta_{\mathrm{FCC1}}}\ln\frac{1-\beta_{\mathrm{FCC1}}+\delta_{\mathrm{FCC1}}}{1-\beta_{\mathrm{FCC1}}-\delta_{\mathrm{FCC1}}}\right)+\left(\frac{\gamma_{\mathrm{FCC1}}}{\sqrt{\gamma_{\mathrm{FCC1}}+1}}\ln\frac{\sqrt{\gamma_{\mathrm{FCC1}}+1}+\beta_{\mathrm{FCC1}}}{\sqrt{\gamma_{\mathrm{FCC1}}+1}-\beta_{\mathrm{FCC1}}}\right)\right]}$ where $\beta_{\mathrm{FCC1}} = \left(\frac{2\pi}{3v_f}\right)^{\frac{1}{3}} - 1,$ $\delta_{\mathrm{FCC1}} = \sqrt{4+2\gamma_{\mathrm{FCC1}}-(\beta_{\mathrm{FCC1}}+1)^2}$
SC2		- $v_f < 0.524$ - Included effect of the Interfacial thermal resistance	$\frac{k_{eff,\mathrm{SC2}}}{k_m} = \frac{1}{1-\left(\frac{6\varepsilon_K v_f}{\pi}\right)^{\frac{1}{3}}\left[1-\frac{\varepsilon_K^{-\frac{2}{3}}\gamma_{\mathrm{SC1}}}{2\sqrt{\varepsilon_K^{-\frac{2}{3}}\gamma_{\mathrm{SC1}}+1}}\ln\frac{\sqrt{\varepsilon_K^{-\frac{2}{3}}\gamma_{\mathrm{SC1}}+1}+1}{\sqrt{\varepsilon_K^{-\frac{2}{3}}\gamma_{\mathrm{SC1}}+1}-1}\right]}$ where $\varepsilon_K = \left(1-\frac{a_K}{r}\right)^3 = (1-\alpha_K)^3 = \left(\frac{r'}{r}\right)^3$

CHAPTER 5
RESULTS AND DISCUSSIONS

The effective thermal conductivity models derived in this work were discussed and compared with the experiments and other well-known models. The effective thermal conductivity models without the interfacial thermal resistance were studied in the section 5.1. Then the effective thermal conductivity models modified with the interfacial thermal resistance were studied in the section 5.2.

All of the experimental data discussed in this chapter were of polymer composite filled with spherical filler particles. The experimental data were cited from references and tabulated in the Appendix. In addition, the relative thermal conductivity, the ratio between the thermal conductivity of the composite and that of the polymer matrix, was used in order to compare various composite systems and to discount any effect of measurement errors.

5.1 Effective Thermal Conductivity Models without the Interfacial Thermal Resistance

The equations of all models without the interfacial thermal resistance were summarized in Table 4.1. It can be observed that these models depended on thermal conductivity of polymer matrix and filler, and volume fraction of filler. Thus the effects of these parameters on each model were considered. Furthermore, in order to discuss the predictive ability of derived models, the values predicted by each model were compared with experimental data and other models.

5.1.1 Effect of Thermal Conductivities of Filler and Polymer and Volume Fraction of Filler on SC1 Model, BCC1 Model, and FCC1 Model

The relationship between the relative effective thermal conductivity (k_{eff}/k_m) and the ratio of thermal conductivity of filler and matrix (k_f/k_m) predicted by SC1 model at various volume fractions of filler is shown in Figure 5.1. It indicated that for value of k_f/k_m below 100 the relative effective thermal conductivity rapidly increased

with increasing k_f/k_m. At 100 $\leq k_f/k_m \leq$ 500, the relative effective thermal conductivity gradually increased with increasing k_f/k_m. At $k_f/k_m >$ 500, there was an insignificant effect of k_f/k_m on the effective thermal conductivity. Thus the effective thermal conductivity depended only on the volume fraction of filler at a sufficiently high ratio of k_f/k_m. Figure 5.2 showed the relationship between k_{eff}/k_m and volume fraction of filler for SC1 model at various values of k_f/k_m. It can be seen that for ratios of k_f/k_m greater than 500:1 the curve predicted by SC1 model overlapped with others. This was a result of a decrease in γ_{SC1} in Eq. (4.21) at high ratio of k_f/k_m; Eq. (4.21) thus predicted that the effective thermal conductivity depended greatly on the volume fraction of filler particles. The behaviors as shown in Figure 5.1 and 5.2 were also found in Nielsen model but the effective thermal conductivity depended only on the volume fraction of filler at the ratios of k_f/k_m greater than 100:1 [39].

At a maximum packing volume fraction of filler particles for simple cubic element ($v_f =$ 0.524), the effective thermal conductivity still depended on the ratio of k_f/k_m as shown in Figure 5.1. This indicated that, at a maximum packing volume fraction of filler particles, the high thermal conductivity of filler dominated the effective thermal conductivity due to the formation of filler particle network. In addition, it should be noted that the slope of predicted curves rapidly increased at volume fraction of filler of 0.524 as shown in Figure 5.2. This referred to the percolation behavior, which is a rapid increase of the effective thermal conductivity over several order of magnitude [53]. Thus it could said that SC1 model predicted a percolation threshold at volume fraction of filler of 0.524. This was a result of the contact of filler particles in the representative volume element of simple cubic at $v_f =$ 0.524.

Figure 5.3 showed the relationship between the relative effective thermal conductivity and the ratio of k_f/k_m predicted by BCC1 model at various volume fractions of filler particles. It could be observed that the behavior similar to SC1 model occurred only at the filler volume fraction of filler particles less than 0.131 due to the same reason with SC1 model. At the volume fraction of filler particles more than 0.131, the relative effective thermal conductivity increased linearly with increasing ratio of k_f/k_m. This indicated that for filler volume fraction more than 0.131 the effective thermal conductivity predicted by BCC1 model depended strongly on both ratio of

k_f/k_m and volume fraction of filler. The strong influences of ratio of k_f/k_m and volume fraction of filler were also shown in Figure 5.4. This was due to the denominator in Eq. (4.93) which was in term of addition; Eq. (4.93) thus predicted high effective thermal conductivities at high ratios of k_f/k_m.

Furthermore, it should be noted that BCC1 model predicted a percolation threshold at volume fraction of filler of 0.131. This percolation behavior was the cause of the addition of resistances that possessed the commutative of addition. Therefore, the geometry of representative volume element of body-centered cubic in case of $v_f = 0.131$ can change to be the contact of filler particles.

FCC1 model gave the prediction similar with BCC1 model as shown in Figure 5.5 and 5.6 but FCC1 model predicted the percolation threshold at $v_f = 0.262$. This was due to the similarity of predictive equations.

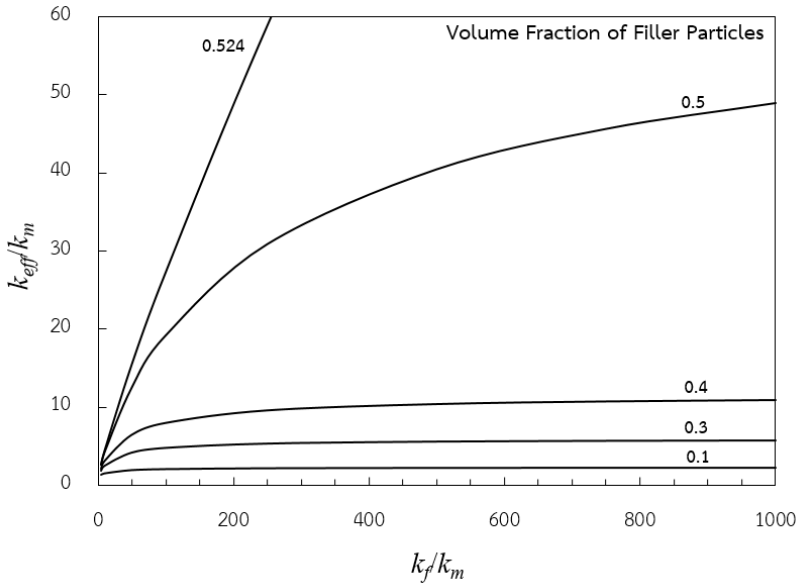

Figure 5.1 The relationship between k_{eff}/k_m and k_f/k_m for SC1 model at various volume fraction of filler particles

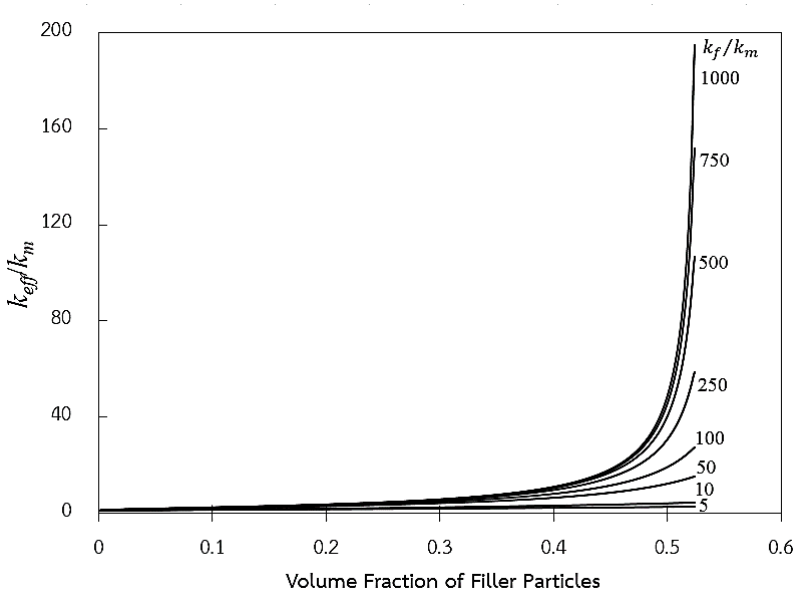

Figure 5.2 The relationship between k_{eff}/k_m and volume fraction of filler particles for SC1 model at various k_f/k_m

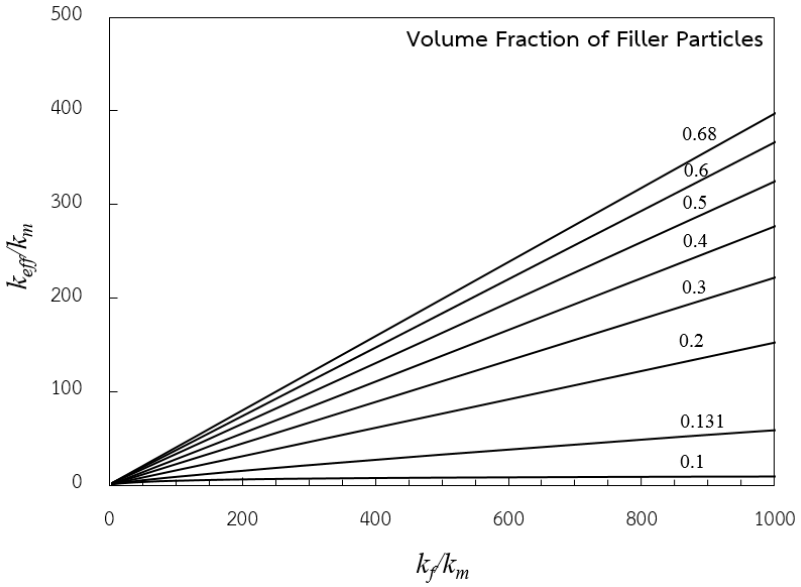

Figure 5.3 The relationship between k_{eff}/k_m and k_f/k_m for BCC1 model at various volume fraction of filler particles

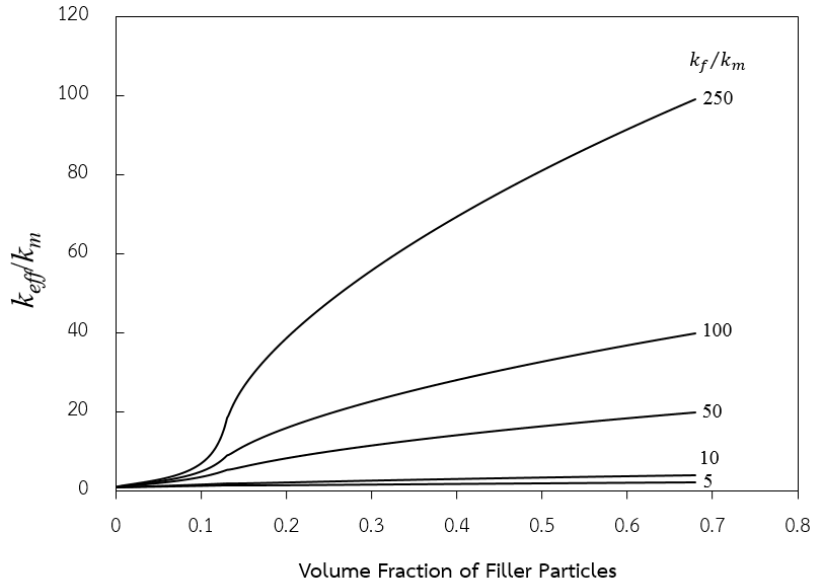

Figure 5.4 The relationship between k_{eff}/k_m and volume fraction of filler particles for BCC1 model at various k_f/k_m

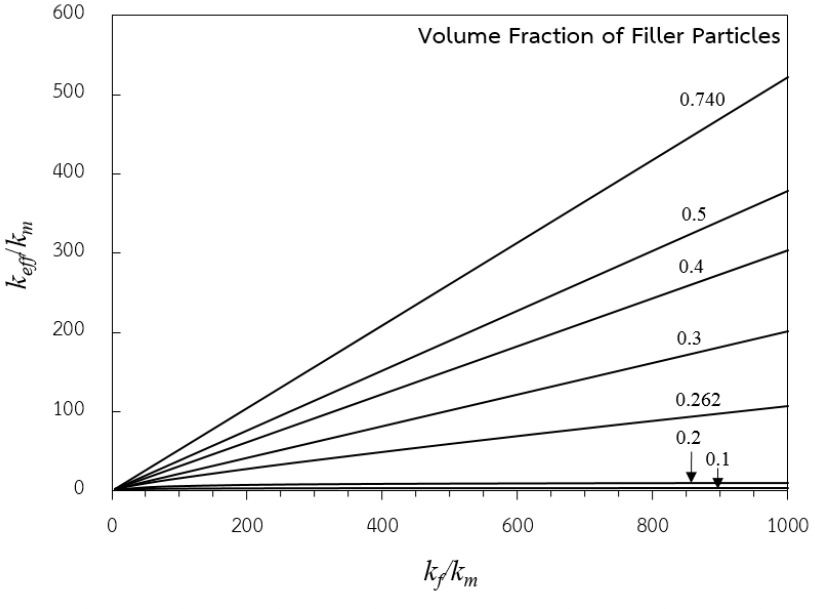

Figure 5.5 The relationship between k_{eff}/k_m and k_f/k_m for FCC1 model at various volume fraction of filler particles

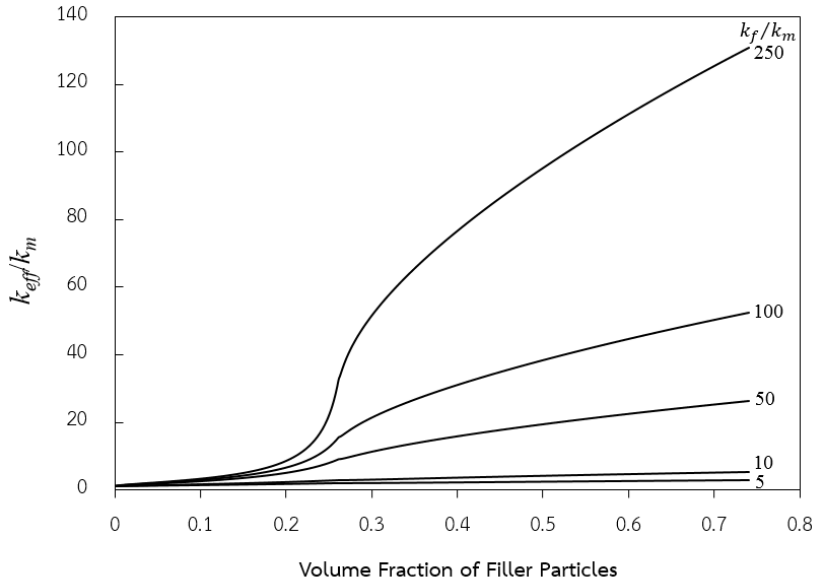

Figure 5.6 The relationship between k_{eff}/k_m and volume fraction of filler particles for FCC1 model at various k_f/k_m

SC1 model, BCC1 model, and FCC1 model gave the different predictions that were discussed in previous paragraphs. The effects of thermal conductivity of filler and polymer and volume fraction of filler on the effective thermal conductivity were very significant for BCC1 model and FCC1 model but not SC1 model in which the effective thermal conductivity depended greatly on the volume fraction of filler for ratios of k_f/k_m greater that 500:1. This difference was due to the different location of a percolation threshold predicted. SC1 model predicted a percolation threshold at filler volume fraction of 0.524, which is its maximum packing volume fraction of filler. Thus the effects of thermal conductivity of filler and polymer and volume fraction of filler were very significant at only the maximum packing volume fraction for SC1 model.

5.1.2 Comparison with Experimental Data and Other Models

In this section, the three models, i.e. SC1 model, BCC1 model, and FCC1 model, were compared with the experiment data of various composite systems with different ratios of k_f/k_m. The predictions of other models, i.e. Maxwell model, Bruggeman model, Hashin model, Cheng and Vachon model, and Liang and Liu model, were also plotted in the same graph in order to compare their performance.

Figure 5.7 showed the overview of relationship between relative effective thermal conductivity and filler volume fraction of EVA/$BaTiO_3$ with k_f/k_m = 10:1. Maxwell model, Bruggeman model, and Hashin model gave the predictions throughout the entire range of filler volume fraction, owing to these models were the exact solutions obtained by an analytical solution of the heat equation for a spherical particle surrounded by matrix without any assumptions on heat flow or temperature patterns [20]. While Cheng and Vachon model, Liang and Liu model, and three models derived in this work were simplified solutions in which unidirectional heat flow and isotherm planes perpendicular to the heat flow were assumed. To derive these second type models, the representative volume element (RVE) was first required. The filler particles were packed in the RVE until reaching the maximum packing volume fraction, which had different values depending on the arrangements of filler particles in the RVE. This led to the limitation of the second type models that could only predict the effective thermal conductivity at the volume fraction of filler under the maximum packing volume fraction. It should be noted in Figure 5.7 that albeit EVA filled with different particle size of BaTiO3, i.e. 9 and 105 μm in diameter showed the different thermal conductivities, all models still gave the prediction depending on volume fraction of filler particles. This was due to the fact that these models never take into account the filler particle size.

When the ratio of k_f/k_m increased to be 992:1 and 1721:1 as shown in Figure 5.8 and 5.9, respectively, the percolation behavior was observed in each model. This was not in agreement with the experimental data, which does not show the percolation behavior. The percolation threshold usually appears in the electrical conductive composites more than thermal conductive composites. This can be explained that the thermal conductivities of the filler particle and of the polymer matrix are comparable to each other, whereas the filler electrical conductivity is 10^{10}-10^{20} times larger than the polymer conductivity [53]. Therefore, models derived in this work might be suitable in case of very high ratio of k_f/k_m. However, this should be further investigated by comparing with the experimental data of composites with very high ratio of k_f/k_m in wide range of volume fraction of filler particles. It should be further noted that the predictions of SC1 model and Liang and Liu model converged

to the same value when the ratios of k_f/k_m increased. The result was due to the same modeling method based on the additivity of resistances in series, and these models had an equivalent RVE in which they contained a sphere. By this way, the arrangement of particles can be rearranged without the effect on the overall thermal resistance of the whole element [45]. However, it should be further stated that this property occurred at sufficiently high ratio of k_f/k_m.

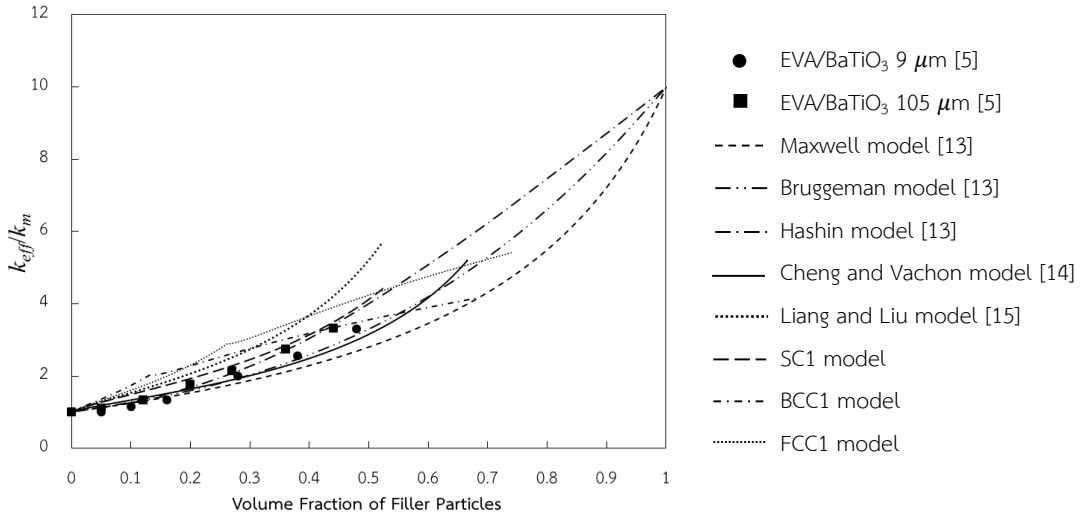

Figure 5.7 Overview of relationship between relative effective thermal conductivity and filler volume fraction of EVA/$BaTiO_3$ with k_f/k_m = 10:1

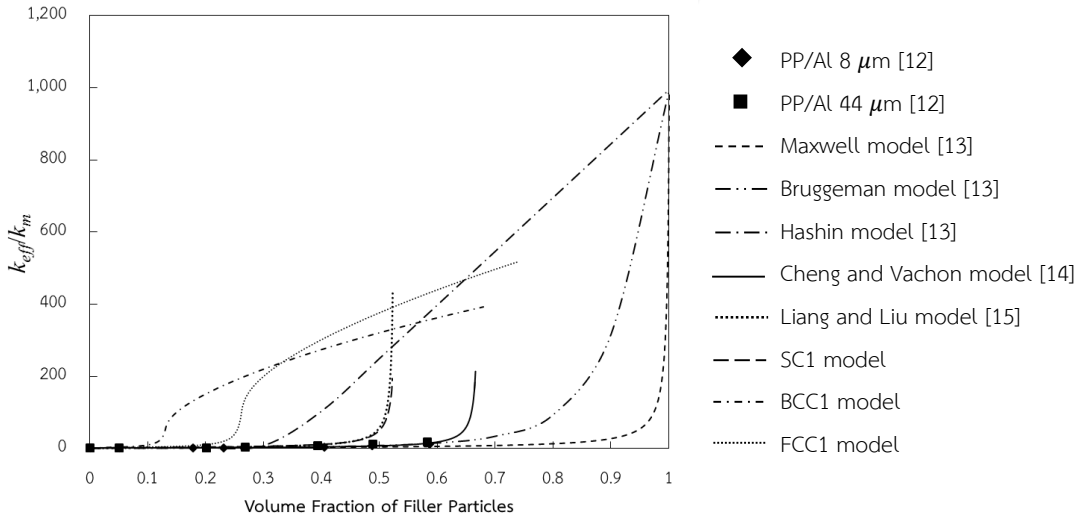

Figure 5.8 Overview of relationship between relative effective thermal conductivity and filler volume fraction of PP/Al with k_f/k_m = 992:1

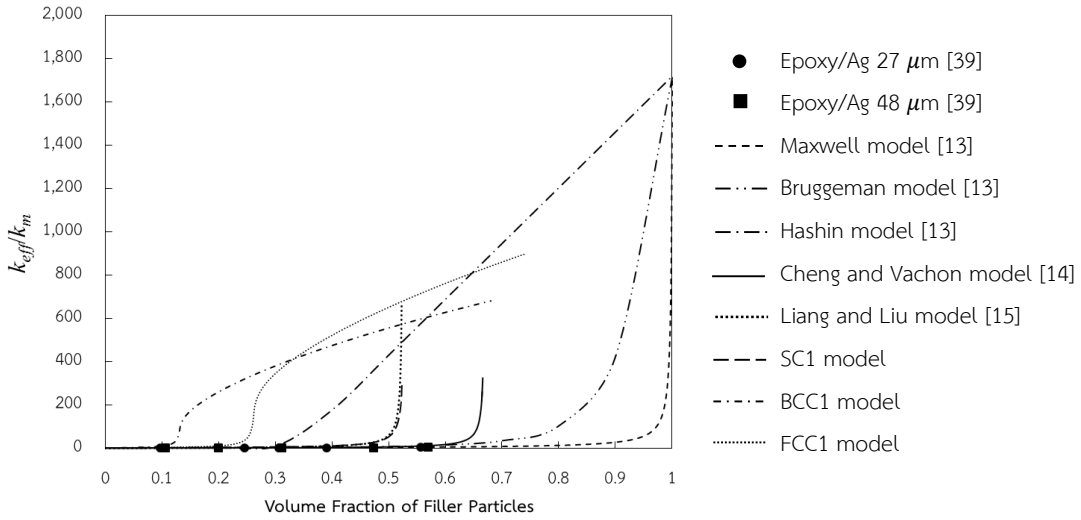

Figure 5.9 Overview of relationship between relative effective thermal conductivity and filler volume fraction of Epoxy/Ag with k_f/k_m = 1721:1

For more apparent observation, the scale of graphs were enlarged as shown in Figure 5.10, 5.11, and 5.12, for composite system with k_f/k_m equal to 10:1, 992:1, and 1721:1, respectively. It could be seen that Hashin model gave a closer prediction to the EVA composite filled with 105 μm $BaTiO_3$ particles and Bruggeman model gave a closer prediction to the EVA composite filled with 9 μm $BaTiO_3$ particles than other models throughout the volume fraction of filler as shown in Figure 5.10. For PP filled with 8 and 44 μm Al particle, it seemed that Bruggeman model and Cheng and Vachon model gave a good agreement with the experimental data as shown in Figure 5.11. For epoxy filled with 27 and 48 μm Ag particles, Maxwell model showed a good prediction throughout the volume fraction of filler as shown in Figure 5.12. These different results indicated that there were no any single model that was applicable to all composite systems.

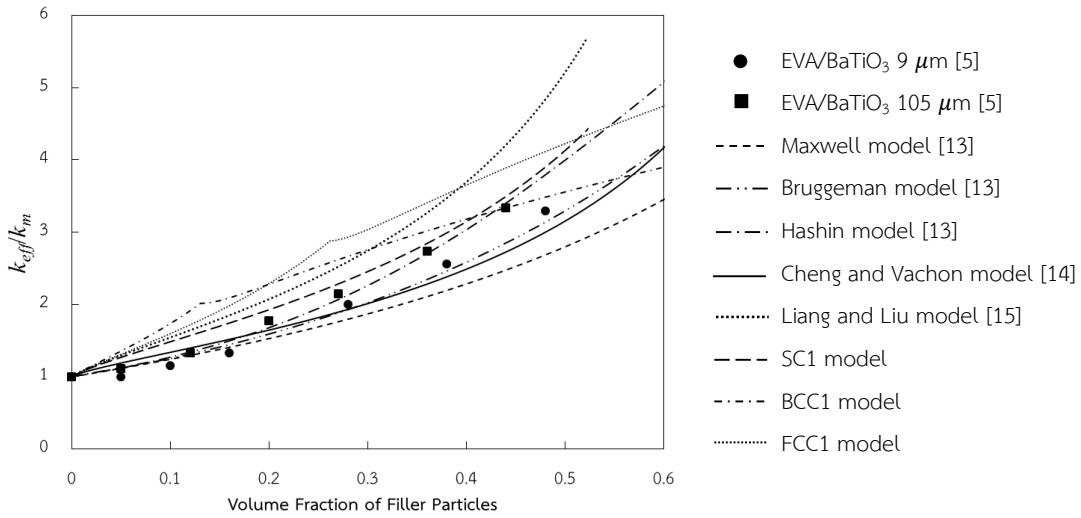

Figure 5.10 Comparison between theoretical predicted effective thermal conductivity and experimental data of EVA/$BaTiO_3$ with k_f/k_m = 10:1

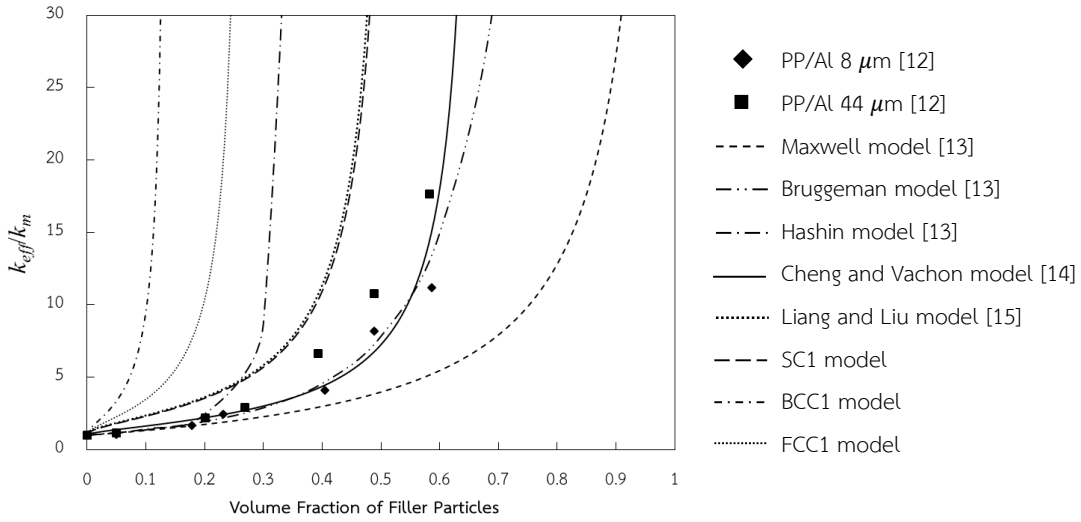

Figure 5.11 Comparison between theoretical predicted effective thermal conductivity and experimental data of PP/Al with k_f/k_m = 992:1

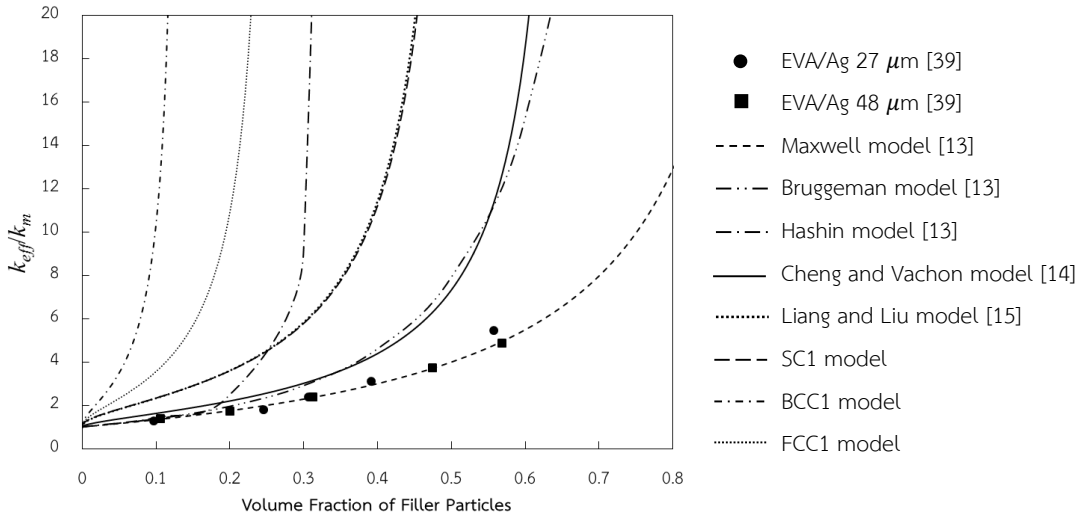

Figure 5.12 Comparison between theoretical predicted effective thermal conductivity and experimental data of Epoxy/Ag with k_f/k_m = 1721:1

The three models derived in this work overestimated the effective thermal conductivities compared with the other theoretical models. BCC1 model gave the most overestimated values, and then followed by FCC1 model, and SC1 model, respectively. Comparing with the models based on the simplified solution, Liang and Liu model gave a more overestimation compared to SC1 model, but less than BCC1 and FCC1 model, at the low ratio of k_f/k_m and similar to SC1 model at the high ratio of k_f/k_m. As described in previous, Liang and Liu model was equivalent to SC1 model at sufficiently high ratio of k_f/k_m. Cheng and Vachon model predicted the effective thermal conductivity in the different manner. It gave an underestimation for EVA/$BaTiO_3$, a reasonable estimation for PP/Al, and an overestimation for Epoxy/Ag. Although Cheng and Vachon model gave the predictions closer to the experimental data than the others, it possessed the instability for the prediction that was difficult to anticipate. In contrast, SC1 model, BCC1 model, and FCC1 model usually gave the overestimation. This result might come from the fact that these models were derived by considering the minimal thermal resistance that directly relates to the bulk or intrinsic thermal conductivity of each material in the composite [15]. Thus these models always overestimated the effective thermal conductivity. To meet the good agreement with the experimental, the interfacial thermal resistance due to the

incomplete bonding between constituents and phonon acoustic mismatch should be taken into account in the model [10]. This would be study in the further section. SC1 model was chosen as a model that would be modified with the interfacial thermal resistance because SC1 model showed a more appropriate prediction than BCC1 model and FCC1 model that gave the very inconsistent predictions with the experimental data; they always showed the percolation threshold at low filler content, which was non-existent in thermally conductive composites.

5.2 Effective Thermal Conductivity Models with the Interfacial Thermal Resistance

5.2.1 Effect of Interfacial Thermal Resistance on SC2 Model (Modified SC1 Model)

The SC2 model derived by modifying SC1 model indicated that the effect of the interfacial thermal resistance on the effective thermal conductivity was controlled by the interfacial thermal resistance factor α_K that its value is related to the ratio of the Kapitza radius and particle radius. As a numerical example, Figure 5.13, 5.14, 5.15, and 5.16 illustrated the relative effective thermal conductivity as a function of volume fraction and α_K with k_f/k_m = 10, 50, 250, and 1000, respectively. It could be observed that for α_K = 0 the effect of the interfacial thermal resistance was neglected and the prediction of SC2 model was similar to that of SC1 model because the equation of SC2 (Eq. (4.166)) reduced to the equation of SC1 (Eq. (4.21)) where ε_K = 0. For α_K > 0, it was noted that the predicted values were lowered and the larger α_K, the lower k_{eff}/k_m would be. In addition, for higher ratio of k_f/k_m, α_K had more effect on the reduction of the effective thermal conductivity. For α_K = 1, it could be seen that the effective thermal conductivity of the composite was the same as that of the matrix. This was due to the contribution of the interfacial thermal resistance was then exactly balanced by the much higher thermal conductivity of filler particles according to the results of the modified Maxwell and Bruggeman models reported by Every *et al* [27]. Furthermore, it was interesting to note that the effect of particle size was automatically included to the model in term of interfacial thermal resistance factor α_K or the ratio of radius of effective filler particle and radius of filler (r'/r). The

relationship between these two factors was given in Eq. (4.154). The value of r'/r is always in the range of 0 – 1. Figure 5.13, 5.14, 5.15, and 5.16 also showed the effective thermal conductivities decreased with decreasing r'/r. For r'/r = 1, the size of particles were not reduced and this was equivalent to the case of α_K = 0 as described previously. For r'/r < 1, this meant that the contribution of filler particles on the heat transfer was reduced due to the presence of interfacial thermal resistance. For r'/r = 0, it could be though that there were not any filler particles, thus the heat conduction was only occurred in the matrix phase. This event is equivalent to the case of α_K = 1.

SC2 model predicted the effective thermal conductivity in the range of $0 \leq \alpha_K \leq 1$, while the modified Maxwell and Bruggeman model predicted the effective thermal conductivity in range of $0 \leq \alpha_K \leq \infty$ [27]. This difference was due to the dissimilar modeling concept for including the effect of the interfacial thermal resistance. SC2 model was developed by determining the effective filler particle, the filler particle surrounded by interfacial layer, that its size would be reduced with increasing the thickness of interfacial layer. In contrast, the modified Maxwell and Bruggeman models were developed by modifying the boundary conditions at the interface with the interfacial thermal conductivity which is the reciprocal of the interfacial thermal resistance [28, 33]. If the interfacial thermal conductivity is very high (the interfacial thermal conductivity will approach to zero), the flow of heat across the interface into the conductive filler will be more difficult, then the conductive filler can less contribute to the heat transfer [28].

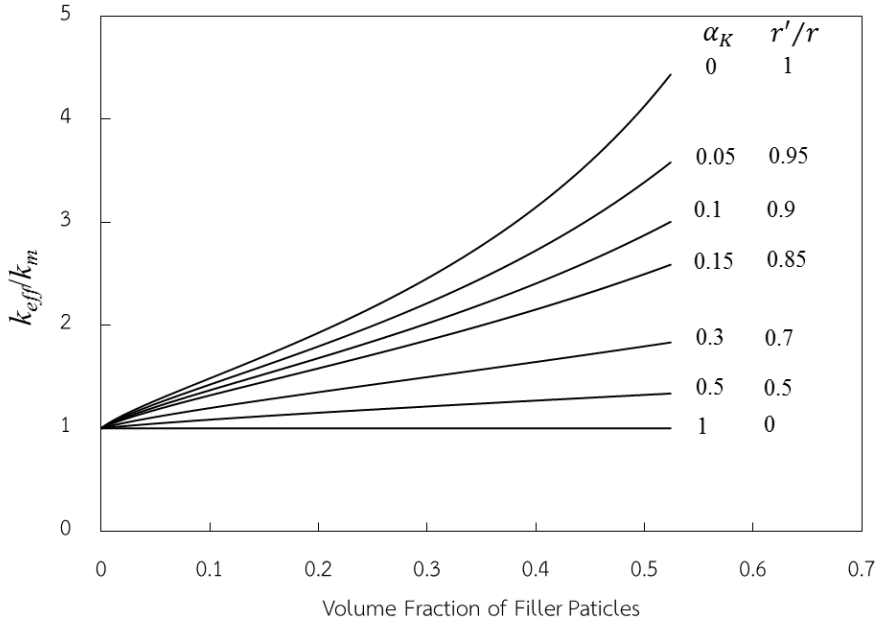

Figure 5.13 Effect of the interfacial thermal resistance on the effective thermal conductivity of polymer matrix filled with spherical filler particles for k_f/k_m = 10

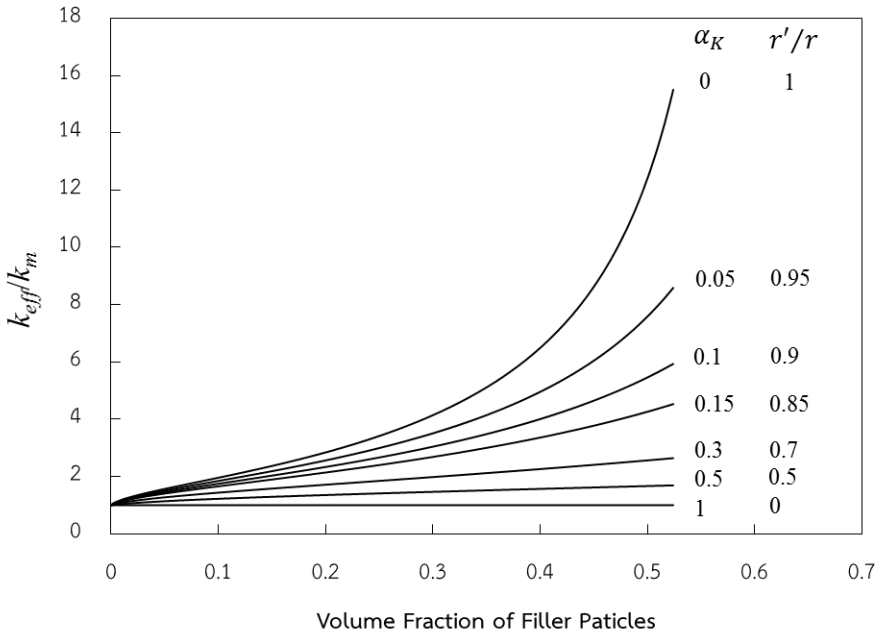

Figure 5.14 Effect of the interfacial thermal resistance on the effective thermal conductivity of polymer matrix filled with spherical filler particles for k_f/k_m = 50

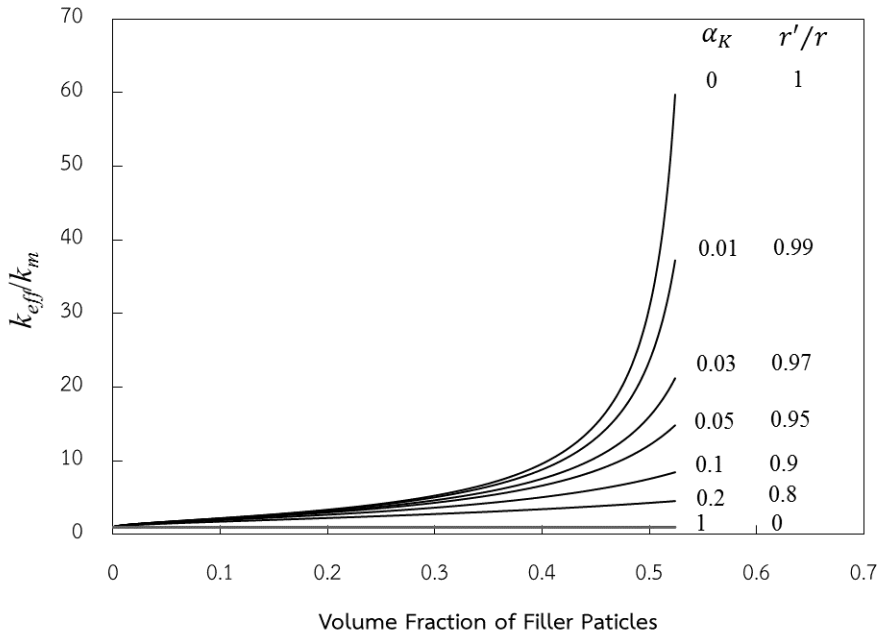

Figure 5.15 Effect of the interfacial thermal resistance on the effective thermal conductivity of polymer matrix filled with spherical filler particles for k_f/k_m = 250

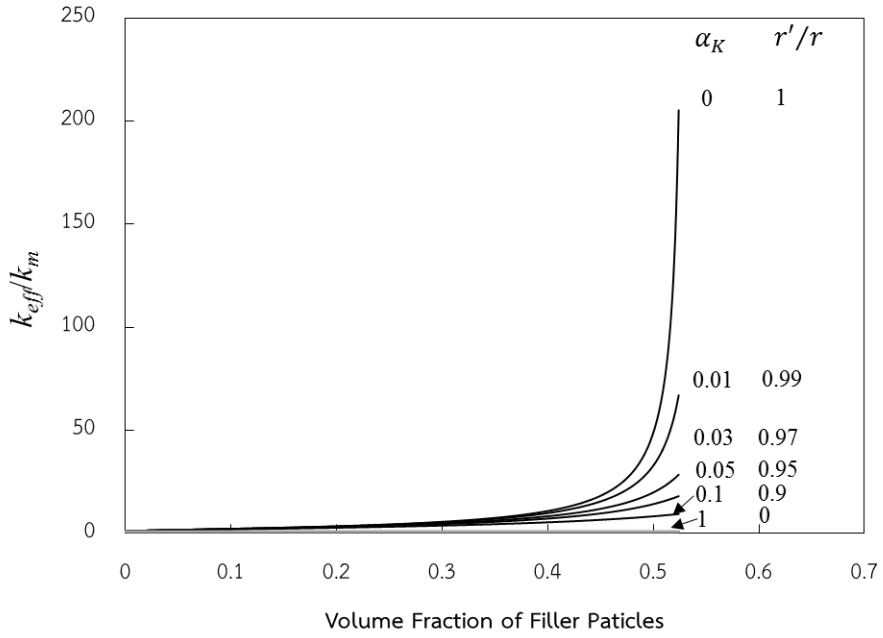

Figure 5.16 Effect of the interfacial thermal resistance on the effective thermal conductivity of polymer matrix filled with spherical filler particles for k_f/k_m = 1000

5.2.2 Comparison with Experimental Data and Other Modified Models

To verifying the ability of SC2 model, it was essential to compare this model with the experimental data. For appropriate experimental data for comparison, both the thermal conductivity and the interfacial thermal resistance measured from a composite must be reported. Unfortunately, there were no any such experimental data. This might come from the difficulty to measure the interfacial thermal resistance [40, 63]. Thus in this work the numerical results predicted by modified model were compared with the experimental data used in the previous section.

The comparison between effective thermal conductivities predicted by SC2 model at various values of α_K and experimental data of EVA filled with 9 and 105 μm BaTiO3 particles were shown in Figure 5.17. It could be observed that the SC2 model could not fit the experimental data by using a value of α_K, different from other models [27, 31]. This indicated that the SC2 model predicted the different value of the interfacial thermal resistance of each composite system depending on the volume fraction of filler and particle size. The similar events were also seen in the Figure 5.18 and 5.19 for PP filled Al particles and Epoxy filled Ag particles, respectively. These might come from the fact that SC2 model was derived based on the ideal arrangement of the uniform spherical particles in the form of simple cubic but the arrangement of particles in real composite system is variant from that ideal pattern due to effects of processing [54], size distribution of filler particles [4], and irregular-shaped particles [70]. The composites might have the same or different arrangement at each volume fraction of filler particles. Therefore, the effect of the arrangement of the particles that deviates from the ideal simple cubic arrangement should be further incorporated into the model.

From Figure 5.17, 5.18, and 5.19, it could be seen that the experimental data of composites filled with smaller particle size always located on the predicted curve with higher α_K (lower r'/r) compared with the composites filled with larger particle size. This represented the larger values of the interfacial thermal resistance of the composites filled with smaller filler particles. This was due to the fact that ,with decreasing average particle radius, the effective thermal conductivity decreases while

the area of interfacial contact per unit volume increases [33]. The interfacial thermal resistance began to play a significant role in the thermal transfer.

The modified Bruggeman model was only one model that could reasonably predict the effect of the interfacial thermal resistance. The modified Maxwell model gave the negative interfacial thermal resistance because it usually underestimates the effective thermal conductivity, albeit α_K = 0 (see Figure 5.10, 5.11, and 5.12). However, the modified Bruggeman model also gave the negative interfacial thermal resistance, if k_f/k_m is lower than 1000 as shown in 5.10 and 5.12. Thus the modified Bruggeman model could be only used for epoxy filled Ag particles with k_f/k_m = 1721:1. It could be seen in Figure 5.19 that the modified Bruggeman model gave the good prediction for epoxy filled Ag particles by used α_K in range of 0.09 – 0.16. This might indicate to the superior performance of the exact solution model type and the differential effective medium theory (DEM). However, this model was suitable for the composite system with $k_f \gg k_m$ according to the suggestion of Every *et al*. [27]. In contrast, SC2 model could use for lower value of the ratio k_f/k_m because it always gave an overestimation over the volume fraction of filler particles.

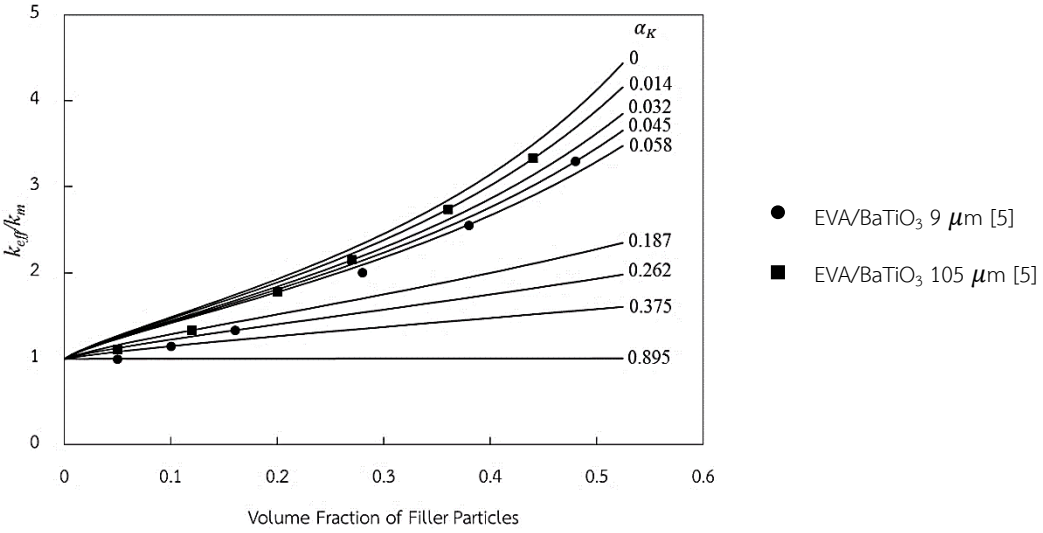

Figure 5.17 Comparison between effective thermal conductivity predicted by SC2 model at various values of α_K and experimental data of EVA/$BaTiO_3$ with k_f/k_m = 10:1

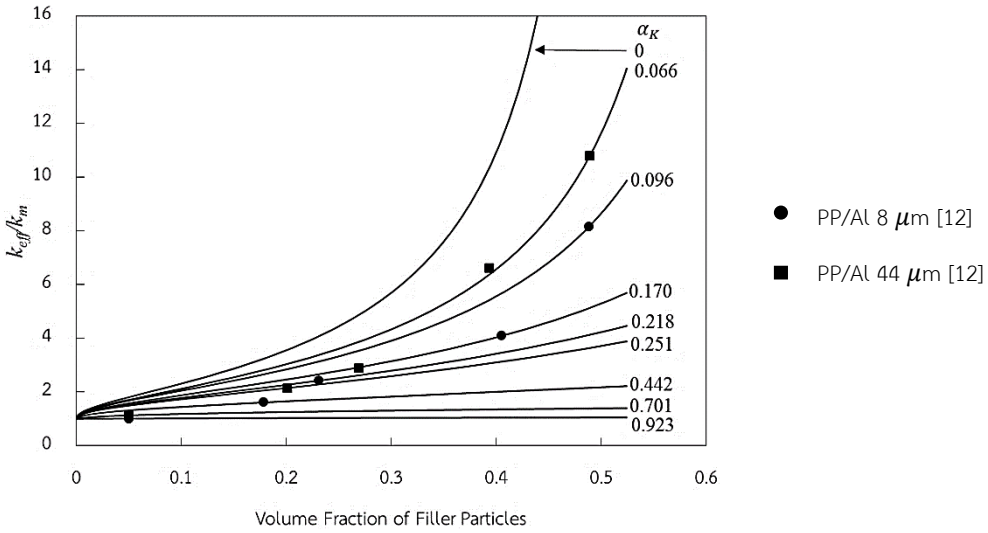

Figure 5.18 Comparison between effective thermal conductivity predicted by SC2 model at various values of α_K and experimental data of PP/Al with k_f/k_m= 992:1

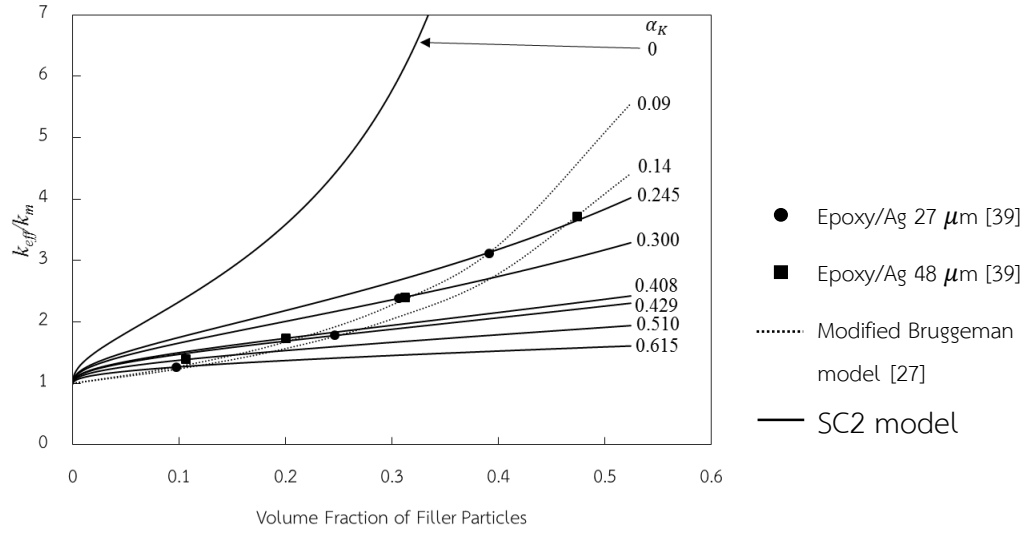

Figure 5.19 Comparison between effective thermal conductivity predicted by SC2 model (solid line) and the modified Bruggeman model (dot line) at various values of α_K and experimental data of Epoxy/Ag with k_f/k_m = 1721:1

The SC2 model were further discussed by substituting the thermal conductivity of Epoxy filled silver particles into predictive equation of SC2 to calculate the properties as tabulated in Table 5.1. The interfacial thermal resistance predicted by the SC2 model decreased with increasing volume fraction of filler particles as shown

in Table 5.1. The interfacial thermal resistance was referred to the combined effect of two thermal resistances, i.e. thermal contact resistance and thermal boundary resistance [33]. The value of thermal boundary resistance was constant for a composite system according to acoustic mismatch model [32]. Thus the decrease of interfacial thermal resistance should be a result of the decrease in the thermal contact resistance that occurred at polymer-filler and filler-filler interfaces [11]. This might be consistent to the formation of some segment of filler network or chains of connected conductive particles at high filler content [33]. Furthermore, it was possible to form the agglomeration of particles at high filler content [71]. The formation of highly thermally conductive networks might minimize the thermal resistance along the conductive paths [4]. This characteristic has never been seen before in the exact solution type models. This might make SC2 model suitable to describe the composites with the presence of some clusters of filler particles at high volume fraction of filler. In addition, this idea might be supported by the ratio of r'/r that increased with the volume fraction of filler particles. This indicated that the contribution of filler on the heat conduction was enhanced. If the relationship between the interfacial thermal resistance and volume fraction of filler was known, the SC2 model could be further modified and might give the better prediction. However, for more accuracy, the SC2 model must further be developed to include the other effect such as arrangement, size distribution, shape, and agglomeration of filler particles apart from the effect of the interfacial thermal resistance.

Furthermore, it should be noted that the values of v_f were the sum of and v_K according to Eq. (4.158). The effective volume fraction of filler v_f' can be though as the volume fraction of filler at a point on the curve predicted by SC1 model. If the values of v_f and thermal conductivities of composite were known from the experiment, the values of v_f' could be found by a graphical method as shown in Figure 5.20. Then the value of α_K or r'/r could be calculated by using Eq. (4.154) and (4.155), respectively. This led to the simple method to find the interfacial thermal resistance.

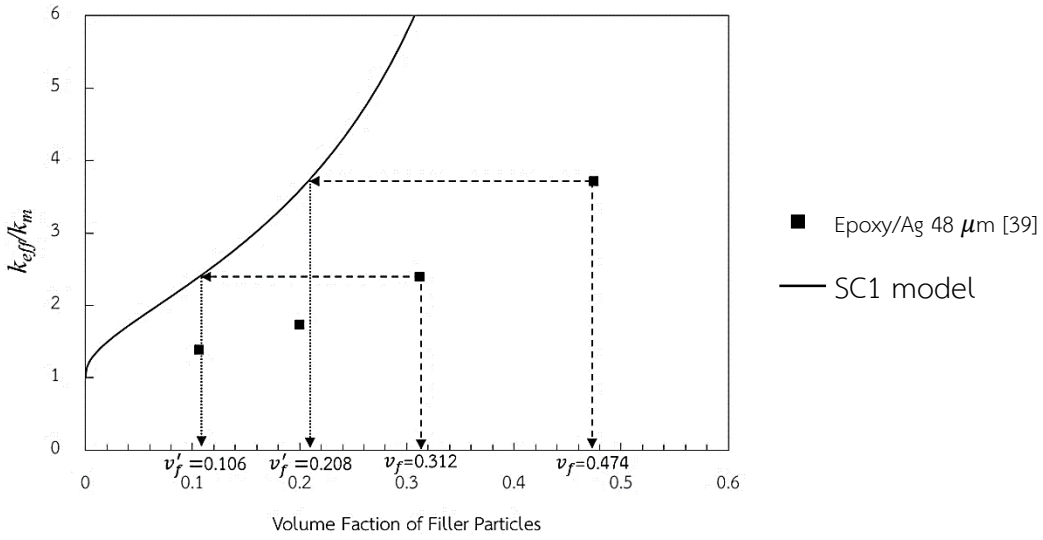

Figure 5.20 Graphical method for finding the effective volume of filler (v_f')

Table 5.1 Epoxy/Ag interfacial thermal resistances predicted by SC2 model

Matrix	Filler	D (μm)	v_f	v_f'	v_K	ε_K	r'/r	α_K	a_K (μm)	R_{int} (m^2K/W)
Epoxy	Silver	48	0.106	0.012	0.094	0.118	0.490	0.510	12.2	5.02×10^{-5}
Epoxy	Silver	48	0.200	0.041	0.159	0.207	0.592	0.408	9.80	4.02×10^{-5}
Epoxy	Silver	48	0.312	0.106	0.206	0.339	0.698	0.302	7.26	2.97×10^{-5}
Epoxy	Silver	48	0.474	0.208	0.266	0.438	0.759	0.241	5.77	2.37×10^{-5}
Epoxy	Silver	27	0.097	0.006	0.091	0.057	0.385	0.615	8.30	3.40×10^{-5}
Epoxy	Silver	27	0.246	0.046	0.200	0.186	0.571	0.429	5.80	2.38×10^{-5}
Epoxy	Silver	27	0.306	0.105	0.201	0.345	0.701	0.299	4.03	1.65×10^{-5}
Epoxy	Silver	27	0.391	0.167	0.224	0.427	0.753	0.247	3.33	1.37×10^{-5}

CHAPTER 6
CONCLUSIONS AND RECOMMENDATIONS

6.1 Conclusions

The three effective thermal conduction models, namely SC1, BCC1, and FCC1 model, for polymer composite filled with spherical particles were successfully derived based on the simplified solution of three ideal arrangements of spherical filler particles in the representative volume elements, i.e. simple cubic, body-centered cubic, and face-centered cubic, respectively. By an analogy between electrical and heat conduction, these models were easily generated and was consistent with the volume fraction of filler. These three models differently predicted that the effective thermal conductivity depended on the ratio between thermal conductivity of filler and polymer matrix (k_f/k_m) and volume fraction of filler. The SC1 model predicted the thermal conductivity of a composite increased with the increasing the ratio of k_f/k_m and for a sufficiently high ratio of k_f/k_m the effective thermal conductivity depended only on the volume fraction of filler. The BCC1 and FCC1 models predicted the same event with SC1 model only at the volume fraction of filler lower than 0.131 for BCC1 model, and 0.262 for FCC1 model. At higher volume fraction of filler, both BCC1 and FCC1 models predicted the effective thermal conductivity strongly increased with increasing the ratio of k_f/k_m. All models gave the overestimation compared to the experimental data and predicted the percolation threshold at volume fraction of filler equal to 0.524 for SC1 model, 0.131 for BCC1 model, and 0.262 for FCC1 model. However, the SC1 model showed more appropriate and reasonable predictions than BCC1 and FCC1 models. Furthermore, SC1 model was also consistent to Liang and Liu model at high ratio of k_f/k_m.

The SC2 model was developed from SC1 model by combining the effect of the interfacial thermal resistance in term of the interfacial layer according to the Kapitza radius concept. The effect of the interfacial thermal resistance on the effective thermal conductivity was in the form of an interfacial thermal resistance factor α_K or the ratio of effective radius and radius of filler r'/r. Thus, the SC2 model gave the

prediction depending on the particle size of filler, apart from the thermal conductivity of filler and polymer matrix (k_f/k_m) and volume fraction of filler. For α_K = 0 or r'/r = 1, the effect of the interfacial thermal resistance was neglected and the SC2 model reduced to SC1 model. For α_K > 0 or r'/r < 1, The SC2 model predicted that the effective thermal conductivity decreased with increasing α_K (decreasing r'/r). Similar to the modified Maxwell and the modified Bruggeman model, the SC2 model predicted the thermal conductivity of the composite equal to that of the matrix for α_K = 1 or r'/r = 0. The comparisons of numerical results with experimental data showed that the SC2 model predicted the interfacial thermal resistance decreased with increasing volume fraction of filler. Furthermore, the smaller particle size led to the higher interfacial thermal resistance than the larger particle size. The SC2 model can be further modified and may give the better prediction if the relationship between the interfacial thermal resistance and volume fraction of filler is known.

6.2 Recommendations

In order to develop a more accurate effective thermal conductivity model, the following recommendations were made.

1. Because the predictive ability of the models strongly depended on the arrangement of filler particles in the representative volume element, thus the arrangement of filler particles in real composite systems should be further studied to find a more appropriate representative volume element for modelling.

2. The effect of the size distribution, shape, and agglomeration of filler particles should be further incorporated into the model.

3. To investigate the ability of the models to predict the percolation behavior, the experimental data measured from the polymer composites with very high ratio of thermal conductivity between filler and polymer and volume fraction of filler in range of 0 to maximum packing volume fraction are required.

4. The relationship between the interfacial thermal resistance and volume fraction of filler should be further investigated to find a correlation that is useful for fitting predicted curve with the experimental data.

5. To verify the ability of the modified model, the appropriate experimental data, the thermal conductivity and the interfacial thermal resistance measured directly from a composite, should be used for comparison.

6. In additional to such appropriate experimental data, the thermal conductivity of the composites should be measured on a wide range of filler volume fraction or up to the maximum packing volume fraction and the necessary data such as the thermal conductivity of polymer matrix and filler, particle size of filler, and so on, which is according to the basic requirements of Mottram [26], should be available.

7. As the lack of the data as listed in 4 and 5 above still is the main problem; the polymer composites should be prepared and their experimental data should be measured in the laboratory.

REFERENCES

1. Dehaghani, H.E., Reiszadeh, M., Chavoshi, A., Nazempour, M., and Vakili, M.H., The effect of zinc oxide and calcium carbonate nanoparticles on the thermal conductivity of polypropylene. Journal of Macromolecular Science, Part B: Physics, 2013. 53(1): p. 93-107.
2. Agarwal, S. and Gupta, R.K., Thermal conductivity of polymer nanocomposites, in Polymer Nanocomposites Handbook. 2010, Taylor and Francis Group, LLC. p. 485-511.
3. Zweben, C., Advances in composite materials for thermal management in electronic packaging. JOM, 1998. 50(6): p. 47-51.
4. Ishida, H. and Rimdusit, S., Very high thermal conductivity obtained by boron nitride-filled polybenzoxazine. Thermochimica Acta, 1998. 320: p. 177-186.
5. Boudenne, A., Ibos, L. and Candau, Y., Thermophysical properties of multiphase polymer systems, in Handbook of Multiphase Polymer Systems, Boudenne, A., et al., Editors. 2011, John Wiley&Son, Ltd.
6. Singh, R. and Sharma, P.K., Effective thermal conductivity of metal filled polymer composites. Indian Journal of Pure & Applied Physics, 2011. 49: p. 112-116.
7. Dehaghani, H.E. and Nazempour, M., Thermal conductivity of nanoparticles filled polymers, in Smart Nanoparticles Technology, Hashim, A., Editor. 2012, InTech. p. 519-540.
8. Yu, S., Hing, P. and Hu, X., Thermal conductivity of polystyrene-aluminum nitride composite. Composites: Part A, 2002. 33: p. 289-292.
9. Zweben, C. Advanced composites and other advanced materials for electronic packaging thermal management. in Advanced Packaging Materials: Processes, Properties and Interfaces, 2001. Proceedings. International Symposium on. 2001.
10. Leung, S.N., Khan, M.O., Chan, E., Naguib, H., Dawson, F., Adinkrah, V., and Hayward, L.L., Analytical modeling and characterization of heat transfer in

thermally conductive polymer composites filled with spherical particulates. Composites: Part B, 2013. 45: p. 43-49.

11. Han, Z. and Fina, A., Thermal conductivity of carbon nanotubes and their polymer nanocomposites: A review. Progress in Polymer Science, 2011. 36: p. 914-944.
12. Boudenne, A., Ibos, L., Fois, M., Gehin, E., and Majeste, J.C., Thermophysical properties of polypropylene/aluminum composites. Journal of Polymer Science: Part B: Polymer Physics, 2004. 42: p. 722-732.
13. Lin, W., Modeling of thermal conductivity of polymer nanocomposites, in Modeling and prediction of polymer nanocomposite properties, Mittal, V., Editor. 2013, Wiley-VCH. p. 169-200.
14. Cheng, S.C. and Vachon, R.I., The prediction of the thermal conductivity of two and three phase solid heterogeneous mixtures. International Journal of Heat and Mass Transfer, 1969. 12: p. 249-264.
15. Liang, J.Z. and Liu, G.S., A new heat transfer model of inorganic particulate-filled polymer composites. Journal of Materials Science, 2009. 44: p. 4715-4720.
16. Liang, J.Z. and Li, F.H., Heat transfer in polymer composites filled with inorganic hollow micro-spheres: A theoretical model. Polymer Testing, 2007. 26: p. 1025-1030.
17. Hatta, H. and Taya, M., Effective thermal conductivity of a misoriented short fiber composite. Journal of Applied Physics, 1985. 58: p. 2478-2486.
18. Hamilton, R.L. and Crosser, O.K., Thermal conductivity of heterogeneous two-component systems. Industrial & Engineering Chemistry Fundamentals, 1962. 1(3): p. 187-191.
19. Nielsen, L.E., The thermal and electrical conductivity of two-phase systems. Industrial & Engineering Chemistry Fundamentals, 1974. 13(1): p. 17-20.
20. Sundstrom, D.W. and Lee, Y.-D., Thermal conductivity of polymers filled with particulate solids. Journal of Applied Polymer Science, 1972. 16(12): p. 3159-3167.

21. Zhang, L.Z., Wang, X.J., Quan, Y.Y. and Pei, L.X., Conjugate heat conduction in filled composite materials considering interactions between the filler and base materials. International Journal of Heat and Mass Transfer, 2013. 64: p. 735-742.
22. Kumlutas, D. and Tavman, I.H., A Numerical and Experimental Study on Thermal Conductivity of Particle Filled Polymer Composites. Journal of Thermoplastic Composite Materials, 2006. 19(4): p. 441-455.
23. Chikhi, M., Agoudjil, B., Haddadi, M. and Boudenne, A., Numerical modelling of the effective thermal conductivity of heterogeneous materials. Journal of Thermoplastic Composite Materials, 2013. 26(3): p. 336-345.
24. Wang, J., Carson, J.K., North, M.F. and Cleland, D.J., A new approach to modelling the effective thermal conductivity of heterogeneous materials. International Journal of Heat and Mass Transfer, 2006. 49: p. 3075-3083.
25. Wang, J., Carson, J.K., North, M.F. and Cleland, D.J., A new structural model of effective thermal conductivity for heterogeneous materials with co-continuous phases. International Journal of Heat and Mass Transfer, 2008. 51: p. 2389-2397.
26. Bigg, D.M., Thermal conductivity of heterophase polymer compositions. Advances in Polymer Science, 1995. 119: p. 1-30.
27. Every, A.G., Tzou, Y., Hasselman, D.P.H. and Raj, R., The effect of particle size on the thermal conductivity of ZnS/diamond composites. Acta Metallurgica et Materialia, 1992. 40(1): p. 123-129.
28. Hasselman, D.P.H. and Johnson, L.F., Effective thermal conductivity of composites with interfacial thermal barrier resistance. Journal of Composite Materials, 1987. 21: p. 508-515.
29. Nan, C.-W., Liu, G., Lin, Y. and Li, M., Interface effect on thermal conductivity of carbon nanotube composites. Applied Physics Letters, 2004. 85(16): p. 3549-3551.
30. Benveniste, Y., Effective thermal conductivity of composites with a thermal contact resistance between the constituents: Nondilute case. Journal of Applied Physics, 1987. 61: p. 2840-2843.

31. Nan, C.W., Birringer, R., Clarke, D.R. and Gleiter, H., Effective thermal conductivity of particulate composites with interfacial thermal resistance. Journal of Applied Physics, 1997. 81: p. 6692-6699.
32. Swartz, E.T. and Pohl, R.O., Thermal boundary resistance. Reviews of Modern Physics, 1989. 61(3): p. 605-668.
33. Pietrak, K. and Wisniewski, T.S., A review of models for effective thermal conductivity of composite materials. Journal of Power Technologies, 2015. 95(1): p. 14-24.
34. Jiajun, W. and Xiao-Su, Y., Effects of interfacial thermal barrier resistance and particle shape and size on the thermal conductivity of AlN/PI composites. Composites Science and Technology, 2004. 64(10–11): p. 1623-1628.
35. Callister, W.D. and Rethwisch, D.G., Materials science and engineering an introduction. 8th ed.: John Wiley&Sons, Inc.
36. Bird, R.B., Stewart, W.E. and Lightfoot, E.N., Transport Phenomena. 2 ed. 2007, New York: John Wiley and Sons, Inc.
37. Kaviany, M., Principles of Heat Transfer. 2002: Wiley.
38. Fiamegkou, E., Athanasopoulos, N. and Kostopoulos, V., Prediction of the effective thermal conductivity of carbon nanotube-reinforced polymer systems. Polymer Composites, 2014. 35(10): p. 1997-2009.
39. Bigg, D.M., Thermally conductive polymer compositions. Polymer Composites, 1986. 7(3): p. 125-140.
40. Pietrak, K. and Wisniewski, T.S., Methods for experimental determination of solid-solid interfacial thermal resistance with application to composite materials. Journal of Power Technologies, 2014. 94(4): p. 270-285.
41. Landry, E.S. and McGaughey, A.J.H., Thermal boundary resistance predictions from molecular dynamics simulations and theoretical calculations. Physical Review B, 2009. 80(16): p. 165304.
42. Shen, M.-x., Cui, Y.-x., He, J. and Zhang, Y.-m., Thermal conductivity model of filled polymer composites. International Journal of Minerals, Metallurgy, and Materials, 2011. 18(5): p. 623-631.

43. Bruggeman, D.A.G., Berechnung verschiedener physikalischer Konstanten von heterogenen substanzen. Annalen der Physik (Leipeig), 1935. 24: p. 636.

44. Torquato, S., Effective electrical conductivity of two-phase disordered composite media. Journal of Applied Physics, 1985. 58(10): p. 3790-3797.

45. Tsao, G.T.N., Thermal conductivity of two-phase materials. Industrial and Engineering Chemistry, 1961. 53(5): p. 395-397.

46. Okamoto, S. and Ishida, H., A new theoretical equation for thermal conductiviy of two-phase systems. Journal of Applied Polymer Science, 1999. 72: p. 1689-1697.

47. Chauhan, D., Singhvi, N. and Singh, R., Effect of geometry of filler particles on the effective thermal conductivity of two-phase systems. International journal of Modern Nonlinear Theory and Application, 2012. 1: p. 40-46.

48. Progelhof, R.C., Throne, J.L. and Ruetsch, R.R., Methods for predicting the thermal conductivity of composite systems: A review. Polymer Engineering and Science, 1976. 16(9): p. 615-625.

49. Ordóñez-Miranda, J., Alvarado-Gil, J.J. and Medina-Ezquivel, R., Generalized Bruggeman Formula for the Effective Thermal Conductivity of Particulate Composites with an Interface Layer. International Journal of Thermophysics, 2010. 31(4-5): p. 975-986.

50. Eshelby, J.D., The Determination of the Elastic Field of an Ellipsoidal Inclusion, and Related Problems. Proceedings of the Royal Society of London. Series A, 1957. 241(1226): p. 376-396.

51. Tong, X., Thermally Conductive Polymer Matrix Composites, in Advanced Materials for Thermal Management of Electronic Packaging. 2011, Springer New York. p. 201-232.

52. Lee, G.-W., Park, M., Kim, J., Lee, J.I., and Yoon, H.G., Enhanced thermal conductivity of polymer composites filled with hybrid filler. Composites Part A: Applied Science and Manufacturing, 2006. 37(5): p. 727-734.

53. Mamunya, Y.P., Davydenko, V.V., Pissis, P. and Lebedev, E.V., Electrical and thermal conductivity of polymers filled with metal powders. European Polymer Journal, 2002. 38(9): p. 1887-1897.

54. Ng, H.Y., Lu, X. and Lau, S.K., Thermal conductivity of boron nitride-filled thermoplastics: Effect of filler characteristics and composite processing conditions. Polymer Composites, 2005. 26(6): p. 778-790.

55. Nurul, M. and Mariatti, M., Effect of thermal conductive fillers on the properties of polypropylene composites. Journal of Thermoplastic Composite Materials, 2013. 26(5): p. 627-639.

56. Sofian, N.M., Rusu, M., Neagu, R. and Neagu, E., Metal Powder-Filled Polyethylene Composites. V. Thermal Properties. Journal of Thermoplastic Composite Materials, 2001. 14(1): p. 20-33.

57. Tekce, H.S., Kumlutas, D. and Tavman, I.H., Effect of Particle Shape on Thermal Conductivity of Copper Reinforced Polymer Composites. Journal of Reinforced Plastics and Composites, 2007. 26(1): p. 113-121.

58. Kochetov, R., Andritsch, T., Morshuis, P.H.F. and Smit, J.J. Effect of filler size on complex permittivity and thermal conductivity of epoxy-based composites filled with BN particles. in Electrical Insulation and Dielectric Phenomena (CEIDP), 2010 Annual Report Conference on. 2010.

59. Han, Z., Wood, J.W., Herman, H., Zhang, C., and Stevens, G.C. Thermal Properties of Composites Filled with Different Fillers. in Electrical Insulation, 2008. ISEI 2008. Conference Record of the 2008 IEEE International Symposium on. 2008.

60. Krupa, I. and Chodák, I., Physical properties of thermoplastic/graphite composites. European Polymer Journal, 2001. 37(11): p. 2159-2168.

61. Huxtable, S.T., et al., Interfacial heat flow in carbon nanotube suspensions. Nature Materials, 2003. 2(11): p. 731-734.

62. Kochetov, R., Korobko, A.V., Andritsch, T., Morshuis, P.H.F., Picken, S.J., and Smit, J.J., Modelling of the thermal conductivity in polymer nanocomposites and the impact of the interface between filler and matrix. Journal of Physics D: Applied Physics, 2011. 44: p. 395401.

63. Chapelle, E., Garnier, B. and Bourouga, B., Interfacial thermal resistance measurement between metallic wire and polymer in polymer matrix composites. International Journal of Thermal Sciences, 2009. 48(12): p. 2221-2227.

64. Gharagozloo-Hubmann, K., Boden, A., Czempiel, G.J.F., Firkowska, I., and Reich, S., Filler geometry and interface resistance of carbon nanofibres: Key parameters in thermally conductive polymer composites. Applied Physics Letters, 2013. 102(21): p. 213103.

65. Fukushima, K., Takezawa, Y. and Adschiri, T., Evaluation of thermal conductive resistance at organic-inorganic interface and effect of interfaces on thermal conductivity of composite materials. Japanese Journal of Applied Physics, 2013. 52: p. 081601.

66. Mori, T. and Tanaka, K., Average Stress in Matrix and Average Elastic Energy of Materials with Misfitting Inclusions. Acta Metallurgica, 1973. 21: p. 571.

67. Felske, J.D., Effective thermal conductivity of composite spheres in a continuous medium with contact resistance. International Journal of Heat and Mass Transfer, 2004. 47(14–16): p. 3453-3461.

68. Andritsch, T., Kochetov, R., Morshuis, P.H.F. and Smit, J.J. Proposal of the polymer chain alignment model. in Electrical Insulation and Dielectric Phenomena (CEIDP), 2011 Annual Report Conference on. 2011.

69. Hahn, H.T. and Tsai, S.W., Introduction to Composite Materials. 1980: Taylor & Francis.

70. White, H.E. and Walton, S.F., Particle packing and particle shape. Journal of the American Ceramic Society, 1937. 20(1-12): p. 155-166.

71. Timofeeva, E.V., Gavrilov, A.N., McCloskey, J.M., Tolmachev, Y.V., Sprunt, S., Lopatina, L.M., and Selinger, J.V., Thermal conductivity and particle agglomeration in alumina nanofluids: Experiment and theory. Physical Review E, 2007. 76(6): p. 061203.

APPENDIX

APPENDIX A

INTEGRATION FORMULA

Two definite integrals of rational functions used in chapter IV were listed here.

1. Integral Involving $\frac{1}{b^2-x^2}$

For $|x| < |b|$, the definite integral involving $\frac{1}{b^2-x^2}$ from e to f can be written as

$$\int_e^f \frac{1}{b^2 - x^2}\,dx = \frac{1}{2b}\left(\ln\left|\frac{b+f}{b-f}\right| - \ln\left|\frac{b+e}{b-e}\right|\right) \tag{A.1}$$

2. Integral Involving $\frac{1}{bx^2+cx+d}$

For $4bd - c^2 < 0$, the definite integral involving $\frac{1}{bx^2+cx+d}$ from e to f can be written as

$$\int_e^f \frac{1}{bx^2 + cx + d}\,dx = \frac{2}{\sqrt{c^2 - 4bd}}\left(\ln\left|\frac{2bf + c - \sqrt{c^2 - 4bd}}{2bf + c + \sqrt{c^2 - 4bd}}\right| - \ln\left|\frac{2be + c - \sqrt{c^2 - 4bd}}{2be + c + \sqrt{c^2 - 4bd}}\right|\right) \tag{A.2}$$

APPENDIX B

TABULATION OF EXPERIMENTAL DATA ON THE THERMAL CONDUCTIVITY OF COMPOSITE MATERIALS

Table B. 1. Thermal conductivity of composites filled with spherical particles

Matrix	Filler	d	k_m	k_f	k_f/k_m	v_f	k_{eff}	k_{eff}/k_m	Ref
EVA	Glass sphere	36	0.27	1.2	4.4	0	0.27	1.0	[5]
EVA	Glass sphere	36	0.27	1.2	4.4	0.03	0.27	1.0	[5]
EVA	Glass sphere	36	0.27	1.2	4.4	0.08	0.29	1.1	[5]
EVA	Glass sphere	36	0.27	1.2	4.4	0.15	0.33	1.2	[5]
EVA	Glass sphere	36	0.27	1.2	4.4	0.29	0.37	1.4	[5]
EVA	Glass sphere	36	0.27	1.2	4.4	0.36	0.45	1.7	[5]
EVA	Glass sphere	36	0.27	1.2	4.4	0.45	0.48	1.8	[5]
EVA	Barium titanate	9	0.27	2.7	10	0	0.27	1.0	[5]
EVA	Barium titanate	9	0.27	2.7	10	0.05	0.27	1.0	[5]
EVA	Barium titanate	9	0.27	2.7	10	0.10	0.31	1.1	[5]
EVA	Barium titanate	9	0.27	2.7	10	0.16	0.36	1.3	[5]
EVA	Barium titanate	9	0.27	2.7	10	0.28	0.54	2.0	[5]
EVA	Barium titanate	9	0.27	2.7	10	0.38	0.69	2.6	[5]
EVA	Barium titanate	9	0.27	2.7	10	0.48	0.89	3.3	[5]
EVA	Barium titanate	105	0.27	2.7	10	0	0.27	1.0	[5]
EVA	Barium titanate	105	0.27	2.7	10	0.05	0.30	1.1	[5]
EVA	Barium titanate	105	0.27	2.7	10	0.12	0.36	1.3	[5]
EVA	Barium titanate	105	0.27	2.7	10	0.20	0.48	1.8	[5]
EVA	Barium titanate	105	0.27	2.7	10	0.27	0.58	2.1	[5]
EVA	Barium titanate	105	0.27	2.7	10	0.36	0.74	2.7	[5]
EVA	Barium titanate	105	0.27	2.7	10	0.44	0.90	3.3	[5]

Table B.1 Thermal conductivity of composites filled with spherical particles (cont.)

Matrix	Filler	d	k_m	k_f	k_f/k_m	v_f	k_{eff}	k_{eff}/k_m	Ref
PP	Aluminum	8	0.239	237	992	0	0.239	1.00	[12]
PP	Aluminum	8	0.239	237	992	0.050	0.242	1.01	[12]
PP	Aluminum	8	0.239	237	992	0.178	0.394	1.65	[12]
PP	Aluminum	8	0.239	237	992	0.231	0.580	2.43	[12]
PP	Aluminum	8	0.239	237	992	0.405	0.980	4.10	[12]
PP	Aluminum	8	0.239	237	992	0.488	1.950	8.16	[12]
PP	Aluminum	8	0.239	237	992	0.587	2.677	11.2	[12]
PP	Aluminum	44	0.239	237	992	0	0.239	1.00	[12]
PP	Aluminum	44	0.239	237	992	0.050	0.271	1.13	[12]
PP	Aluminum	44	0.239	237	992	0.201	0.515	2.15	[12]
PP	Aluminum	44	0.239	237	992	0.269	0.691	2.89	[12]
PP	Aluminum	44	0.239	237	992	0.393	1.580	6.61	[12]
PP	Aluminum	44	0.239	237	992	0.489	2.575	10.8	[12]
PP	Aluminum	44	0.239	237	992	0.583	4.222	17.7	[12]
Epoxy	Silver	48	0.244	420	1721	0	0.244	1.00	[39]
Epoxy	Silver	48	0.244	420	1721	0.106	0.339	1.39	[39]
Epoxy	Silver	48	0.244	420	1721	0.200	0.423	1.73	[39]
Epoxy	Silver	48	0.244	420	1721	0.312	0.584	2.39	[39]
Epoxy	Silver	48	0.244	420	1721	0.474	0.906	3.71	[39]
Epoxy	Silver	48	0.244	420	1721	0.569	1.187	4.86	[39]
Epoxy	Silver	27	0.244	420	1721	0	0.244	1.00	[39]
Epoxy	Silver	27	0.244	420	1721	0.097	0.309	1.27	[39]
Epoxy	Silver	27	0.244	420	1721	0.246	0.434	1.78	[39]
Epoxy	Silver	27	0.244	420	1721	0.306	0.583	2.39	[39]
Epoxy	Silver	27	0.244	420	1721	0.391	0.760	3.11	[39]
Epoxy	Silver	27	0.244	420	1721	0.557	1.326	5.43	[39]

APPENDIX C

Publication

MACRO 2014 was taken place on 6 – 11 July 2014 at Chiang Mai International Convention and Exhibition Center (CMICE), Chiang Mai, Thailand. Part of this thesis was published on the "PROCEEDING MACRO 2014", in the section of "Polymer Processing and Composites" on page of 177 – 180.

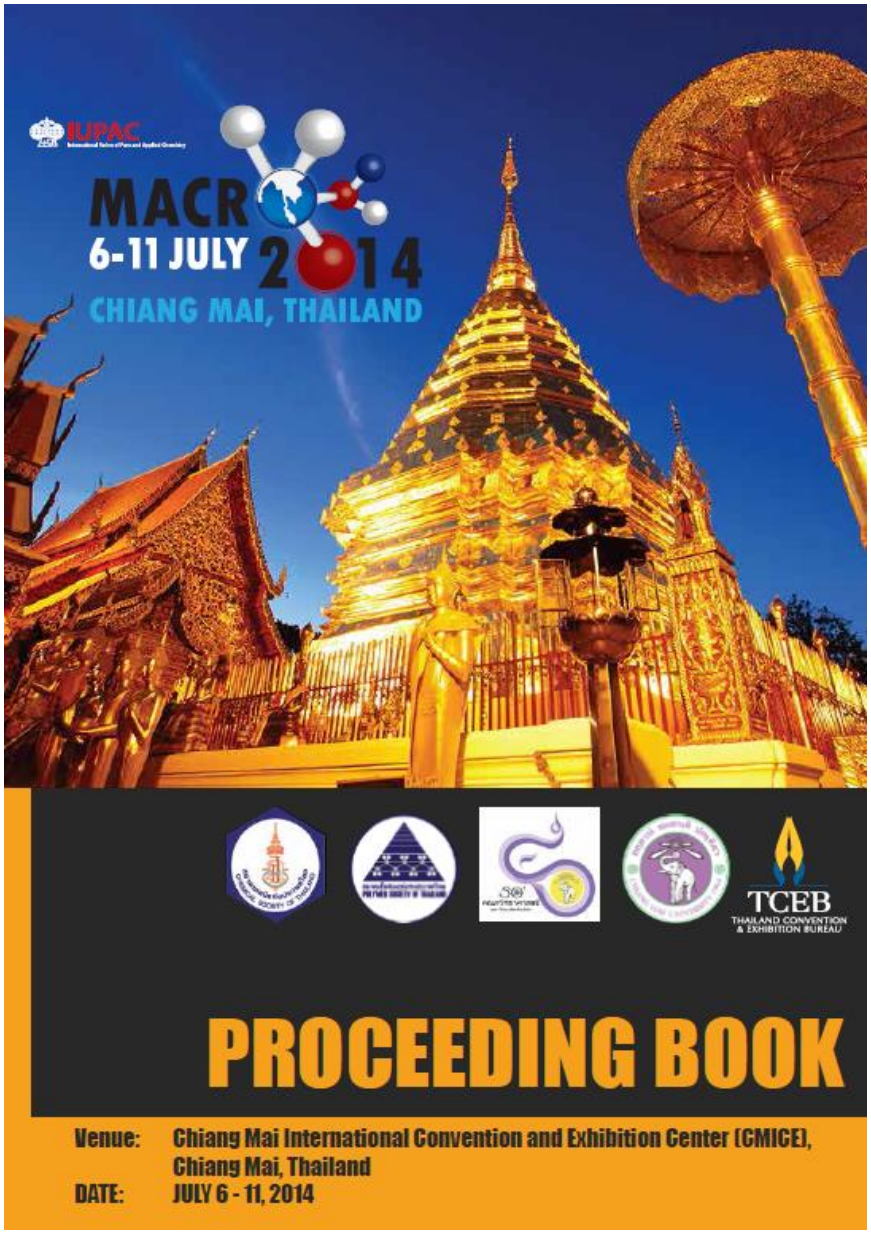

Thermal conductivity model of spherical particulate filled polymer composites

Nuttakan Kuttanate, Varun Taepaisitphongse*

Department of Chemical Engineering, Faculty of Engineering, Chulalongkorn University, Bangkok 10330, Thailand
Phone: +66-2218-6878, Fax: +66-2218-6877,
**E-mail: varun.t@chula.ac.th*

Introduction

Polymers are presently common materials used in electronic devices due to their remarkable properties such as light weight, corrosion resistance and easy processing. However, most polymers have low thermal conductivity and this causes a limitation for polymer application in electronic devices because the materials used in these devices should possess high thermal conductivity to protect the damage from heat during operation [1]. Therefore, it is essential to improve the thermal conductivity of polymer materials. A simple method to solve this problem is the preparation as the polymer composite by mixing the high thermal conductive filler into the polymer matrix. The thermal conduction behavior of final polymer composite material depends on type, shape, arrangement and content of filler [2]. Accordingly, the understanding of heat transfer mechanism of polymer composite is necessary.

In this article, the thermal conductivity model was developed to understand the heat transfer mechanism of polymer composite and the effects of fillers. The model was derived based on a series of thermal resistance along the heat flow direction. The three ideal arrangements of spherical particulate, i.e. simple cubic, body-centered cubic and face-centered cubic, were selected as the heat transfer element. These proposed models showed different prediction behavior depending on the filler arrangement and loading.

Models for effective thermal conductivity

Several models have been developed by the different methods to predict the effective thermal conductivity (k_{eff}) of filled polymer composites [2]. Tsao [3] developed a probabilistic model based on the series and parallel models for effective thermal conductivity. Afterwards, this model was further developed by Cheng and Vachon [4]. They proposed a parabolic distribution of the discontinuous phase. The constants of the parabolic distribution were presented as a function of the filler phase volume fraction (ϕ_f). The Cheng and Vachon equation assumed that the thermal conductivity of fillers (k_f) always are higher than the thermal conductivity of polymer matrix (k_m) and was given as

$$\frac{1}{k_{eff}} = \frac{1}{\sqrt{C(k_f - k_m)[k_m + B(k_f - k_m)]}} \times \ln\frac{\sqrt{k_m + B(k_f - k_m)} + \frac{B}{2}\sqrt{C(k_f - k_m)}}{\sqrt{k_m + B(k_f - k_m)} - \frac{B}{2}\sqrt{C(k_f - k_m)}} + \frac{1-B}{k_m} \quad (1)$$

where $B = (3\phi_f/2)^{1/2}$, $C = -4/B$.

Recently, a new theoretical model of heat transfer in polymer composites was established based on the law of minimal thermal resistance and the equal law of the specific equivalent thermal conductivity by Liang and Liu [5]. The effective thermal conductivity was given by

$$k_{eff} = \frac{1}{\frac{1}{k_m} - \frac{1}{k_m}\left(\frac{6\phi_f}{\pi}\right)^{\frac{1}{3}} + \frac{2}{k_m\left(\frac{4\pi}{3\phi_f}\right)^{\frac{1}{3}} + \left(\frac{2\phi_f}{9\pi}\right)^{\frac{1}{3}}\pi(k_f - k_m)}} \quad (2)$$

Development of the theoretical models

Heat transfer elements. In a simple case, polymer composite is supposed that it consists of uniform spherical particles dispersed homogeneously in polymer matrix. The particles can be considered as being arranged similar to atoms in a crystal structure and the concept of unit cell analogous to crystallography can be applied [6]. In this work, three ideal arrangements, i.e. simple cubic, body-centered cubic and face-centered cubic, were chosen as heat transfer element as shown in Figure 1. Suppose the side length of the cube and the particle diameter is a and $2r$, respectively, an expression of the filler volume fraction was derived for each element as follows:

simple cubic : $\phi_{f,sc} = \frac{4\pi r^3}{3a^3}$ (3)

body-centered cubic : $\phi_{f,bcc} = \frac{8\pi r^3}{3a^3}$ (4)

face-centered cubic : $\phi_{f,fcc} = \frac{16\pi r^3}{3a^3}$ (5)

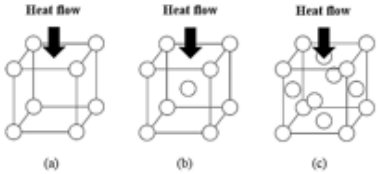

Figure 1. Heat transfer element in form of (a) simple cubic, (b) body-centered cubic and (c) face-centered cubic.

Modeling. The effective thermal conductivity of a polymer composite was derived by considering a series of thermal resistors along the heat flow direction. According to Leung *et al.* [7], the differences between the physical values and the mathematical models depend on the filler loading and their distribution in polymer matrix. Consequently, in this work, the heat transfer models of simple cubic element, body-centered element and face-centered cubic element were divided into eight cases by filler contents as shown in Figures 2, 3 and 4, respectively.

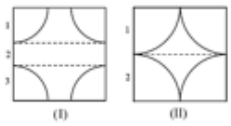

Figure 2. Side view of simple cubic element for polymer composites filled with (I) <52.36 vol.% and (II) 52.36 vol.% fillers.

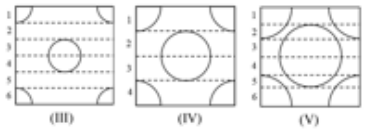

Figure 3. Side view of body-centered cubic element for polymer composites filled with (III) <13.08 vol.%, (IV) 13.08 vol.% and (V) >13.08 vol.% fillers.

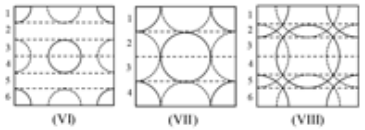

Figure 4. Side view of face-centered cubic element for polymer composites filled with (VI) <26.18 vol.%, (VII) 26.18 vol.% and (VIII) >26.18 vol.% fillers.

Each layer of elements possessed thermal resistances equal to R_i, where i was the layer number as shown in Figures 2, 3 and 4, respectively. These elements can be thought of thermal resistors connected in series along the heat flow direction. The heat flow enters into the element from top of the cube. Thermal interfacial resistance was neglected in this work. The total thermal resistance (R_{total}) of each element can be expressed as

$$R_{total} = \sum_{i=1}^{n} R_i \quad (6)$$

where n is the overall amount of layers of each element.

From the Fourier's law, the heat flow (Q) across the element can be expressed as

$$Q = k_{eff} a^2 \frac{\Delta T}{a} = k_{eff} a \Delta T \tag{7}$$

The thermal resistance is given as

$$R_{total} = \frac{\Delta T}{Q} = \frac{1}{k_{eff} a} \tag{8}$$

Considering a thin layer of the element with thickness dy along the heat flow direction, the heat flow across the layer of thickness dy is

$$Q = k_m A_m \frac{dT}{dy} + k_f A_f \frac{dT}{dy} = \bar{k} A \frac{dT}{dy} \tag{9}$$

where A_m, A_f and A are the cross-sectional areas of the polymer matrix, filler and overall sections, respectively, and

$$\bar{k} = k_m \frac{A_m}{A} + k_f \frac{A_f}{A} \tag{10}$$

The thermal resistance of each layer can be determined by

$$R_i = \int \frac{1}{kA} dy = \int \frac{1}{k_m A_m + k_f A_f} dy \tag{11}$$

Case I: simple cubic element with filler content < 52.36 vol.%. The thermal resistance for each layer was determined by

$$R_1 = R_3 = \frac{1}{\pi(k_f - k_m)} \int_0^r \frac{1}{u_1^2 - y^2} dy \tag{12}$$

$$R_2 = \frac{a - 2r}{k_m a^2} \tag{13}$$

where

$$u_1 = \sqrt{\frac{k_m a^2}{\pi(k_f - k_m)} + r^2} \tag{14}$$

Case II: simple cubic element with filler content = 52.36 vol.%. The thermal resistance for each layer was determined by

$$R_1 = R_2 = \frac{1}{\pi(k_f - k_m)} \int_0^r \frac{1}{u_1^2 - y^2} dy \tag{15}$$

Case III: body-centered cubic element with filler content < 13.08 vol.%. The thermal resistance for each layer was determined by

$$R_1 = R_3 = R_4 = R_6 = \frac{1}{\pi(k_f - k_m)} \int_0^r \frac{1}{u_1^2 - y^2} dy \tag{16}$$

$$R_2 = R_5 = \frac{\frac{a}{2} - 2r}{k_m a^2} \tag{17}$$

Case IV: body-centered cubic element with filler content = 13.08 vol.%. The thermal resistance for each layer was determined by

$$R_1 = R_2 = R_3 = R_4 = \frac{1}{\pi(k_f - k_m)} \int_0^r \frac{1}{u_1^2 - y^2} dy \tag{18}$$

Case V: body-centered cubic element with filler content > 13.08 vol.%. The thermal resistance for each layer was determined by

$$R_1 = R_6 = \frac{1}{\pi(k_f - k_m)} \int_0^{\frac{a}{2} - r} \frac{1}{u_1^2 - y^2} dy \tag{19}$$

$$R_2 = R_5 = \frac{1}{\pi(k_f - k_m)} \int_{\frac{a}{2} - r}^r \frac{1}{-2y^2 + ay + v_1} dy \tag{20}$$

$$R_3 = R_4 = \frac{1}{\pi(k_f - k_m)} \int_r^{\frac{a}{2}} \frac{1}{u_1^2 - (\frac{a}{2} - y)^2} dy \tag{21}$$

where

$$v_1 = \frac{k_m a^2}{\pi(k_f - k_m)} + 2r^2 - \frac{a^2}{4} \tag{22}$$

Case VI: face-centered cubic element with filler content < 26.18 vol.%. The thermal resistance for each layer was determined by

$$R_1 = R_3 = R_4 = R_6 = \frac{1}{2\pi(k_f - k_m)} \int_0^r \frac{1}{u_2^2 - y^2} dy \tag{23}$$

$$R_2 = R_5 = \frac{a - 4r}{2k_m a^2} \tag{24}$$

where

$$u_2 = \sqrt{\frac{k_m a^2}{2\pi(k_f - k_m)} + r^2} \tag{25}$$

Case VII: face-centered cubic element with filler content = 26.18 vol.%. The thermal resistance for each layer was determined by

$$R_1 = R_2 = R_3 = R_4 = \frac{1}{2\pi(k_f - k_m)} \int_0^r \frac{1}{u_2^2 - y^2} dy \tag{26}$$

Case VIII: face-centered cubic element with filler content > 26.18 vol.%. The thermal resistance for each layer was determined by

$$R_1 = R_6 = \frac{1}{2\pi(k_f - k_m)} \int_0^{\frac{a}{2} - r} \frac{1}{u_2^2 - y^2} dy \tag{27}$$

$$R_2 = R_5 = \frac{1}{2\pi(k_f - k_m)} \int_{\frac{a}{2} - r}^r \frac{1}{-2y^2 + ay + v_2} dy \tag{28}$$

$$R_3 = R_4 = \frac{1}{2\pi(k_f - k_m)} \int_r^{\frac{a}{2}} \frac{1}{u_2^2 - (\frac{a}{2} - y)^2} dy \tag{29}$$

where

$$v_2 = \frac{k_m a^2}{2\pi(k_f - k_m)} + 2r^2 - \frac{a^2}{4} \tag{30}$$

The total resistance for cases I-VIII derived by taking the integration and substituting the results into Eq. (6) can be expressed as Eqs. (31)-(38), respectively.

$$R_{total,I} = \frac{1}{\pi(k_f - k_m)u_1} \ln\left|\frac{u_1 + r}{u_1 - r}\right| + \frac{a - 2r}{k_m a^2} \tag{31}$$

$$R_{total,II} = \frac{1}{\pi(k_f - k_m)u_1} \ln\left|\frac{u_1 + r}{u_1 - r}\right| \tag{32}$$

$$R_{total,III} = \frac{2}{\pi(k_f - k_m)u_1} \ln\left|\frac{u_1 + r}{u_1 - r}\right| + \frac{a - 4r}{k_m a^2} \tag{33}$$

$$R_{total,IV} = \frac{2}{\pi(k_f - k_m)u_1} \ln\left|\frac{u_1 + r}{u_1 - r}\right| \tag{34}$$

$$R_{total,V} = \frac{2}{\pi(k_f - k_m)u_1} \ln\left|\frac{u_1 + \frac{a}{2} - r}{u_1 - \frac{a}{2} + r}\right| + \frac{4}{\pi(k_f - k_m)\sqrt{a^2 + 8v_1}} \ln\left(\frac{4r - a + \sqrt{a^2 + 8v_1}}{4r - a - \sqrt{a^2 + 8v_1}}\right) \tag{35}$$

$$R_{total,VI} = \frac{1}{\pi(k_f - k_m)u_2} \ln\left|\frac{u_2 + r}{u_2 - r}\right| + \frac{a - 4r}{k_m a^2} \tag{36}$$

$$R_{total,VII} = \frac{1}{\pi(k_f - k_m)u_2} \ln\left|\frac{u_2 + r}{u_2 - r}\right| \tag{37}$$

$$R_{total,VIII} = \frac{1}{\pi(k_f - k_m)u_2} \ln\left|\frac{u_2 + \frac{a}{2} - r}{u_2 - \frac{a}{2} + r}\right| + \frac{2}{\pi(k_f - k_m)\sqrt{a^2 + 8v_2}} \ln\left(\frac{4r - a + \sqrt{a^2 + 8v_2}}{4r - a - \sqrt{a^2 + 8v_2}}\right) \tag{38}$$

The effective thermal conductivity for each element can then be calculated by Eq. (8).

Results and Discussion

Based on a series of thermal resistance along the heat flow direction, the total resistances of polyamide 6 filled with copper particles (average particle size 50 μm) (PA6/Cu) at various filler contents were calculated by Eqs. (31) – (38) then the effective thermal conductivities can be calculated by Eq. (8). The calculated values were compared with the experimental thermal conductivity of PA6/Cu composite cited from [8] as shown in Figure 5 for overview of predicted values and Figure 6 for comparative values. From the results, the predictive values of each model depended on the filler content only. In this work, three ideal arrangements of particulate were used as representative volume element. It was clear that body-centered cubic model offered the most overestimated values and then followed by face-centered cubic model and simple cubic model, respectively. Leung *et al*. [7] suggested that these differences were attributed to the thermal contact resistance at the interfaces between particles and polymer matrix due to the incomplete bonding and phonon acoustic mismatch; this was ignored in this work. Also, these ideal particulate arrangement could be a cause of the differences apart from the thermal contact resistance. In real system, the arrangement of particles of polymer composites is variant from the ideal arrangement due to effects of processing [9], size distribution of filler particles [10], and irregular-shaped particles [11]. Furthermore, the agglomeration of particles results in nonspherical geometries of the agglomerates such as a dendritic or fractal structure which affects to the thermal conductivity enhancement [12]. Thus, the irregularly-shaped agglomerates should be included in further work, such as considering in the form of equivalent spherical diameter.

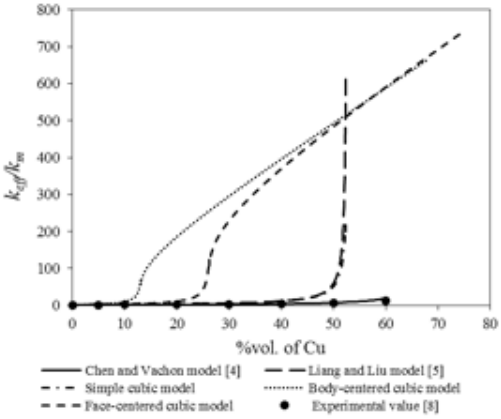

Figure 5. Overview of relationship between effective thermal conductivity and filler volume contents of PA6/Cu.

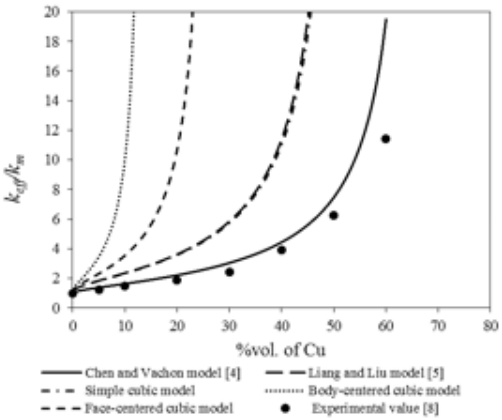

Figure 6. Comparison between theoretical predicted effective thermal conductivity and experimental data of PA6/Cu with different filler volume contents.

It should be noted in Figure 6 that percolation behavior, which is a rapid increase of the effective thermal conductivity over several order of magnitude [13], was observed when filler volume contents were equal to 52.36 vol.% for simple cubic model (case II), 13.08 vol.% for body-centered cubic model (case IV) and 26.18 vol.% for face-centered cubic model (case VII). In contrast, the experimental data did not show the percolation behavior. Different from electrical conductivity, it was known that most polymer composites showed an absence of percolation behavior for their thermal conductivity because the difference between the thermal conductivity of fillers and polymer matrices was relatively small for most systems [9]. However, these percolation behavior indicated the influence of the different arrangement of filler particles in the heat transfer element upon the predictive ability of the models.

From such differences, it is suggested that there should be a suitable arrangement of filler particles for heat transfer element modeling. In this work, simple cubic arrangement offered the best predicted values compared with the others two arrangements. Besides simple cubic arrangement, Liang and Liu [5] proposed the thermal conductivity model based on the same principal but a heat transfer element was a spherical particle located in the center of a cube. This model provided the satisfactory results in their work and the predicted values were similar with the simple cubic model in this article. Unfortunately, both models could not predict the effective thermal conductivity where filler content was more than 52.36 vol.% and they usually overestimated the effective thermal conductivity. However, it indicated that there must be an equivalent heat transfer element that has the same quantity of filler particles but different arrangement of particles. Based upon the additivity of resistances in series, the arrangement of particles can be rearranged without the effect on the overall thermal resistance of the whole element [3]. By this principal, Cheng and Vachon [4] proposed a theoretical model that assumed a parabolic distribution of the discontinuous phase and determined the constant of the parabolic distribution as a function of the discontinuous phase volume fraction. This model was shown to predict the effective thermal conductivity closer to the experimental data than the other models as shown in Figure 6. This inferred that the model based on a series of thermal resistance should be developed further by using the appropriate function representing distribution or arrangement of filler particle in polymer matrices.

Conclusions

The theoretical models based on a series of thermal resistance along one dimensional heat conduction had been proposed by using three ideal filler arrangements as heat transfer elements, i.e. simple cubic, body-centered cubic and face-centered cubic. Each model overestimated the effective thermal conductivity as a function of the filler content. The behavior of predictive values were also significantly affected by the filler arrangement models. Hence, more appropriate filler arrangement used as the heat transfer element should be further studied for developing the effective thermal conductivity model of polymer composites.

References

(1) Zweben, C. *JOM.* **1998**, *50*, 47.
(2) Shen, M.; Cui, Y.; He, J.; Zhang, Y. *International Journal of Minerals, Metallurgy, and Materials* **2011**, *18*, 623.
(3) Tsao, G.T.N. *Industrial & Engineering Chemistry* **1961**. *53*, 395.
(4) Cheng, S.C.; Vachon, R.I. *International Journal of Heat and Mass Transfer* **1969**, *12*, 249.
(5) Liang, J.Z.; Liu, G.S. *Journal of Materials Science* **2009**, *44*, 4715.
(6) Andritsch, T.; Kochetov, R.; Morshuis, P.H.F.; Smit, J.J. *Electrical Insulation and Dielectric Phenomena (CEIDP)* **2011**, 624.
(7) Leung, S.N.; Khan, M.O.; Chan, E.; Naguib, H.; Dawson, F.; Adinkrah, V.; Lakatos-Hayward, L. *Composites Part B: Engineering* **2013**, *45*, 43.
(8) Tekce, H.S.; Kumlutas, D.; Tavman, I.H. *Journal of Reinforced Plastics and Composites* **2007**, *26*, 113.
(9) Ng, H.Y.; Lu, X.; Lau, S.K. *Polymer Composites* **2005**, *26*, 778.
(10) Ishida, H.; Rimdusit, S. *Thermochimica Acta* **1998**, *320*, 177.
(11) White, H.E.; Walton, S.F. *Journal of the American Ceramic Society* **1937**, *20*, 155.
(12) Timofeeva, E.V.; Gavrilov, A.N.; McCloskey, J.M.; Tolmachev, Y.V.; Sprunt, S.; Lopatina, L.M.; Selinger, J.V. *Physical Review E* **2007**, *76*, 061203.
(13) Mamunya, Y.P.; Davydenko, V.V.; Pissis, P.; Lebedev, E.V. *European Polymer Journal* **2002**, *38*, 1887.

VITA

Mr. Nuttakan Kuttanate was born in Chiang Mai, Thailand on November 29, 1989. He completed high school at Dara Academy School, Chiang Mai, Thailand in 2007 and received a Bachelor degree of Petrochemical and Polymeric Material Engineering from the Department of Materials Science and Engineering, Faculty of Engineering and Industrial Technology, Silpakorn University, Nakhon Pathom, Thailand in 2011. He began his graduate study for a Master of Engineering degree at the Department of Chemical Engineering, Faculty of Engineering, Chulalongkorn University, Bangkok, Thailand in 2012. During his graduate study, he presented part of his thesis titled "Thermal conductivity model of spherical particulate filled polymer composites" in the poster session at the MACRO 2014 organized by the International Union of Pure and Applied Chemistry (IUPAC) in Chiang Mai, Thailand during 6 - 11 July 2014.